UNIVERSITY OF AMSTERDAM

UvA-DARE (Digital Academic Repository)

Search for a CP-odd Higgs boson decaying into a heavy CP-even Higgs boson and a Z boson in the $\ell^+\ell^-\bar{t}t$ and $\nu\nu b\bar{b}$ final states using 140 fb^{-1} of data collected with the ATLAS detector

ATLAS Collaboration

DOI
10.1007/JHEP02(2024)197

Publication date
2024

Document Version
Final published version

Published in
Journal of High Energy Physics

License
CC BY

Link to publication

Citation for published version (APA):
ATLAS Collaboration (2024). Search for a CP-odd Higgs boson decaying into a heavy CP-even Higgs boson and a *Z* boson in the $\ell^+\ell^-\bar{t}t$ and $\nu\nu b\bar{b}$ final states using 140 fb^{-1} of data collected with the ATLAS detector. *Journal of High Energy Physics*, *2024*(2), Article 197. https://doi.org/10.1007/JHEP02(2024)197

General rights
It is not permitted to download or to forward/distribute the text or part of it without the consent of the author(s) and/or copyright holder(s), other than for strictly personal, individual use, unless the work is under an open content license (like Creative Commons).

Disclaimer/Complaints regulations
If you believe that digital publication of certain material infringes any of your rights or (privacy) interests, please let the Library know, stating your reasons. In case of a legitimate complaint, the Library will make the material inaccessible and/or remove it from the website. Please Ask the Library: https://uba.uva.nl/en/contact, or a letter to: Library of the University of Amsterdam, Secretariat, P.O. Box 19185, 1000 GD Amsterdam, The Netherlands. You will be contacted as soon as possible.

UvA-DARE is a service provided by the library of the University of Amsterdam (https://dare.uva.nl)

Download date:07 Sep 2026

Published for SISSA by Springer

Received: November 8, 2023
Accepted: February 10, 2024
Published: February 26, 2024

Search for a CP-odd Higgs boson decaying into a heavy CP-even Higgs boson and a Z boson in the $\ell^+\ell^- t\bar{t}$ and $\nu\bar{\nu}b\bar{b}$ final states using 140 fb^{-1} of data collected with the ATLAS detector

The ATLAS collaboration

E-mail: atlas.publications@cern.ch

Abstract: A search for a heavy CP-odd Higgs boson, A, decaying into a Z boson and a heavy CP-even Higgs boson, H, is presented. It uses the full LHC Run 2 dataset of pp collisions at $\sqrt{s} = 13$ TeV collected with the ATLAS detector, corresponding to an integrated luminosity of 140 fb^{-1}. The search for $A \to ZH$ is performed in the $\ell^+\ell^- t\bar{t}$ and $\nu\bar{\nu}b\bar{b}$ final states and surpasses the reach of previous searches in different final states in the region with $m_H > 350$ GeV and $m_A > 800$ GeV. No significant deviation from the Standard Model expectation is found. Upper limits are placed on the production cross-section times the decay branching ratios. Limits with less model dependence are also presented as functions of the reconstructed $m(t\bar{t})$ and $m(b\bar{b})$ distributions in the $\ell^+\ell^- t\bar{t}$ and $\nu\bar{\nu}b\bar{b}$ channels, respectively. In addition, the results are interpreted in the context of two-Higgs-doublet models.

Keywords: Hadron-Hadron Scattering

ArXiv ePrint: 2311.04033

Open Access, Copyright CERN,
for the benefit of the ATLAS Collaboration.
Article funded by SCOAP^3.

https://doi.org/10.1007/JHEP02(2024)197

JHEP02(2024)197

Contents

1 Introduction **1**

2 ATLAS detector **3**

3 Data and simulated event samples **4**

4 Object reconstruction **5**

5 Event selection and background estimation **7**
5.1 $\ell^+\ell^- t\bar{t}$ selection 7
5.2 $\nu\bar{\nu}b\bar{b}$ selection 9

6 Systematic uncertainties **11**

7 Statistical analysis **13**

8 Results **14**
8.1 Upper limits on the production cross-section for $A \to ZH \to \ell^+\ell^- t\bar{t}/\nu\bar{\nu}b\bar{b}$ 17
8.2 Interpretation in the context of 2HDM 18
8.3 Model-independent limits 22

9 Conclusion **23**

A Upper limits on the production cross sections for additional $\tan\beta$ values **25**

The ATLAS collaboration **37**

1 Introduction

The discovery of a Higgs boson at the Large Hadron Collider (LHC) [1, 2] raised the question of whether this particle is part of an extended scalar sector, a scenario which arises in several models that attempt to explain the shortcomings of the Standard Model (SM), such as the hierarchy problem, the excess of matter over antimatter in the observable universe and the existence of dark matter. This question has motivated experimental searches for extended scalar sectors at the LHC [3]. A simple such extension that has received a lot of attention is the two-Higgs-doublet model (2HDM) [4, 5]. The 2HDM is popular due to its very rich phenomenology and the fact that it is motivated by several new physics scenarios such as supersymmetry [6], dark matter [7, 8] and axion [9] models, electroweak baryogenesis [10] and neutrino mass models [11].

A second Higgs doublet leads to five Higgs bosons after electroweak symmetry breaking. The phenomenology depends on many parameters, including the masses of the Higgs bosons

JHEP02(2024)197

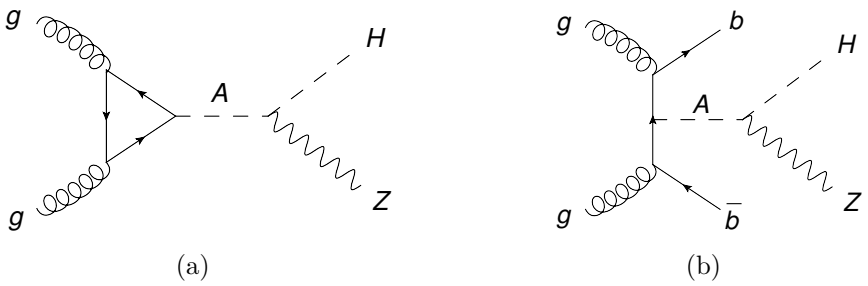

Figure 1. Feynman diagrams for the ggF (a) and bbA (b) production modes. The searches presented in this paper target final states in which the H boson decays into $t\bar{t}$ or $b\bar{b}$ and the Z boson decays into $\ell^+\ell^-$ or $\nu\bar{\nu}$.

and the parameters of the Higgs potential. Phenomenological studies often assume CP-conservation and discrete symmetries that eliminate quartic terms odd in either of the doublets [12]. This leads to two CP-even Higgs bosons, h and H, with $m_h < m_H$, one CP-odd boson, A, and two charged scalars, $H^\pm$. This model has seven free parameters, usually taken to be the masses of the Higgs bosons (m_h, m_H, m_A, $m_{H^\pm}$), the ratio of the vacuum expectation values of the two doublets ($\tan\beta$), the potential parameter (m_{12}), and the mixing angle (α) of the CP-even Higgs bosons. It is usually assumed that the h boson is the Higgs boson that was discovered at the LHC and has $m_h \simeq 125\,\text{GeV}$. In this scenario, h has the same couplings to fermions and vector bosons as the SM Higgs boson at lowest order in the limit that $\cos(\beta-\alpha)=0$, known as the alignment limit.

Precision electroweak measurements [13] suggest that the masses of two of the heavy Higgs bosons in the 2HDM are degenerate. This has motivated many LHC searches, such as for the $A \to Zh$ process [14, 15], where $m_A = m_H$ is assumed when interpreting the results. The scenario $m_A \neq m_H$ has strong motivation from electroweak baryogenesis models [16–20]; in particular, $m_A > m_H$ is favoured [17] for a strong first-order phase transition to have occurred in the early universe. The A boson mass is also constrained to be not far above 1 TeV [16, 21], whereas the h boson is required to have properties similar to those of a SM Higgs boson and hence it is compatible with the Higgs boson that was observed at the LHC [17].

In such a scenario, the most promising experimental signature is an A boson produced either via gluon-gluon fusion (ggF, figure 1(a)) or in association with b-quarks (bbA, figure 1(b)), with a subsequent decay into ZH, which dominates when the mass difference $m_A - m_H$ becomes large. The signature of the $A \to ZH$ process has been sought at the LHC in final states where the Z boson decays leptonically ($Z \to \ell^+\ell^-$) and the H boson decays into $b\bar{b}$, WW or $\tau\tau$ [22–24]. These final states, although very sensitive, cannot probe the parameter space in which $m_H > 2m_{\text{top}}$, where the $H \to t\bar{t}$ decay becomes dominant. This parameter space was probed recently with $A \to ZH$ and $H \to hh$ [25], but this decay chain is not sensitive in the alignment limit.

The first search presented in this paper aims to cover this unexplored phase space by searching for $A \to ZH$ in the $\ell^+\ell^- t\bar{t}$ final state. Top-quark pairs ($t\bar{t}$) in which one top-quark decays semileptonically and the other decays hadronically are considered. This leads to a signature with three leptons (electrons or muons) and at least four jets, two of which are expected to have originated from b-quarks.

JHEP02(2024)197

In addition, a search for $A \to ZH$ with the Z boson decaying into neutrinos and the H boson decaying into a pair of b-quarks is performed. This constitutes the first search at the LHC for $b\bar{b}$ resonances with a mass up to 2 TeV produced in association with missing transverse momentum, and complements the sensitivity of the $\ell^+\ell^- b\bar{b}$ search [22] at high m_A, due to the higher branching ratio of the Z boson decay into neutrinos [14]. Moreover, this search could also be reinterpreted in the context of hierarchical 2HDMs with extra mediators coupling to dark matter [8], thus also complementing the existing searches [26] in the high m_H regime.

2 ATLAS detector

The ATLAS detector [27] at the LHC covers nearly the entire solid angle around the collision point.[1] It consists of an inner tracking detector surrounded by a thin superconducting solenoid, electromagnetic and hadron calorimeters, and a muon spectrometer incorporating three large superconducting air-core toroidal magnets.

The inner-detector system (ID) is immersed in a 2 T axial magnetic field and provides charged-particle tracking in the range $|\eta| < 2.5$. The high-granularity silicon pixel detector covers the vertex region and typically provides four measurements per track, the first hit normally being in the insertable B-layer installed before Run 2 [28, 29]. It is followed by the silicon microstrip tracker, which usually provides eight measurements per track. These silicon detectors are complemented by the transition radiation tracker (TRT), which enables radially extended track reconstruction up to $|\eta| = 2.0$. The TRT also provides electron identification information based on the fraction of hits (typically 30 in total) above a higher energy-deposit threshold corresponding to transition radiation.

The calorimeter system covers the pseudorapidity range $|\eta| < 4.9$. Within the region $|\eta| < 3.2$, electromagnetic calorimetry is provided by barrel and endcap high-granularity lead/liquid-argon (LAr) calorimeters, with an additional thin LAr presampler covering $|\eta| < 1.8$ to correct for energy loss in material upstream of the calorimeters. Hadron calorimetry is provided by the steel/scintillator-tile calorimeter, segmented into three barrel structures within $|\eta| < 1.7$, and two copper/LAr hadron endcap calorimeters. The solid angle coverage is completed with forward copper/LAr and tungsten/LAr calorimeter modules optimised for electromagnetic and hadronic energy measurements respectively.

The muon spectrometer (MS) comprises separate trigger and high-precision tracking chambers measuring the deflection of muons in a magnetic field generated by the superconducting air-core toroidal magnets. The field integral of the toroids ranges between 2.0 and 6.0 T m across most of the detector. Three layers of precision chambers, each consisting of layers of monitored drift tubes, cover the region $|\eta| < 2.7$, complemented by cathode-strip chambers in the forward region, where the background is highest. The muon trigger system covers the range $|\eta| < 2.4$ with resistive-plate chambers in the barrel, and thin-gap chambers in the endcap regions.

[1] ATLAS uses a right-handed coordinate system with its origin at the nominal interaction point (IP) in the centre of the detector and the z-axis along the beam pipe. The x-axis points from the IP to the centre of the LHC ring, and the y-axis points upwards. Cylindrical coordinates (r, ϕ) are used in the transverse plane, ϕ being the azimuthal angle around the z-axis. The pseudorapidity is defined in terms of the polar angle θ as $\eta = -\ln\tan(\theta/2)$. Angular distance is measured in units of $\Delta R \equiv \sqrt{(\Delta\eta)^2 + (\Delta\phi)^2}$.

JHEP02(2024)197

Interesting events are selected by the first-level trigger system implemented in custom hardware, followed by selections made by algorithms implemented in software in the high-level trigger [30]. The first-level trigger accepts events from the 40 MHz bunch crossings at a rate below 100 kHz, which the high-level trigger reduces in order to record events to disk at about 1 kHz.

An extensive software suite [31] is used in data simulation, in the reconstruction and analysis of real and simulated data, in detector operations, and in the trigger and data acquisition systems of the experiment.

3 Data and simulated event samples

The search presented here uses 140 fb^{-1} of proton-proton collision data at a centre-of-mass energy ($\sqrt{s}$) of 13 TeV recorded by the ATLAS detector during the years 2015–2018 (Run 2). All events were required to pass basic data-quality requirements which ensure that all components of the ATLAS detector were functioning correctly [32].

For the analysis targeting the $\ell^+\ell^- t\bar{t}$ final state, events were recorded using a logical OR of single-electron triggers with transverse momentum (p_{T}) thresholds varying from 24 to 26 GeV or single-muon triggers with p_{T} thresholds varying from 20 to 26 GeV and a combination of quality and isolation requirements. Offline, the leptons were required to be geometrically matched to the corresponding trigger object and to have a p_{T} threshold 1–2 GeV above the high-level trigger threshold to operate in the region where the trigger reaches its maximum efficiency. For the analysis targeting the $\nu\bar{\nu}b\bar{b}$ final state, events were recorded by the missing transverse momentum ($E_{\text{T}}^{\text{miss}}$) triggers with thresholds varying between 70 and 110 GeV, which become fully efficient for an offline $E_{\text{T}}^{\text{miss}}$ value of approximately 200 GeV. The trigger efficiencies in simulation are corrected to match those observed in data. For the $E_{\text{T}}^{\text{miss}}$ triggers, this is done following the procedure in ref. [33]. Events with one or two leptons that are used to define background-enriched control regions in the $\nu\bar{\nu}b\bar{b}$ channel are selected with the same single-lepton triggers as in the $\ell^+\ell^- t\bar{t}$ channel.

Simulated signal events were generated with MadGraph5_aMC@NLO (MG5aMC) 2.3.3 [34], requiring an s-channel A boson that decays into a Z boson and H boson, and using the UFO model provided in ref. [8] to calculate the loop-induced ggF process with a finite m_{top} value.[2] Both the ggF and bbA production modes (shown in figure 1) were generated at leading order (LO) in QCD for various combinations of (m_A, m_H) using the NNPDF3.0nlo set of parton distribution functions (PDF) [35], with the former including contributions from top-quark loop-induced processes but neglecting contributions from bottom-loop induced processes, which have a negligible impact on the kinematic distributions. The ggF samples were generated at $\tan\beta = 1$ and the bbA production samples were generated at $\tan\beta = 5$. Simulated events with different values of $\tan\beta$ were obtained via matrix-element reweighting [36]. The decay widths of the A and H bosons were calculated by MG5aMC at LO and finite-width effects were included in the simulation. The decays of the Z and H bosons were simulated using MadSpin [37, 38].

[2]This UFO model contains a priori an extra CP-odd Higgs boson a that mixes with the CP-odd Higgs boson A of the 2HDM with a mixing angle $\sin\theta$. This is completely decoupled in the signal generation by setting $\sin\theta = 0$, thereby effectively yielding a 2HDM with five physical Higgs bosons.

JHEP02(2024)197

Pythia 8.244 [39] was used to model the parton shower and hadronisation, using the A14 [40] set of tuned parameters (tune). Non-resonant diagrams, in which the ZH final state is produced through a top-quark box were found to have a negligible impact and thus were not included in the simulation. The interference between the resonant diagram shown in figure 1 and the non-resonant box diagrams, and also the SM $t\bar{t}Z$ process, was studied using the UFO model provided in ref. [41] and found to be negligible. The generation of events in the $\nu\bar{\nu}b\bar{b}$ final state required $E_{\mathrm{T}}^{\mathrm{miss}} > 100\,\mathrm{GeV}$, which increased the efficiency of the simulation by improving the acceptance. Simulated events in the $\ell^+\ell^- t\bar{t}$ final state were filtered to select events with at least one top-quark decaying semileptonically, with no kinematic requirements on the generator-level leptons.

Simulated events for the background processes were generated as shown in table 1. The decays of bottom and charm hadrons were simulated using EvtGen 1.6.0 [42], except for the samples generated using Sherpa [43], in which case these decays were generated within Sherpa.

The effect of multiple interactions in the same and neighbouring bunch crossings (pile-up) in all simulated samples was modelled by overlaying each hard-scattering event with simulated inelastic proton-proton events generated with Pythia 8.186 [44] using the NNPDF2.3lo PDF set and the A3 tune [45]. The simulated events were weighted to reproduce the distribution of the average number of interactions per bunch crossing observed in the data. All generated background samples were passed through the Geant4-based [46] detector simulation [47] of the ATLAS detector. The ATLFAST-II simulation [47] was used for the signal samples. The simulated events were reconstructed in the same way as the data (see section 4).

4 Object reconstruction

Tracks measured in the ID are used to reconstruct interaction vertices [89]. The one with the highest sum of squared transverse momenta of associated tracks is selected as the primary vertex and its position is taken as the proton-proton collision point in the reconstruction of physics objects.

Electrons are reconstructed from a track matched to a cluster built from energy deposits in the calorimeter [90]. They are identified using a multivariate likelihood technique [91], using the 'loose' working point (WP) for the $\nu\bar{\nu}b\bar{b}$ channel and the 'medium' WP for the $\ell^+\ell^- t\bar{t}$ channel, and they are required to fulfil loose calorimeter isolation criteria. Electrons must have $p_{\mathrm{T}} > 7\,\mathrm{GeV}$ and $|\eta| < 2.47$. To ensure that they are compatible with the primary vertex, the track associated with the electron candidate is required to have $\sigma(d_0) < 5$ and $|z_0 \sin\theta| < 0.5$ mm, where $\sigma(d_0)$ is the significance of the transverse impact parameter, z_0 is the longitudinal impact parameter and θ is the polar angle of the track.

Muons are reconstructed by matching track segments in the MS to a track in the ID [92]. They are identified by using selections on the quality of the tracks and the compatibility of the ID and MS measurements, and they are required to satisfy the 'loose' identification WP and loose isolation criteria combining calorimeter and track information [92]. Muons are required to have $p_{\mathrm{T}} > 7\,\mathrm{GeV}$, $|\eta| < 2.5$, $\sigma(d_0) < 3$ and $|z_0 \sin\theta| < 0.5$ mm.

Hadronically decaying τ-leptons are reconstructed from calorimeter-cell energy clusters [93] formed by the anti-k_t algorithm [94, 95] with a radius parameter of $R = 0.4$.

JHEP02(2024)197

Process	Matrix element	QCD order	PDF	Parton shower	Tune	Cross-section	Special settings
$t\bar{t}$	Powheg v2 [51–54]	NLO	NNPDF3.0nlo [35]	Pythia 8.230 [39]	A14 [40]	NNLO+NNLL QCD [55–61]	$h_{\text{damp}} = 1.5 m_{\text{top}}$
tW	Powheg v2 [52–54, 62]	NLO	NNPDF3.0nlo [35]	Pythia 8.230 [39]	A14 [40]	NLO+NNLL QCD [63, 64]	DS scheme [50]
Single top t-channel	Powheg v2 [52–54, 65]	NLO	NNPDF3.0nlo [35]	Pythia 8.230 [39]	A14 [40]	NLO QCD [66, 67]	4-flavour scheme
Single top s-channel	Powheg v2 [52–54, 65]	NLO	NNPDF3.0nlo [35]	Pythia 8.230 [39]	A14 [40]	NLO QCD [66, 67]	5-flavour scheme
V+jets	Sherpa 2.2.1 [68]	0,1 jets @ NLO 2,3,4 jets @ LO	NNPDF3.0nnlo [35]	Sherpa [43]	default	NNLO [69]	MEPS@NLO [70–73]
Diboson $q\bar{q} \to VV$	Sherpa 2.2.1 [68]	0,1 jets @ NLO 2,3 jets @ LO	NNPDF3.0nnlo [35]	Sherpa [43]	default	NLO QCD	MEPS@NLO [70–73]
Diboson $gg \to VV$	Sherpa 2.2.2 [68]	0,1 jets @ LO	NNPDF3.0nnlo [35]	Sherpa [43]	default	NLO QCD	MEPS@NLO [70–73]
$q\bar{q} \to Vh$	Powheg v2 [54]	NLO	NNPDF3.0nlo [35]	Pythia 8.212 [39]	AZNLO [74]	NNLO QCD + NLO EW [77–83]	MiNLO [75, 76]
$gg \to Zh$	Powheg v2 [54]	NLO	NNPDF3.0nlo [35]	Pythia 8.212 [39]	AZNLO [74]	NLO+NLL QCD [84–86]	-
$t\bar{t}V$	MG5aMC 2.3.3 [34]	NLO	NNPDF3.0nlo [35]	Pythia 8.210 [39]	A14 [40]	NLO QCD + NLO EW [87]	$t\bar{t}\ell\ell$ scaled by $\mathcal{O}(\alpha_s^3\alpha)$ off-shell correction
$t\bar{t}H$	Powheg v2 [51–54, 88]	NLO	NNPDF3.0nlo [35]	Pythia 8.230 [39]	A14 [40]	NLO QCD + NLO EW [87]	-
tZq	MG5aMC 2.3.3 [34]	NLO	NNPDF3.0nlo [35]	Pythia 8.230 [39]	A14 [40]	NLO QCD	4-flavour scheme, off-shell effects, top decays in MadSpin [37, 38]
$t\bar{t}t\bar{t}$ $t\bar{t}\,WW$	MG5aMC 2.3.2 [34]	LO	NNPDF3.1lo [35]	Pythia 8.186 [44]	A14 [40]	LO QCD	top decays in MadSpin [37, 38]
tWZ	MG5aMC 2.6.2 [34]	LO	NNPDF3.1lo [35]	Pythia 8.235 [39]	A14 [40]	LO QCD	top decays in MadSpin [37, 38], DR scheme [50]
VVV	Sherpa 2.2.2 [68]	0 jets @ NLO 1,2 jets @ LO	NNPDF3.0nnlo [35]	Sherpa [43]	default	NLO QCD	-

Table 1. List of generators used for the simulation of different processes. (N)(N)LO or (N)NLL refers to (next-to-)(next-to-)leading order or (next-to-)next-to-leading-logarithm accuracy in the perturbative expansion of the cross-sections, while EW refers to the inclusion of electroweak corrections at the order indicated. For all samples using the A14 or AZNLO tune, the NNPDF2.3lo [48] or CTEQ6L1 [49] PDF set was used, respectively. The diagram removal (DR) and diagram subtraction (DS) schemes [50] were used to remove the overlap between the $t\bar{t}Z/tWZ$ and $t\bar{t}/tW$ processes, respectively. V denotes a W or Z boson.

Either one or three tracks must lie within a cone of size $\Delta R = 0.2$ around the direction of the hadronically decaying τ candidate, which is identified using a recurrent neural network [96] and the 'loose' WP. The τ-lepton candidates must have $p_{\text{T}} > 15\,\text{GeV}$ and $|\eta| < 2.5$, excluding the calorimeter barrel/endcap transition region ($1.37 \leq |\eta| \leq 1.52$).

Jets are reconstructed from particle-flow objects formed from ID tracks and calorimeter energy clusters [97] by using the anti-k_t algorithm with a radius parameter of $R = 0.4$. Jets with $|\eta| < 2.5$ ($2.5 < |\eta| < 4.5$) are classified as central (forward) jets and are required to have $p_{\text{T}} > 20$ (30) GeV. Central jets with $20\,\text{GeV} < p_{\text{T}} < 60\,\text{GeV}$ and $|\eta| < 2.4$ are required to pass the 'tight' jet vertex tagger (JVT) [98] WP that suppresses jets originating from pile-up interactions.

Jets containing b-hadrons, hereafter referred to as b-jets, are identified using the DL1r tagger [99]. A WP corresponding to a 77% efficiency in simulated inclusive $t\bar{t}$ events is used for

JHEP02(2024)197

the $\ell^+\ell^- t\bar{t}$ channel, while a WP corresponding to a 70% efficiency is used for the $\nu\bar{\nu}b\bar{b}$ channel. The decays of the b-hadrons can produce muons which are vetoed when building particle-flow objects and therefore are not included in the energy of the reconstructed jets. To correct for this effect, the four-momentum of the closest non-isolated muon that satisfies $\Delta R(b\text{-jet}, \mu) < \min(0.4, 0.04+10/p_{\mathrm{T}}(\mu)[\mathrm{GeV}])$ is added to the four-momentum of the b-jet. The corrected four-momentum is used when defining the event selection criteria described in the following section.

The event's missing transverse momentum, $\vec{E}_{\mathrm{T}}^{\mathrm{miss}}$ (or $E_{\mathrm{T}}^{\mathrm{miss}}$ for its modulus), is defined as the negative vector sum of the transverse momenta of all the observable electron, muon and jet objects described above, plus a soft term comprising ID tracks that are matched to the primary vertex but not to any of the already included objects [100]. An $E_{\mathrm{T}}^{\mathrm{miss}}$ significance variable ($\mathcal{S}_{\mathrm{MET}}$) which is sensitive to fake-$E_{\mathrm{T}}^{\mathrm{miss}}$ effects is defined using the expected resolutions of all objects used in the $E_{\mathrm{T}}^{\mathrm{miss}}$ reconstruction and the correlations between them [101].

An overlap removal procedure is applied to avoid any double-counting between the reconstructed leptons, including the hadronically decaying τ-leptons, and jets [33].

5 Event selection and background estimation

The final state resulting from the $A \to Z(\to \ell^+\ell^-)H(\to t\bar{t})$ signal process, where one top-quark decays semileptonically and the other decays hadronically, is expected to contain three high-p_{T} leptons, two of which should have an invariant mass close to the Z boson mass, m_Z, and a resonant $t\bar{t}$ pair. The main backgrounds expected in the $\ell^+\ell^- t\bar{t}$ channel consist of $t\bar{t}Z$ events, which have a non-resonant $m(t\bar{t})$ spectrum, and events with a jet misidentified as a lepton which mostly arise from the $t\bar{t}$ process with both top quarks decaying semileptonically.

The $A \to Z(\to \nu\bar{\nu})H(\to b\bar{b})$ signal process leads to a final state with large $E_{\mathrm{T}}^{\mathrm{miss}}$, no leptons, at least two b-jets and a resonant $m(b\bar{b})$ spectrum. The main backgrounds in the $\nu\bar{\nu}b\bar{b}$ channel arise from $Z+$heavy-flavour (denoted by Zhf)[3] and $t\bar{t}$ processes.

Differences between the signal and background processes in lepton multiplicity, flavour, charge and kinematics are exploited to define background-enriched control regions that can be used to constrain the main backgrounds, as described in the following sections.

A common preselection is applied to the $\ell^+\ell^- t\bar{t}$ and $\nu\bar{\nu}b\bar{b}$ channels to reject events without a reconstructed primary vertex or events containing jets with properties consistent with beam-induced background processes, cosmic-ray showers or noisy calorimeter cells [102]. The subsequent channel-specific selections are described in the following sections.

5.1 $\ell^+\ell^- t\bar{t}$ selection

In the $\ell^+\ell^- t\bar{t}$ channel, the dominant background consists of $t\bar{t}Z$ events, which, unlike signal events, produce a non-resonant $m(t\bar{t})$ spectrum. Another major background consists of $t\bar{t}$ events with two prompt leptons from the top-quark decays and an extra lepton which is expected to originate from b-hadron decays in 60% of cases or a jet misidentified as a lepton in

[3] Jets in simulated events are labelled as b/c-jets if a b/c-hadron with $p_{\mathrm{T}} > 5\,\mathrm{GeV}$ is found within a cone of size $\Delta R = 0.3$ around the jet axis, or as light jets (l-jets) otherwise. In the $\nu\bar{\nu}b\bar{b}$ channel the W/Z+jets events are divided according to the true flavour of the jets that constitute the Higgs boson candidate, into heavy flavour, consisting of bb, bc, bl and cc, and light flavour, consisting of cl and ll. These components are denoted in the following by Vhf and Vlf, respectively.

JHEP02(2024)197

the remaining 40% of cases. Other backgrounds arise from multi-boson events and events with a single top quark produced in association with vector bosons; these backgrounds generally have lower lepton p_{T}, a non-resonant $m(t\bar{t})$ spectrum, and can be accompanied by Z bosons. Events are therefore separated into signal (SR), control (CR) and validation (VR) regions using a combination of requirements on the following three kinematic quantities: the p_{T} of the third-highest-p_{T} lepton ($p_{\mathrm{T}}(\ell_3)$), the mass of the Z boson candidate (m_Z^{cand}) and the invariant mass of the H boson candidate (m_H^{cand}), as defined below.

Events in all regions are required to have exactly three leptons (electrons or muons), leading to the four flavour combinations eee, $ee\mu$, $\mu\mu e$, and $\mu\mu\mu$. The leptons must have $p_{\mathrm{T}} > 7\,\mathrm{GeV}$, with the highest-$p_{\mathrm{T}}$ lepton having $p_{\mathrm{T}} > 27\,\mathrm{GeV}$. Furthermore, only events with at least four jets and exactly two b-tagged jets are retained.[4] The events which do not contain any pairs of leptons with opposite-sign charges and the same flavour (OSSF), namely the $e^{\pm}e^{\pm}\mu^{\mp}$ and $\mu^{\pm}\mu^{\pm}e^{\mp}$ combinations, are selected for the same-sign (`ss`) region, which serves as the $t\bar{t}$ CR. Events with at least one OSSF lepton pair are considered further in the selection of the SR and other CRs and VRs.

The following regions are defined by requirements on $p_{\mathrm{T}}(\ell_3)$: the region with $p_{\mathrm{T}}(\ell_3) > 13\,\mathrm{GeV}$ (denoted by `L3hi`) is enriched in signal events, whereas the region with $7\,\mathrm{GeV} < p_{\mathrm{T}}(\ell_3) < 13\,\mathrm{GeV}$ (denoted by `L3lo`) is enriched in background events.

The Z candidate is defined as the OSSF lepton pair whose invariant mass is closest to m_Z [103], and only events with $|m_Z^{\mathrm{cand}} - m_Z| < 20\,\mathrm{GeV}$ are retained. Events that satisfy $|m_Z^{\mathrm{cand}} - m_Z| < 10\,\mathrm{GeV}$ define the `Zin` region, where more signal events are expected, and the remaining events define the `Zout` region. In the `ss` region, the Z candidate is reconstructed from the pair of leptons with same-sign charges and the same flavour, and only events with $|m_Z^{\mathrm{cand}} - m_Z| < 20\,\mathrm{GeV}$ are selected.

A combination of the $p_{\mathrm{T}}(\ell_3)$ and m_Z^{cand} requirements allows the definition of several regions, enriched in either signal or background events. The signal events generally populate the `L3hi_Zin` region. Two signal-depleted regions are also defined: `L3lo_Zin`, with roughly equal contributions from Zhf, $t\bar{t}$ and $t\bar{t}Z$ background processes, and `L3hi_Zout`, with a relatively large contribution from $t\bar{t}$ and $t\bar{t}Z$ background processes. These signal-depleted regions cannot be used as CRs to simultaneously constrain the normalisation of the Zhf, $t\bar{t}$ and $t\bar{t}Z$ backgrounds because they receive fairly similar background contributions and have a limited number of events. They are therefore only used as VRs to verify that the fit model (described in section 7) can describe the data in regions that are kinematically close to the SR.

The semileptonically decaying top-quark candidate (t_{lep}) is reconstructed from the lepton that is not used in the reconstruction of the Z candidate, the b-jet which is the closest in ΔR to this lepton, and $\vec{E}_{\mathrm{T}}^{\mathrm{miss}}$. To improve the resolution in $m_{t_{\mathrm{lep}}}$, the longitudinal-momentum component of the neutrino from the t_{lep} decay is calculated by constraining the mass of the lepton-neutrino system to be equal to the W boson mass, m_W.[5] The hadronically decaying top-quark candidate (t_{had}) is reconstructed from the light-jet pair with mass m_{jj} closest to m_W and the b-jet that is not used in the t_{lep} reconstruction. To improve the resolution in

[4] For the bbA production mode, it was found that the majority of events with three or more b-jets ($\gtrsim 60\%$) are reconstructed in the 2-b-tag region, since the additional b-jets are soft and forward.

[5] In the resulting quadratic equation, the neutrino p_z is taken from the real component in the case of complex solutions or the smaller component of the two solutions if both solutions are real.

JHEP02(2024)197

$m_{t_{\text{had}}}$, the four-momenta of the light-jet pair that constitutes the hadronic W candidate are rescaled by m_W/m_{jj}.

The H candidate is defined as the sum of the four-momenta of t_{lep} and t_{had}, while the A candidate is reconstructed as the sum of the four-momenta of the H candidate and the Z candidate. The fact that the H and Z candidates for signal events are produced by the decay of a resonance constrains the kinematic properties of these candidates; the constraints depend on the m_A and m_H values of the signal hypothesis. In particular, the H candidate is expected to be produced more centrally than background events. It is found that requiring the pseudorapidity of the H candidate in the rest frame of the A candidate to satisfy $\left|\eta^{ZH\text{-r.fr.}}_{H\text{-cand}}\right| < 2.2 + 0.0004 \cdot m(t\bar{t})$ [GeV] $- 0.0011 \cdot m(\ell^+\ell^- t\bar{t})$ [GeV] provides the optimal sensitivity across the whole (m_A, m_H) plane. The parameters of the linear function defining this requirement are determined by a fit to the values of the $\left|\eta^{ZH\text{-r.fr.}}_{H\text{-cand}}\right|$ cut that maximise the expected significance for each (m_A, m_H) hypothesis.

The presence of a signal would manifest itself as a resonance in the $m(t\bar{t})$ and $m(\ell^+\ell^- t\bar{t})$ distributions, as well as in the distribution of the mass difference $\Delta m = m(\ell^+\ell^- t\bar{t}) - m(t\bar{t})$ [41]. The region that is expected to contain most of the signal events for a given mass hypothesis m_H is constructed using a sliding window defined by the condition $|m(t\bar{t}) - m_H| < N \cdot \sigma$, where $\sigma \approx 0.16 \cdot m_H$ is the resolution in $m(t\bar{t})$ and $N = 2$ (1.5) for $m_H < (\geq) 500\,\text{GeV}$, and this region is referred to as the `Hin` SR. The sideband regions with a lower or higher $m(t\bar{t})$ value define the `Hlo` and `Hhi` CRs, which are used to constrain the normalisation of the simulated $t\bar{t}Z$ sample. The N factor, which defines the width of the signal region, is optimised to achieve the highest signal significance.

The four-momentum vector of the H candidate is rescaled by $m_H/m(t\bar{t})$ to improve the resolution in $m(\ell^+\ell^- t\bar{t})$. The rescaling is performed only in the SR, where the resonance is expected, and is applied to both the simulated events and data events. After this rescaling, the resolution in $m(\ell^+\ell^- t\bar{t})$ improves by as much as a factor of three, particularly for signal hypotheses with small $m_A - m_H$ values, and ranges from 3% to 20% for small and large $m_A - m_H$ values, respectively.

The fraction of signal events passing the full event selection varies from 2% to 3.5%, depending on the mass hypothesis, and the fraction increases slightly with increasing m_H.

A summary of the selection criteria that define the different regions considered in the statistical analysis is given in table 2.

5.2 $\nu\bar{\nu}b\bar{b}$ selection

In the $\nu\bar{\nu}b\bar{b}$ channel, the events are split into regions with different lepton multiplicities. The signal is expected to manifest in the region with no leptons. A region consisting of exactly two leptons of the same flavour (`2L`),[6] enriched in Zhf events, and a region with one electron and one muon (`e`μ), enriched in $t\bar{t}$ events, are used to constrain the corresponding background normalisations. Finally, a region with exactly one lepton (`1L`) is used as a VR. The SR, CR

[6] In principle, the `2L` region could also contain signal from the $A \to ZH \to \ell^+\ell^- b\bar{b}$ process. Based on the constraints on the cross-section for this process derived in ref. [22] and given that the `2L` region is included in the statistical analysis as a single bin (see section 7) it has been estimated that the impact of such a signal contamination in the `2L` control region would be smaller than 3%, with a negligible impact on the analysis, and is therefore neglected.

JHEP02(2024)197

Requirement	Regions				
	ss (CR)	L3hi__Zout (VR)	L3hi__Zin		L3lo__Zin (VR)
			Hlo / Hhi (CR)	Hin (SR)	
Number of leptons	3				
$p_{\mathrm{T}}(\ell_1)$	$> 27\,\mathrm{GeV}$				
Number of jets	≥ 4				
Number of b-jets	2				
$\left\lvert\eta^{ZH\text{-r.fr.}}_{H\text{-cand}}\right\rvert$	$< 2.2 + 0.0004 \cdot m(t\bar{t})[\mathrm{GeV}] - 0.0011 \cdot m(\ell^+\ell^- t\bar{t})[\mathrm{GeV}]$				
$p_{\mathrm{T}}(\ell_3)$	$> 13\,\mathrm{GeV}$				$> 7\,\mathrm{GeV}$ & $< 13\,\mathrm{GeV}$
Lepton flavour	$ee\mu/\mu\mu e$	$eee/ee\mu/\mu\mu e/\mu\mu\mu$			
OSSF lepton pairs	0	≥ 1			
$\lvert m_Z^{\mathrm{cand}} - m_Z\rvert$	$< 20\,\mathrm{GeV}$	$> 10\,\mathrm{GeV}$ & $< 20\,\mathrm{GeV}$	$< 10\,\mathrm{GeV}$		
$\lvert m(t\bar{t}) - m_H\rvert$ $m_H < 500\,\mathrm{GeV}$	-		$> 0.32 \cdot m_H$	$< 0.32 \cdot m_H$	-
$m_H \geq 500\,\mathrm{GeV}$			$> 0.24 \cdot m_H$	$< 0.24 \cdot m_H$	

Table 2. Event selection for the $\ell^+\ell^- t\bar{t}$ channel. The SR, CR and VR symbols next to the region name indicate that this region is used as a signal, control or validation region in the fit, respectively.

and VR regions are further divided into regions with exactly two and at least three b-jets, which target the ggF and bbA production modes, respectively.

In events with at least one lepton, the highest-p_{T} lepton is required to have $p_{\mathrm{T}}(\ell_1) > 27\,\mathrm{GeV}$. Events in all regions are required to have $p_{\mathrm{T}}(V) > 150\,\mathrm{GeV}$ (V denotes a Z or W boson), where $p_{\mathrm{T}}(V) = E_{\mathrm{T}}^{\mathrm{miss}}$ in the region with no leptons, $p_{\mathrm{T}}(V) = |\vec{p_{\mathrm{T}}}(\ell) + \vec{E}_{\mathrm{T}}^{\mathrm{miss}}|$ in the 1L region and $p_{\mathrm{T}}(V) = |\vec{p_{\mathrm{T}}}(\ell_1) + \vec{p_{\mathrm{T}}}(\ell_2)|$ in the 2L and eμ regions. Events are also required to have at least two b-jets. A veto on events with more than five jets or events containing any hadronically decaying τ-lepton (τ^{had}) candidates is applied to suppress the $t\bar{t}$ background.

To suppress the background from multi-jet events, only events in which the smallest azimuthal angle between $\vec{E}_{\mathrm{T}}^{\mathrm{miss}}$ and any jet, $\min_i \Delta\phi(\vec{E}_{\mathrm{T}}^{\mathrm{miss}}, \vec{p}_i^{\mathrm{jet}})$, is larger than $\pi/10$ are selected. This background is further suppressed by selecting events with $\mathcal{S}_{\mathrm{MET}} > 3$ ($\mathcal{S}_{\mathrm{MET}} > 10$) in the region with one (zero) lepton(s). These selection criteria are found to reduce the multi-jet contamination to a negligible level. In contrast, a selection $\mathcal{S}_{\mathrm{MET}} < 5$ is applied in the 2L region to reduce the contamination from the $t\bar{t}$ background and maximise the purity in the Zhf background in this CR. The purity of the Zhf background in the 2L region is further increased by retaining only events that satisfy $|m_Z^{\mathrm{cand}} - m_Z| < 10\,\mathrm{GeV}$.

The H candidate is reconstructed from the two highest-p_{T} b-jets and only events with $m(b\bar{b}) > 50\,\mathrm{GeV}$ are retained. The ΔR between the b-jets forming the H candidate is required to be smaller than 3.3 (3.5) for events with exactly two (at least three) b-jets.

To further suppress the $t\bar{t}$ background in events with no leptons, two top-quark-mass proxy variables are defined as follows [26]:

$$m_{\mathrm{top}}^{\mathrm{near/far}} = \sqrt{2 p_{\mathrm{T},b_{\mathrm{near/far}}} E_{\mathrm{T}}^{\mathrm{miss}} \left[1 - \cos\Delta\phi\left(\vec{p}_{\mathrm{T},b_{\mathrm{near/far}}}, \vec{E}_{\mathrm{T}}^{\mathrm{miss}}\right)\right]},$$

where near (far) refers to the H candidate's b-jet that is nearer to (farther from) the $\vec{E}_{\mathrm{T}}^{\mathrm{miss}}$ in azimuthal angle. The b-jet closer to $\vec{E}_{\mathrm{T}}^{\mathrm{miss}}$ in azimuthal angle is used for the calculation of $m_{\mathrm{top}}^{\mathrm{near}}$, whereas the b-jet farther from $\vec{E}_{\mathrm{T}}^{\mathrm{miss}}$ is used for $m_{\mathrm{top}}^{\mathrm{far}}$. Events are retained only if $m_{\mathrm{top}}^{\mathrm{near}} > 180\,\mathrm{GeV}$ and $m_{\mathrm{top}}^{\mathrm{far}} > 200\,\mathrm{GeV}$.

JHEP02(2024)197

Requirement	Regions				
	2L (CR)	eμ (CR)	1L (VR)	0L	
				Hlo / Hhi (CR)	Hin (SR)
Number of jets	2–5				
Number of b-jets	≥ 2				
$m(b\bar{b})$	$> 50\,\text{GeV}$				
Number of τ^{had}	0				
$p_{\text{T}}(V)$	$> 150\,\text{GeV}$				
$\min_i \Delta\phi(\vec{E}_{\text{T}}^{\text{miss}}, \vec{p}_i^{\text{jet}})$	$> \pi/10$				
$\Delta R(b_1, b_2)$	< 3.3 (2 b-jets) < 3.5 (≥ 3 b-jets)				
Number of leptons	2		1	0	
Lepton flavour	$ee/\mu\mu$	$e\mu$	e/μ	—	
$p_{\text{T}}(\ell_1)$	$> 27\,\text{GeV}$			—	
$\lvert m_Z^{\text{cand}} - m_Z \rvert$	$< 10\,\text{GeV}$	—			
$\mathcal{S}_{\text{MET}}$	< 5	—	> 3	> 10	
$m_{\text{top}}^{\text{near}}$	—			$> 180\,\text{GeV}$	
$m_{\text{top}}^{\text{far}}$	—			$> 200\,\text{GeV}$	
$\lvert m(b\bar{b}) - m_H \rvert$	—			$> 0.2 \cdot m_H$	$< 0.2 \cdot m_H$

Table 3. Event selection for the $\nu\bar{\nu}b\bar{b}$ channel. The SR, CR and VR symbols next to the region name indicate that this region is used as a signal, control or validation region in the fit, respectively.

The presence of a signal would manifest as a broad resonance in the distribution of the A candidate transverse mass ($m_{\text{T}}(VH)$) in the final state with no leptons. The region which is expected to contain most of the signal events for a given mass hypothesis m_H is constructed using a sliding window defined by the condition $|m(b\bar{b}) - m_H| < 2 \cdot \sigma$, where $\sigma = 0.1 \cdot m_H$ is the resolution in $m(b\bar{b})$. The adjacent regions with a lower or higher $m(b\bar{b})$ define the Hlo and Hhi regions, which are used as CRs in the statistical analysis. The Hlo and Hhi regions contain events from a mix of background processes, so they constrain all the background processes present there, rather than a specific one.

The four-momentum vector of the H candidate is rescaled by $m_H/m(b\bar{b})$ to improve the resolution in $m_{\text{T}}(VH)$. The rescaling is performed only in the SR, where the resonance is expected, and is applied to both the simulated events and data events. The resolution in $m_{\text{T}}(VH)$ after this rescaling ranges from 8% for signal hypotheses with high m_H and low $m_A - m_H$ values, to 27% for signal hypotheses with low m_H and high $m_A - m_H$ values.

The fraction of signal events passing the full event selection varies from less than 1% for signal events with low $m_A - m_H$, which also have low $E_{\text{T}}^{\text{miss}}$, to about 21% for signal events with high $m_A - m_H$.

A summary of the selection requirements applied in the SR, VRs and CRs is shown in table 3.

6 Systematic uncertainties

Experimental uncertainties from detector effects and theoretical uncertainties related to the modelling of the simulated signal and background processes affect the normalisation and

JHEP02(2024)197

shape of the final discriminating variable (see section 7) as well as the relative normalisation of events in the SR and CRs.

Uncertainties arising from the calibration of the jet energy scale and resolution are derived as functions of the jet p_{T} and η [104]. Uncertainties arising from the identification of b-jets are derived in refs. [99, 105, 106]. Uncertainties related to the reconstruction and identification of leptons are derived in refs. [90, 92]. Uncertainties in the reconstruction of $E_{\mathrm{T}}^{\mathrm{miss}}$ are taken into account as described in ref. [107]. The number of pile-up collisions in simulation is reweighted to match the data and a 4% variation of this reweighting factor is assigned as an uncertainty. The uncertainty in the total integrated luminosity is 0.83% [108], obtained using the LUCID-2 detector [109] for the primary luminosity measurements.

For the V+jets and diboson processes, uncertainties are estimated by comparing the nominal Sherpa samples with alternative samples simulated with MG5aMC 2.2.2 interfaced to Pythia 8.186 and including up to four jets in the matrix element calculated at LO accuracy in QCD. Uncertainties related to multi-jet merging and resummation are calculated by varying the associated scales in Sherpa.

For the $t\bar{t}Z$ process, the uncertainty related to the modelling of the parton shower is obtained by comparing the nominal sample with a sample simulated with MG5aMC 2.3.3 interfaced to Herwig 7.13 [110]. An additional uncertainty related to the modelling of initial- and final-state radiation is obtained using the associated eigentune of the A14 tune [40].

For the $t\bar{t}$ process, an uncertainty related to the NLO matching is obtained by comparing the nominal sample with a sample simulated with MG5aMC 2.6.0 interfaced to Pythia 8.230, while the parton shower uncertainty is obtained by comparison with a sample simulated with Powheg+Herwig 7.04 [111, 112]. The initial- and final-state radiation uncertainties are obtained by varying the renormalisation scale in the initial- and final-state emissions by a factor of two. The downward variation of the renormalisation scale in initial-state emissions is accompanied by an upward variation of the h_{damp} parameter by a factor of two.

For the tW process, an additional uncertainty related to the removal of the overlap with the $t\bar{t}$ process is obtained by comparing the nominal sample evaluated using the diagram subtraction technique with a sample which uses the diagram removal technique.

For all simulated samples, the uncertainties due to missing higher orders in QCD are estimated by independent variations of the renormalisation and factorisation scales by a factor of two, while the PDF and α_{s} uncertainties are calculated using the PDF4LHC prescription [113].

Systematic uncertainties for background processes that contribute less than 1% to the total background are neglected.

Statistical uncertainties are dominant in the $\ell^+\ell^- t\bar{t}$ channel for all (m_A, m_H) hypotheses, while in the $\nu\bar{\nu}b\bar{b}$ analysis the systematic uncertainties dominate. The dominant systematic uncertainties in the $\nu\bar{\nu}b\bar{b}$ channel are related to the modelling of the Zhf and Whf background processes as well as to the jet energy scale and resolution.

The relative contributions from the different sources of uncertainty for representative (m_A, m_H) hypotheses in the two channels are shown in table 4. The fractional impact is calculated by considering the square of the uncertainty in the signal strength parameter (μ) arising from a group of uncertainties (as listed in the left column of the table), divided by

JHEP02(2024)197

Source of uncertainty	Fractional squared uncertainty in μ				
	$\ell^+\ell^- t\bar{t}$ signals (m_A, m_H) [GeV]		$\nu\bar{\nu}b\bar{b}$ signals (m_A, m_H) [GeV]		
	(700, 500)	(1200, 800)	(400, 130)	(700, 300)	(1200, 800)
Total statistical uncertainty	0.91	0.90	0.19	0.27	0.48
Total systematic uncertainty	0.09	0.10	0.81	0.73	0.52
Statistical uncertainties					
Data statistics	0.40	0.72	0.16	0.24	0.48
$t\bar{t}Z$ normalisation	0.36	0.14		neglected	
Zhf normalisation	not free to float, included in 'Other'		0.01	0.05	0.12
$t\bar{t}$ normalisation	0.01	0.02	0.06	0.01	0.01
Systematic uncertainties					
Jets	0.02	0.01	0.15	0.10	0.10
b-tagging	< 0.01	< 0.01	0.02	< 0.01	0.05
$E_{\mathrm{T}}^{\mathrm{miss}}$ soft-term and pile-up	< 0.01	< 0.01	0.01	0.01	< 0.01
Luminosity	< 0.01	< 0.01	< 0.01	< 0.01	< 0.01
Other experimental sources	< 0.01	< 0.01	< 0.01	< 0.01	< 0.01
$t\bar{t}Z$ modelling	0.03	0.05		not applied	
$t\bar{t}$ modelling	0.01	0.02	0.05	0.01	0.01
Zhf modelling	included in 'Other'		0.21	0.47	0.30
Whf modelling	neglected		0.14	0.04	0.10
tW modelling	neglected		0.02	0.03	< 0.01
Other modelling sources	0.01	0.02	0.08	0.01	< 0.01
Signal modelling	< 0.01	< 0.01	< 0.01	< 0.01	< 0.01
MC sample size	0.01	0.01	0.05	0.05	0.05

Table 4. Fractional squared uncertainty in μ from the different sources of uncertainty for different (m_A, m_H) values in the $\ell^+\ell^- t\bar{t}$ and $\nu\bar{\nu}b\bar{b}$ channels.

the square of the total uncertainty in μ. The value of μ used is determined by the fit to data. Due to correlations, the sum of the impacts of different systematic uncertainties may not be equal to the total impact of all systematic uncertainties. Statistical uncertainties include the uncertainties due to the size of the data sample and the uncertainties associated with the background process normalisations which are free to float in the fit. The row "MC sample size" refers to the systematic uncertainty due to the finite number of generated events in the simulation.

7 Statistical analysis

To extract the final result of the search presented here, a binned profile likelihood fit [114] to the data is used. The likelihood function $\mathcal{L}(\mu, \theta)$ is constructed from a product of Poisson probabilities $\mathrm{Pois}(N_{\mathrm{obs}}|\mu s+b)$ for observing N_{obs} data events when μs signal and b background events are expected in each bin of the fitted distribution. It contains the parameter-of-interest μ, which is a factor multiplying the nominal signal cross-section and is extracted by maximising the likelihood. Background processes whose event yields are constrained using data have freely floating normalisations in the likelihood function (see table 4). The uncertainties due to the limited number of simulated background events are incorporated in the likelihood as

JHEP02(2024)197

nuisance parameters (NP) using Poisson probability density functions following a simplified version of the Beeston-Barlow technique [115].

The rest of the systematic uncertainties are incorporated in the fit as NP, constrained using Gaussian probability density functions. These include (i) the NP corresponding to the normalisation uncertainty in the measured phase space, added for each background sample whose normalisation is not left to float freely in the fit, (ii) the NP corresponding to the uncertainty in the acceptance difference between the different regions considered in the fit and (iii) the NP corresponding to the uncertainty in the distribution shape of the fitted final discriminating variable.

In the $\ell^+\ell^- t\bar{t}$ channel, the normalisation of the $t\bar{t}$ background is constrained by using the `ss` region, and the normalisation of the $t\bar{t}Z$ background is constrained by using the `Hlo` and `Hhi` regions, so these normalisations are allowed to float freely in the fit. A simultaneous fit is performed to the data yields in the `ss`, `Hlo` and `Hhi` CRs and to the Δm distribution in the `Hin` SR, which is the final discriminating variable for this channel.

In the $\nu\bar{\nu}b\bar{b}$ channel, the normalisations of the $t\bar{t}$ and Zhf background processes are allowed to float freely in the likelihood function, since they are constrained by using the `e`μ and `2L` regions, respectively. Due to a known mismodelling of Zhf events [14, 26, 33], which is expected to be more severe in the $\geq$ 3-b-tag region, two decorrelated normalisation factors are used for the Zhf background in the 2-b-tag and $\geq$ 3-b-tag regions. The $t\bar{t}$ events populating the $\geq$ 3-b-tag region can arise either from events with at least three real b-jets, via $t\bar{t} + (g \to b\bar{b})$, or from the misidentification of a c-jet originating from a W boson produced in the top-quark decays. The contributions of the two processes depend on $m(b\bar{b})$, with the former dominating in the high $m(b\bar{b})$ region. To account for the different underlying processes, two decorrelated normalisation factors are applied to the $t\bar{t}$ background in the 2-b-tag and $\geq$ 3-b-tag regions. A simultaneous fit of the $m_{\mathrm{T}}(VH)$ distribution, which is the final discriminating variable for this channel, is performed in the `2L`, `e`μ, `Hlo` and `Hhi` CRs and the `Hin` SR including both the 2-b-tag and $\geq$ 3-b-tag regions. Eight bins of the $m_{\mathrm{T}}(VH)$ distribution are used in the `2L` 2-b-tag region, but only two bins in the `e`μ region and a single bin in the `2L` $\geq$ 3-b-tag, `Hlo` and `Hhi` regions.

Since a large number of events satisfy the selection criteria, both the significance of any excess and the upper limits are calculated in the asymptotic approximation [114]. Upper limits on μ are extracted using the profile-likelihood test statistic and the $\mathrm{CL_s}$ prescription [116] by performing fits for multiple (m_A, m_H) values. All upper limits mentioned in section 8 correspond to a confidence level (CL) of 95%.

8 Results

No significant deviation from the background-only hypothesis is observed in the likelihood fits. The largest excess over the SM background prediction, amounting to a local significance of $2.85\,\sigma$, is observed in the $\ell^+\ell^- t\bar{t}$ channel, for the signal hypothesis corresponding to $(m_A, m_H) = (650, 450)\,\mathrm{GeV}$. The global significance for the $\ell^+\ell^- t\bar{t}$ channel is estimated following refs. [117, 118] to be $2.35\,\sigma$.

The yields and post-fit distributions presented here are obtained from background-only fits to the data in the SR and CRs. The constraints from these fits are also applied to the

JHEP02(2024)197

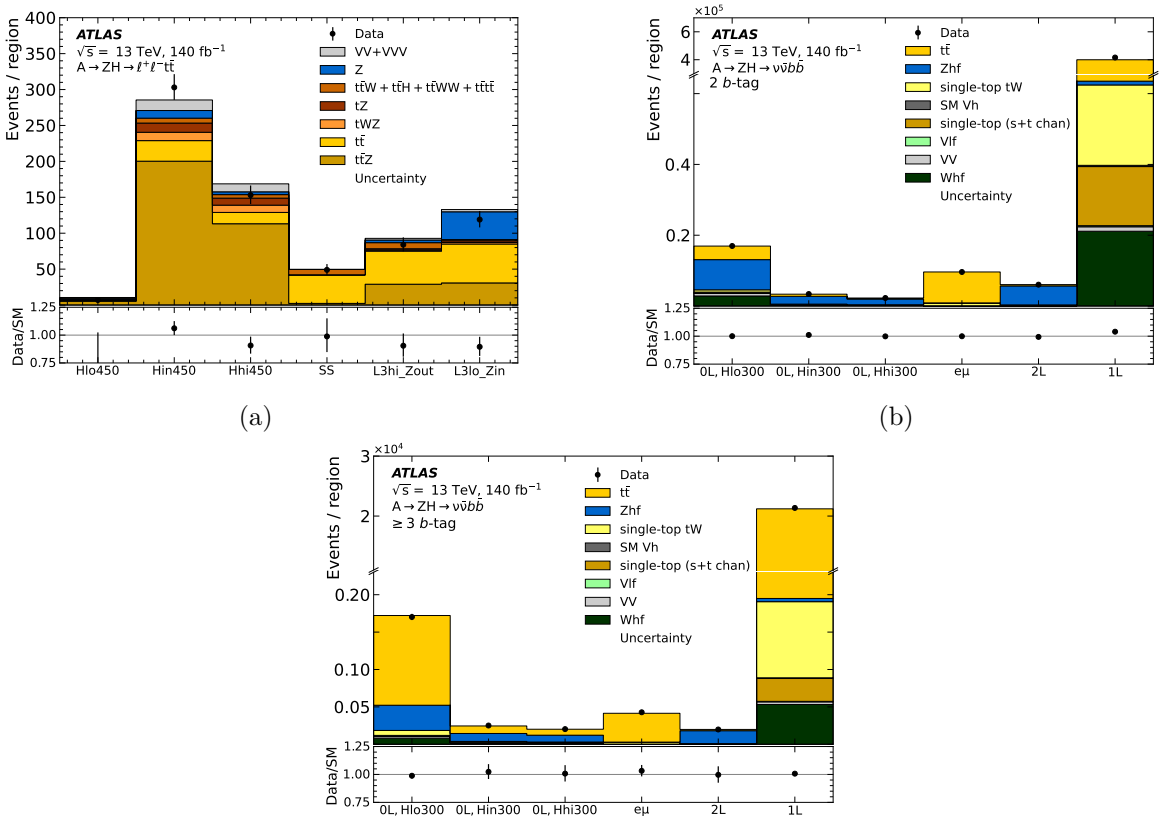

Figure 2. Yields in the SR, CRs and VRs used in the $\ell^+\ell^- t\bar{t}$ channel (a) and in the 2-b-tag (b) and $\geq$ 3-b-tag (c) regions of the $\nu\bar{\nu}b\bar{b}$ channel. The yields are obtained from a background-only fit to data. The region names are defined in tables 2 and 3. The value next to the region name refers to the m_H hypothesis. The data are represented as black points and the associated error bars represent the statistical uncertainty. The hatched band indicates the combined statistical and systematic uncertainty for the sum of backgrounds.

VRs to gauge whether the fit can describe the data in regions that are kinematically close to the SR and CRs but are not included in the fits. Representative yields in the SR, CRs and VRs are shown in figure 2 and tables 5, 6 and 7. Representative distributions of the fit discriminant and the mass of the H candidate in the SR are shown in figures 3 and 4.

The normalisation factors in the $\ell^+\ell^- t\bar{t}$ channel are found to be compatible with unity for the $t\bar{t}Z$ background, while for the $t\bar{t}$ background they range from 1.5 to 1.8 for the different m_H hypotheses with an uncertainty of 0.5. The $t\bar{t}$ normalisation factor is higher than unity due to mismodelling of $t\bar{t}$ events with a non-prompt or misidentified lepton; this has been verified with a data-driven method. In the $\nu\bar{\nu}b\bar{b}$ channel, the normalisation factors for the $t\bar{t}$ background are compatible with unity, while for the Zhf background they are in the range 1.2–1.3 with an uncertainty of 0.1 in the 2-b-tag region and in the range 1.4–1.7 with an uncertainty of 0.2 in the $\geq$ 3-b-tag regions. The Zhf normalisation factors are higher than unity due to mismodelling of the Zhf process in Sherpa [14, 26, 33]. In the $\ell^+\ell^- t\bar{t}$ channel, the $t\bar{t}$ template corresponds to $t\bar{t}$ events with two prompt leptons and one non-prompt or

JHEP02(2024)197

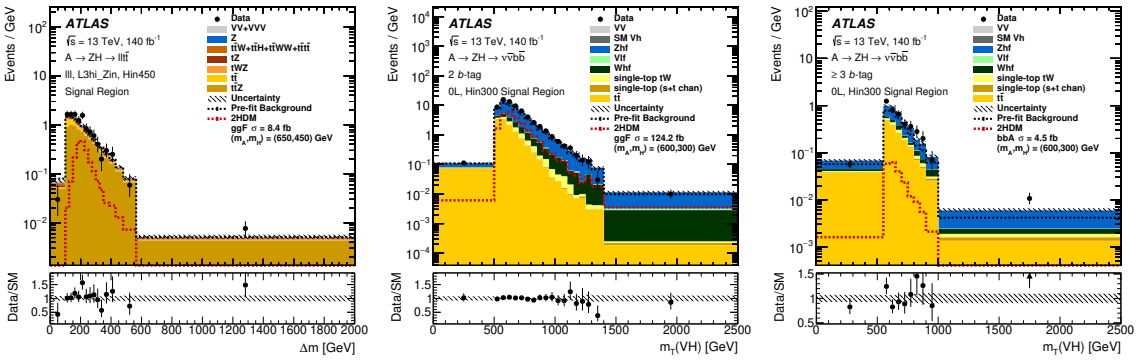

(a) (b) (c)

Figure 3. The distribution of the fit discriminant $\Delta m = m(\ell^+\ell^- t\bar{t}) - m(t\bar{t})$ in the SR of the $\ell^+\ell^- t\bar{t}$ channel for the $m_H = 450\,\text{GeV}$ hypothesis (a). The distribution of the fit discriminant $m_\text{T}(VH)$ in the SR of the $\nu\bar{\nu}b\bar{b}$ channel in the 2-b-tag (b) and $\geq$ 3-b-tag (c) region, for the $m_H = 300\,\text{GeV}$ hypothesis. The background yields are obtained from a background-only fit to data. Signal distributions corresponding to ggF or bbA production normalised to the theory cross-section are shown for comparison. The data are represented as black points and the associated error bars represent the statistical uncertainty. The hatched band indicates the combined statistical and systematic uncertainty for the sum of backgrounds. The quantity on the vertical axis is the number of events divided by the bin width in GeV.

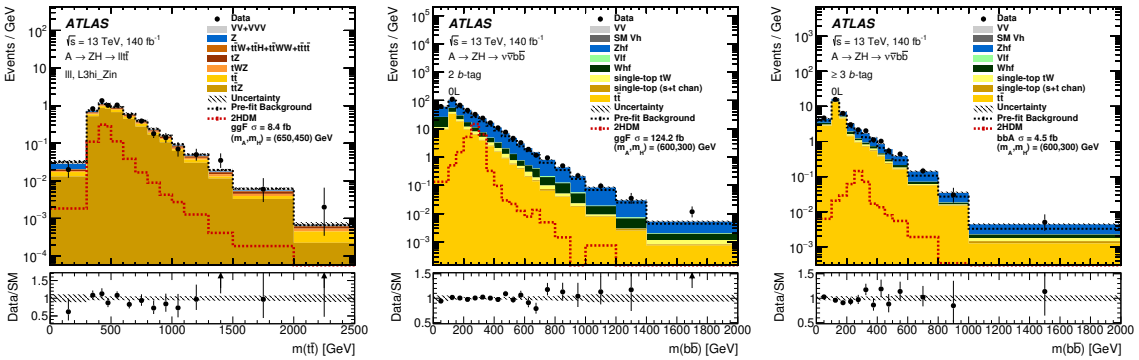

(a) (b) (c)

Figure 4. The $m(t\bar{t})$ distribution in the `L3hi_Zin` region of the $\ell^+\ell^- t\bar{t}$ channel (a) and the $m(b\bar{b})$ distribution in the $\nu\bar{\nu}b\bar{b}$ channel in the 2-b-tag (b) and $\geq$ 3-b-tag (c) `0L` region. The background yields are obtained from a background-only fit to data. Signal distributions corresponding to ggF or bbA production normalised to the theory cross-section are shown for comparison. The data are represented as black points and the associated error bars represent the statistical uncertainty. The hatched band indicates the combined statistical and systematic uncertainty for the sum of backgrounds. The quantity on the vertical axis is the number of events divided by the bin width in GeV.

JHEP02(2024)197

	L3hi_Zin				(VR)	(VR)
	Hlo450 (CR)	Hin450 (SR)	Hhi450 (CR)	ss (CR)	L3hi_Zout	L3lo_Zin
$t\bar{t}Z$	5.1 ± 0.9	200 ± 22	113 ± 13	2.3 ± 0.6	29.0 ± 3.2	30.8 ± 3.4
$t\bar{t}$	1.2 ± 0.8	29 ± 9	16 ± 6	40 ± 7	46 ± 14	54 ± 17
tWZ	0.40 ± 0.14	12 ± 4	10 ± 4	0.13 ± 0.04	1.6 ± 0.5	2.2 ± 0.7
tZq	0.6 ± 0.4	13 ± 8	10 ± 6	0.046 ± 0.032	1.8 ± 1.2	2.4 ± 1.6
VV+VVV	1.5 ± 0.5	15 ± 4	11.1 ± 3.5	0.034 ± 0.013	2.3 ± 0.6	3.1 ± 0.9
Z	1.5 ± 1.1	11 ± 4	3.9 ± 1.6	0.025 ± 0.010	3.7 ± 1.4	39 ± 15
$t\bar{t}W$+$t\bar{t}H$+$t\bar{t}WW$+$t\bar{t}t\bar{t}$	0.16 ± 0.05	6.8 ± 0.9	4.9 ± 0.9	7.4 ± 1.8	8.4 ± 1.8	1.63 ± 0.27
Total background	10.5 ± 1.5	285 ± 15	169 ± 10	50 ± 7	93 ± 13	133 ± 21
Data	7	303	153	49	84	119

Table 5. Yields in the $\ell^+\ell^- t\bar{t}$ channel obtained from the background-only fit to data using Hin450 as the signal region. The indicated uncertainties include statistical and systematic components. The value next to the region name refers to the m_H hypothesis.

	0L					
	Hlo300 (CR)	Hin300 (SR)	Hhi300 (CR)	2L (CR)	eμ (CR)	1L (VR)
$t\bar{t}$	3800 ± 400	600 ± 80	290 ± 40	370 ± 60	8700 ± 500	336000 ± 28000
Single-top (s-, t-chan)	93 ± 18	26 ± 4	16.7 ± 3.1	0.70 ± 0.15	12.4 ± 0.7	16700 ± 1100
Single-top tW	600 ± 400	160 ± 90	90 ± 60	43 ± 23	800 ± 500	23000 ± 12000
Whf	2800 ± 900	330 ± 100	230 ± 70	2.8 ± 1.0	29 ± 9	21000 ± 7000
Zhf	8500 ± 900	2200 ± 120	1620 ± 90	5370 ± 120	18.1 ± 1.3	1070 ± 90
Vlf	44 ± 8	10.8 ± 1.7	12.3 ± 2.3	23 ± 5	0.35 ± 0.08	330 ± 60
$VHbb$	210 ± 130	0.8 ± 0.5	0.48 ± 0.31	60 ± 40	0.37 ± 0.23	350 ± 220
VV	770 ± 150	15.4 ± 1.7	12.3 ± 1.6	207 ± 24	1.63 ± 0.20	1260 ± 140
Total background	16960 ± 170	3350 ± 50	2270 ± 50	6080 ± 90	9620 ± 110	400000 ± 26000
Data	16961	3389	2266	6037	9618	415808

Table 6. Yields in the 2-b-tag regions of the $\nu\bar{\nu}b\bar{b}$ channel obtained from the background-only fit to data using Hin300 as the signal region. The indicated uncertainties include statistical and systematic components. The value next to the region name refers to the m_H hypothesis.

misidentified lepton, while in the $\nu\bar{\nu}b\bar{b}$ channel it corresponds to $t\bar{t}$ events with two prompt leptons, so the two normalisation factors obtained above are not comparable.

8.1 Upper limits on the production cross-section for $A \to ZH \to \ell^+\ell^- t\bar{t}/\nu\bar{\nu}b\bar{b}$

Upper limits on the production cross-section for the A boson times the decay branching ratios, $B(A \to ZH) \times B(H \to t\bar{t})$ in the $\ell^+\ell^- t\bar{t}$ channel and $B(A \to ZH) \times B(H \to b\bar{b})$ in the $\nu\bar{\nu}b\bar{b}$ channel, are derived for the ggF and bbA production modes and are shown in figures 5 and 6. While the limits generally depend on the natural width of the A and H bosons, for the parameter space that is relevant for this search only the width of the A boson matters, with the width of the H boson always being very small compared to the experimental resolution. The width of the A boson increases as $m_A - m_H$ increases and is roughly independent of $\tan\beta$ for $\tan\beta \gtrsim 5$ but becomes larger for smaller values of $\tan\beta$ (i.e. $\tan\beta \lesssim 5$). This implies that the limits provided in figures 5 and 6 for $\tan\beta = 10$ are generally applicable for $\tan\beta \gtrsim 5$, while the limits provided for $\tan\beta = 1$ are not applicable for other $\tan\beta$ values. Upper limits

JHEP02(2024)197

	0L					
	Hlo300 (CR)	Hin300 (SR)	Hhi300 (CR)	2L (CR)	eμ (CR)	1L (VR)
$t\bar{t}$	1200 ± 70	101 ± 8	80 ± 9	16.9 ± 3.1	385 ± 26	19300 ± 1400
Single-top (s-, t-chan)	11.0 ± 1.2	3.9 ± 0.5	4.0 ± 0.4	—	0.28 ± 0.10	310 ± 27
Single-top tW	70 ± 50	13 ± 8	8 ± 7	1.2 ± 0.8	27 ± 19	1000 ± 700
Whf	82 ± 28	18 ± 6	14 ± 5	0.13 ± 0.04	1.2 ± 0.4	530 ± 170
Zhf	340 ± 50	106 ± 10	91 ± 10	173 ± 13	0.60 ± 0.16	43 ± 5
Vlf	0.73 ± 0.33	0.14 ± 0.05	0.17 ± 0.04	0.0040 ± 0.0020	—	6.9 ± 2.8
$VHbb$	3.7 ± 2.4	0.48 ± 0.31	0.42 ± 0.27	1.1 ± 0.7	0.010 ± 0.007	5.3 ± 3.4
VV	21 ± 4	3.7 ± 0.5	3.3 ± 0.4	6.6 ± 0.9	0.037 ± 0.018	35 ± 4
Total background	1720 ± 40	245 ± 9	201 ± 8	199 ± 12	415 ± 19	21200 ± 1300
Data	1702	251	203	198	428	21356

Table 7. Yields in the $\geq$ 3-b-tag regions of the $\nu\bar{\nu}b\bar{b}$ channel obtained from the background-only fit to data using Hin300 as the signal region. The indicated uncertainties include statistical and systematic components. The value next to the region name refers to the m_H hypothesis.

for other $\tan\beta$ values are provided in figures 9 to 12 in the appendix. Limits for intermediate $\tan\beta$ values can be obtained by interpolating between the limits for the given $\tan\beta$ values.

To obtain more realistic limits, instead of using narrow-width A bosons, the signals are generated with a natural width that corresponds to the prediction of the 2HDM for $\tan\beta = 1$ in ggF production and $\tan\beta = 10$ in bbA production. For the 2HDM benchmarks considered and the parameter space that is relevant for this search (see section 8.2), the $\tan\beta$ and Higgs boson mass values are enough to define the A boson width. The choice $\tan\beta = 10$ is made for bbA production because at this value this production mechanism is dominant in the benchmark models discussed in section 8.2 (Type-II and flipped 2HDM). In the 2HDM benchmarks considered here, the width of the A boson relative to its mass is a few percent for low m_A values and increases at high m_A. For example, for the m_A range shown in figures 5(a) and 5(b) for the $\ell^+\ell^- t\bar{t}$ channel, the A boson width ranges from 4.3% to 37% of its mass.

The observed upper limit in the $\ell^+\ell^- t\bar{t}$ channel in the case of ggF production varies from 75.0 fb for $(m_A, m_H) = (1200, 600)$ GeV to 992 fb for $(m_A, m_H) = (550, 450)$ GeV; this is to be compared with the respective expected limits of 90.8 fb and 582 fb. The observed upper limit in the $\ell^+\ell^- t\bar{t}$ channel in the case of bbA production varies from 79.4 fb for $(m_A, m_H) = (800, 400)$ GeV to 636 fb for $(m_A, m_H) = (650, 450)$ GeV; this is to be compared with the respective expected limits of 162 fb and 257 fb. Similarly, for the $\nu\bar{\nu}b\bar{b}$ channel, the observed upper limit in the case of ggF production varies from 6.2 fb for $(m_A, m_H) = (1200, 300)$ GeV to 3700 fb for $(m_A, m_H) = (350, 150)$ GeV; this is to be compared with the respective expected limits of 10.6 fb and 3520 fb. Finally, for the $\nu\bar{\nu}b\bar{b}$ channel, the observed upper limit in the case of bbA production varies from 3.62 fb for $(m_A, m_H) = (1200, 200)$ GeV to 1750 fb for $(m_A, m_H) = (350, 150)$ GeV; this is to be compared with the respective expected limits of 9.92 fb and 1910 fb.

8.2 Interpretation in the context of 2HDM

The upper limits shown in section 8.1 are interpreted in the context of the CP-conserving 2HDM. For this interpretation, several assumptions are made to reduce the number of free parameters in the model. The $H^\pm$ bosons are assumed to have the same mass as the A

JHEP02(2024)197

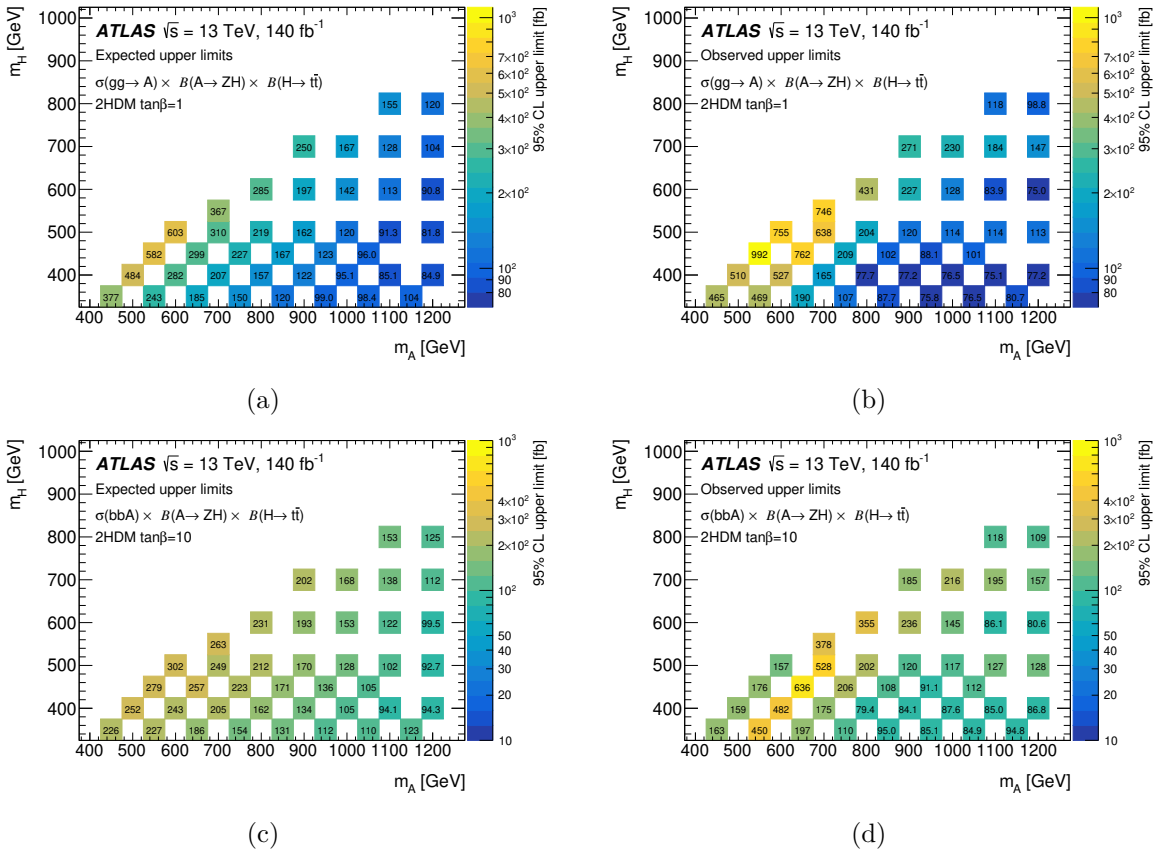

Figure 5. Expected (a,c) and observed (b,d) upper limits at 95% CL on $\sigma(gg \to A) \times B(A \to ZH) \times B(H \to t\bar{t})$ (a,b) and $\sigma(b\bar{b}A) \times B(A \to ZH) \times B(H \to t\bar{t})$ (c,d) in the (m_A, m_H) plane. The limits are shown for either $\tan\beta = 1$ or $\tan\beta = 10$ in ggF or bbA production, respectively. The $\tan\beta$ value is relevant only for the choice of A boson width.

boson, whereas $m_H < m_A$ is assumed for the masses of the A and H bosons. The 2HDM parameter m_{12}^2 is fixed to $m_A^2 \tan\beta/(1+\tan^2\beta)$. The h boson is assumed to have a mass of 125 GeV and its couplings to fermions and vector bosons are set to be the same as those of the SM Higgs boson at lowest order by choosing $\cos(\beta-\alpha) = 0$. The widths of the A and H bosons are taken from the predictions of the 2HDM. These assumptions leave three free parameters: m_A, m_H and $\tan\beta$. In addition, there are four possible arrangements of the Yukawa couplings, which are known as type-I, type-II, lepton specific and flipped 2HDM. For the parameter space that is relevant for this search, the widths of the A and H bosons differ very little across the different 2HDM types in comparison with the experimental mass resolution. In the same parameter space, the A boson width is larger than the H boson width, so the quoted limits from this search cannot be interpreted as limits for the $H \to ZA$ process. The cross-sections for A boson production in the 2HDM are calculated with corrections up to NNLO in QCD for ggF and bbA production in the five-flavour scheme as implemented in SusHi [119–122]. For bbA production, a cross-section in the four-flavour scheme is also calculated as described in refs. [123, 124] and the results are combined with the five-flavour scheme calculation following ref. [125]. The Higgs boson branching ratios are calculated using

JHEP02(2024)197

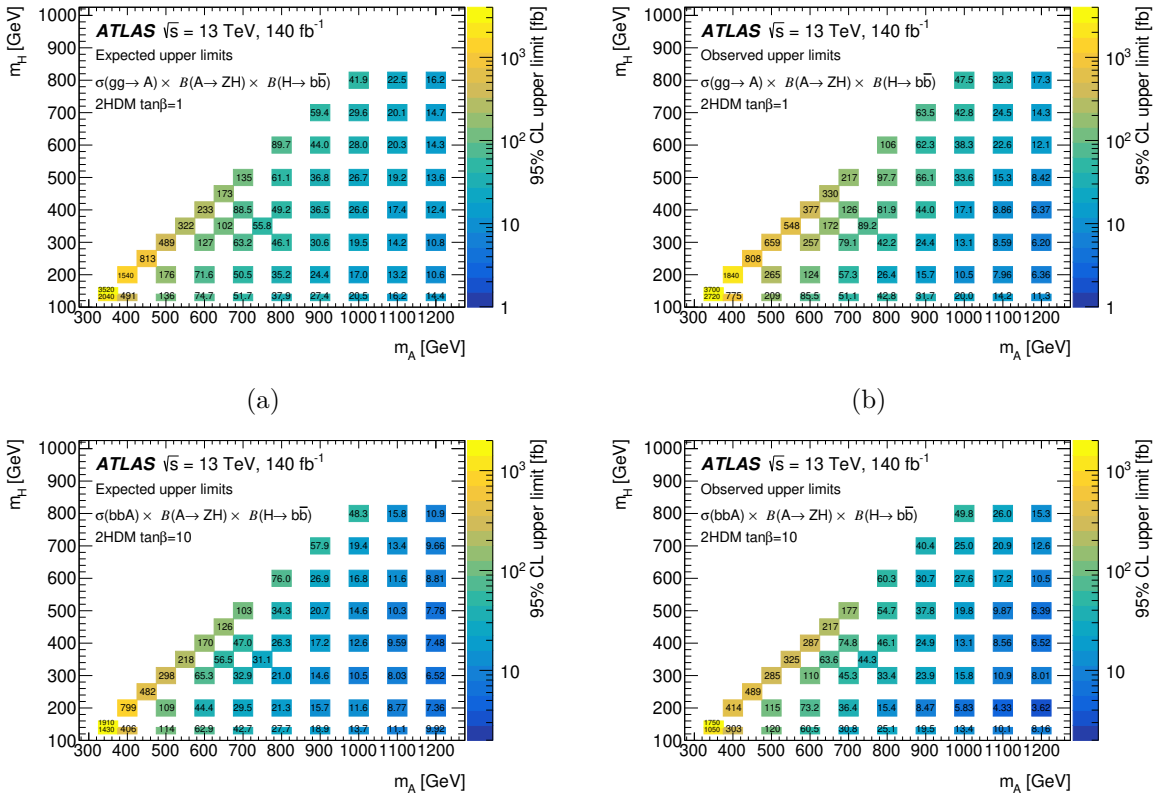

Figure 6. Expected (a,c) and observed (b,d) upper limits at 95% CL on $\sigma(gg \to A) \times B(A \to ZH) \times B(H \to b\bar{b})$ (a,b) and $\sigma(b\bar{b}A) \times B(A \to ZH) \times B(H \to b\bar{b})$ (c,d) in the (m_A, m_H) plane. The limits are shown for either $\tan\beta = 1$ or $\tan\beta = 10$ in ggF or bbA production, respectively. The $\tan\beta$ value is relevant only for the choice of A boson width.

2HDMC [126]. The procedure used to calculate the cross-sections and branching ratios, as well as to choose the 2HDM parameter values, follows ref. [87].

The upper limits are interpreted as constraints in the (m_A, m_H) plane for several $\tan\beta$ values. The widths of the A and H bosons change as a function of $\tan\beta$ and these variations are taken into account when calculating the constraints. The results are quoted only for cases in which the width of the A boson is no more than 25% of m_A. Figures 7(a) and 7(b) show the constraints from the $\ell^+\ell^- t\bar{t}$ channel for the type-I and type-II 2HDM, respectively. Constraints from this channel for the lepton-specific 2HDM are very similar to type-I. Constraints from the $\nu\bar{\nu}b\bar{b}$ channel are shown in figure 7(c) for the type-I 2HDM, and in figures 7(d) and 7(e) for the type-II 2HDM. These results extend the reach of the $A \to ZH \to \ell\ell b\bar{b}$ search reported in ref. [22], especially in parts of the parameter space with $m_H > 350\,\text{GeV}$ and $m_A > 800\,\text{GeV}$.

The fact that the observed exclusion limit for the $\ell^+\ell^- t\bar{t}$ channel is smaller than the expected exclusion limit in the region around $(m_A, m_H) = (650, 450)\,\text{GeV}$ in figures 7(a) and 7(b) is a consequence of the small data excess observed in figure 3(a). Similarly, in the $\nu\bar{\nu}b\bar{b}$ channel, at low $\tan\beta$ in figure 7(d) the expected and observed limits diverge because of a small excess of events for $550\,\text{GeV} \lesssim m_T(VH) \lesssim 650\,\text{GeV}$. Finally, differences seen between the limits at high $\tan\beta$ are affected by small excesses or deficits in the data; in

JHEP02(2024)197

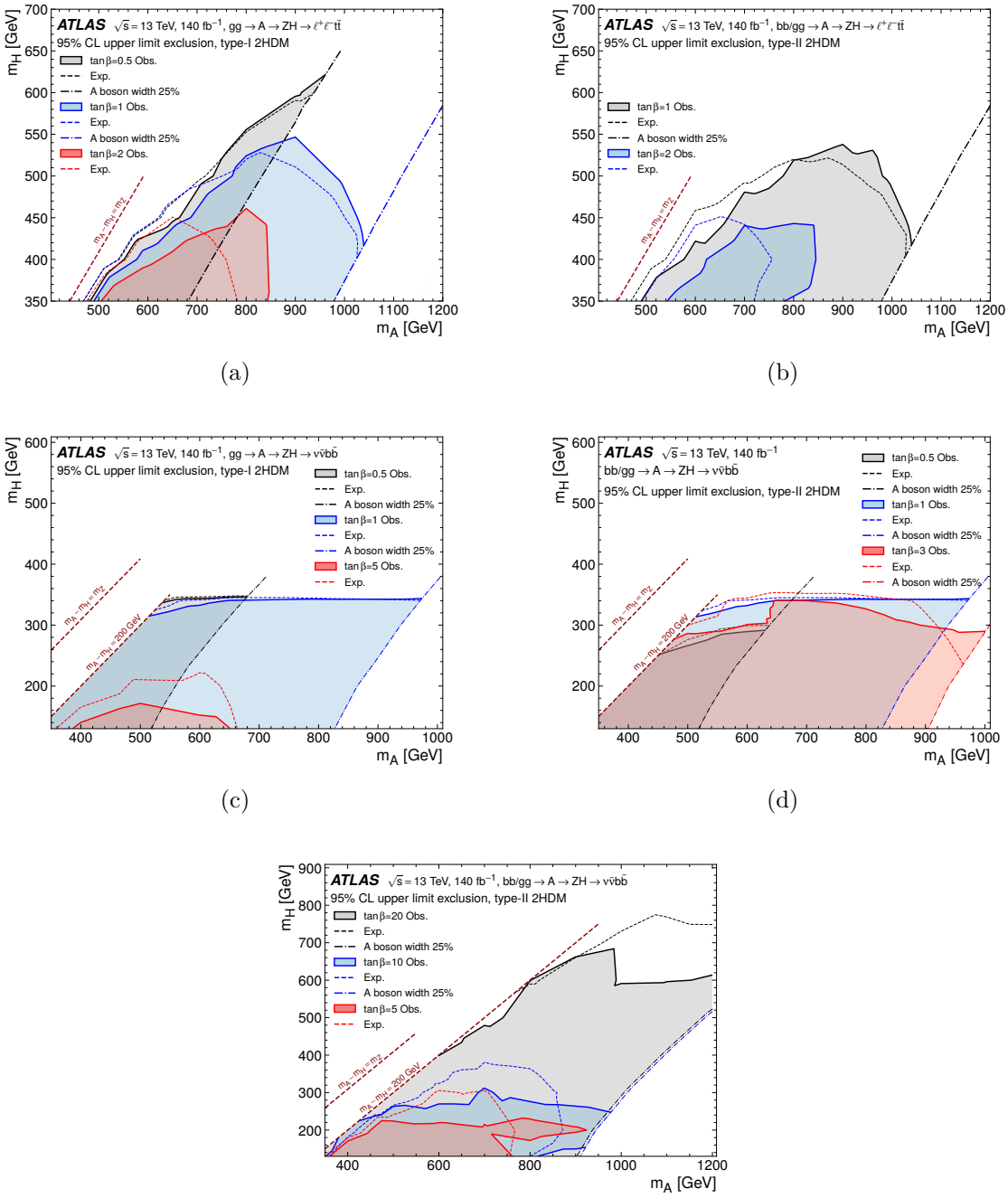

Figure 7. Observed and expected 95% CL exclusion regions in the (m_A, m_H) plane for various $\tan\beta$ values for the $\ell^+\ell^- t\bar{t}$ channel, type-I (a) and type-II (b) 2HDM, and $\nu\bar{\nu}b\bar{b}$ channel, type-I (c) and type-II (d,e) 2HDM. The line at $m_A - m_H = 200\,\text{GeV}$ shown in (c–e) corresponds to the edge of the analysis sensitivity due to the $E_{\text{T}}^{\text{miss}}$ requirement.

JHEP02(2024)197

particular, the smaller observed exclusion limit in the region with $(m_A, m_H) = (600, 300)$ GeV is due to the excess observed in figure 3(c).

8.3 Model-independent limits

The upper limits presented above are based on the assumption that the Z and H candidates in the final state are produced resonantly and therefore have a significant model dependence. In addition to the 2HDM interpretation, limits with less model dependence are derived with a slight modification of the fit model as follows. Assuming that a resonance X that decays into a $t\bar{t}$ or $b\bar{b}$ pair is produced in association with a Z boson, the number of signal events that will be recorded by the detector in a given bin of the reconstructed $m(t\bar{t})$ or $m(b\bar{b})$ distribution will be equal to the integrated luminosity times the 'visible cross-section' $\sigma_{\text{vis}}(Z(\ell\ell)X(t\bar{t}))$ or $\sigma_{\text{vis}}(Z(\nu\bar{\nu})X(b\bar{b}))$.

Upper limits at 95% CL are placed on $\sigma_{\text{vis}}(Z(\ell\ell)X(t\bar{t}))$ and $\sigma_{\text{vis}}(Z(\nu\bar{\nu})X(b\bar{b}))$ using the fit model described in section 7, except that the $m(t\bar{t})$ or $m(b\bar{b})$ distributions for the events that pass the SR selection are fitted using three bins. The signal template is constructed by adding a single signal event in the central bin of the $m(t\bar{t})$ or $m(b\bar{b})$ distribution, with the adjacent bins used as CRs. The corresponding `ss` region or `e`μ and `2L` regions are also used as CRs in this fit without any modification. Using the $m(t\bar{t})$ or $m(b\bar{b})$ distributions instead of the Δm or $m_{\text{T}}(VH)$ distributions in the fit ensures that the limit thus obtained is independent of how the Z and H candidates are produced, and using a large bin that contains all of the signal events ensures that the limit does not depend strongly on the lineshape of the $t\bar{t}$ or $b\bar{b}$ resonance.[7]

To obtain the upper limits on the visible cross-section as functions of $m(t\bar{t})$ and $m(b\bar{b})$, multiple independent fits are performed, each time using different SRs, defined by the bin edges shown in figure 8. These limits can be used to estimate sensitivities for theories involving high-mass $t\bar{t}$ or $b\bar{b}$ resonances, by comparing the upper limit shown in figure 8 with the visible cross-section predicted by a specific theory, given by

$$\sigma_{\text{vis}}^{\text{theory}} = \sigma_{\text{theory}} \times B \times (\mathcal{A} \cdot \epsilon)_{m(t\bar{t})/m(b\bar{b})},$$

where σ_{theory} is the inclusive signal cross-section, B is the product of the branching ratios for the decay chain and $(\mathcal{A} \cdot \epsilon)_{m(t\bar{t})/m(b\bar{b})}$ is the acceptance times efficiency for reconstructing a signal-model event in a given bin of the $m(b\bar{b})$ or $m(t\bar{t})$ distribution. The use of the limits shown in figure 8 requires the value of $(\mathcal{A} \cdot \epsilon)_{m(t\bar{t})/m(b\bar{b})}$ for a given signal model to be obtained from a Monte Carlo 'truth'-level analysis that reproduces the event selection described in section 5, incorporating the detector effects, for example via fast simulation packages such as DELPHES [127] or smearing routines such as the ones provided in the RIVET framework [128, 129]. The applicability of these limits is not guaranteed outside the phase space in which $(\mathcal{A} \cdot \epsilon)$ values are provided, or when the derived $(\mathcal{A} \cdot \epsilon)$ values differ significantly from the values provided in this publication.

[7] For signals that predict a $t\bar{t}$ or $b\bar{b}$ resonance with a mass that lies between the bin edges in figure 8, the limits from all bins in which the signal contributes have to be combined, taking into account their respective acceptances.

JHEP02(2024)197

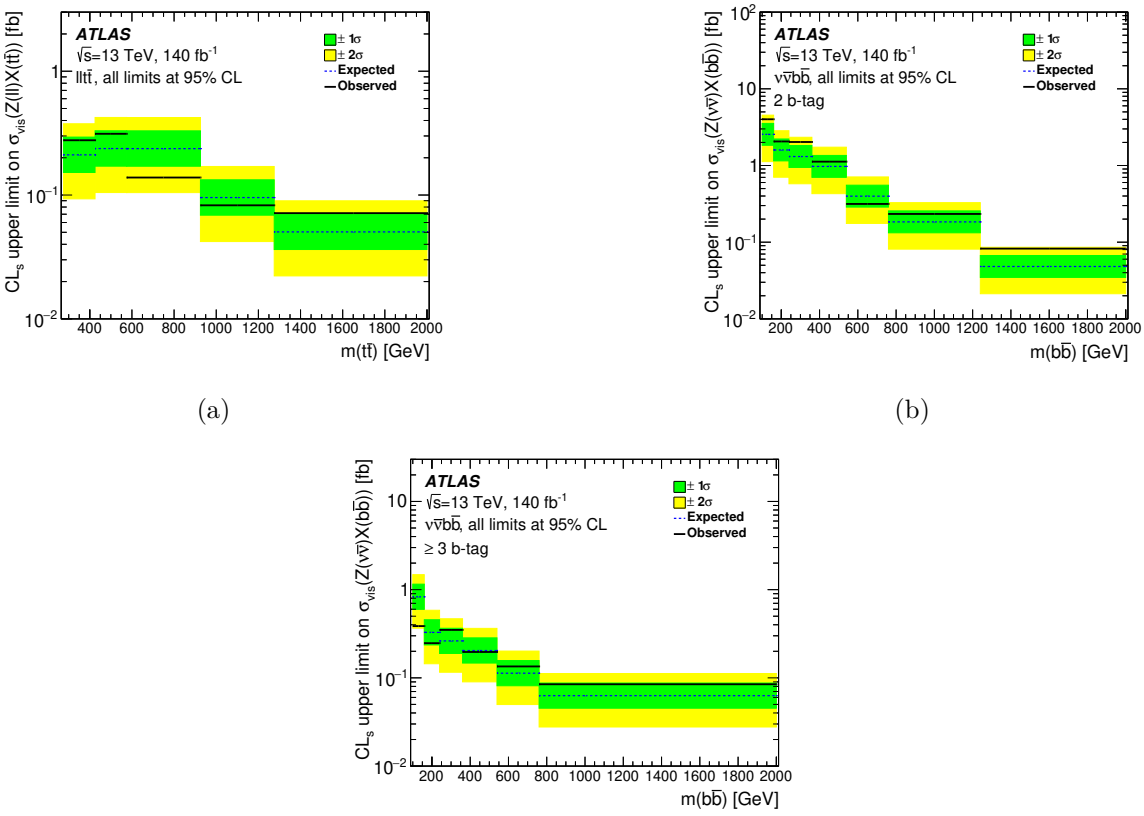

Figure 8. Observed (solid line) and expected (dashed line) 95% CL upper limits on $\sigma_{\text{vis}}(Z(\ell\ell)X(t\bar{t}))$ (a) and $\sigma_{\text{vis}}(Z(\nu\bar{\nu})X(b\bar{b}))$ obtained from the 2-b-tag (b) and $\geq$ 3-b-tag (c) regions. The limits are obtained in bins of reconstructed $m(t\bar{t})$ and $m(b\bar{b})$. The green and yellow bands correspond to the $\pm 1\,\sigma$ and $\pm 2\,\sigma$ intervals for the expected upper limits, respectively.

9 Conclusion

A search for the decay of a heavy CP-odd Higgs boson A into a heavy CP-even Higgs boson H is presented, using the full LHC Run 2 dataset of 13 TeV proton-proton collisions corresponding to an integrated luminosity of 140 fb^{-1} recorded by the ATLAS detector. Two channels are considered in the present search. The $\ell^+\ell^- t\bar{t}$ channel, which probes H boson decays into a pair of top quarks and Z boson decays into a pair of charged leptons, provides sensitivity in the $m_H > 350$ GeV region. The $\nu\bar{\nu}b\bar{b}$ channel, which probes H boson decays into a pair of b-quarks and Z boson decays into neutrinos, extends the sensitivity of previous searches in parts of the parameter space with $m_A > 800$ GeV and $m_H < 350$ GeV.

No significant excess over the SM background prediction is observed. Upper limits are set at the 95% confidence level on the production cross-section times the decay branching ratios. These results are interpreted in the context of the two-Higgs-doublet models and yield an exclusion range significantly larger than those obtained by previous searches sensitive to this parameter space. In addition, upper limits are quoted as a function of reconstructed $m(t\bar{t})$ and $m(b\bar{b})$, assuming the production of a $t\bar{t}$ or $b\bar{b}$ resonance.

JHEP02(2024)197

Acknowledgments

We thank CERN for the very successful operation of the LHC, as well as the support staff from our institutions without whom ATLAS could not be operated efficiently.

We acknowledge the support of ANPCyT, Argentina; YerPhI, Armenia; ARC, Australia; BMWFW and FWF, Austria; ANAS, Azerbaijan; CNPq and FAPESP, Brazil; NSERC, NRC and CFI, Canada; CERN; ANID, Chile; CAS, MOST and NSFC, China; Minciencias, Colombia; MEYS CR, Czech Republic; DNRF and DNSRC, Denmark; IN2P3-CNRS and CEA-DRF/IRFU, France; SRNSFG, Georgia; BMBF, HGF and MPG, Germany; GSRI, Greece; RGC and Hong Kong SAR, China; ISF and Benoziyo Center, Israel; INFN, Italy; MEXT and JSPS, Japan; CNRST, Morocco; NWO, Netherlands; RCN, Norway; MEiN, Poland; FCT, Portugal; MNE/IFA, Romania; MESTD, Serbia; MSSR, Slovakia; ARRS and MIZŠ, Slovenia; DSI/NRF, South Africa; MICINN, Spain; SRC and Wallenberg Foundation, Sweden; SERI, SNSF and Cantons of Bern and Geneva, Switzerland; MOST, Taiwan; TENMAK, Türkiye; STFC, United Kingdom; DOE and NSF, United States of America. In addition, individual groups and members have received support from BCKDF, CANARIE, Compute Canada and CRC, Canada; PRIMUS 21/SCI/017 and UNCE SCI/013, Czech Republic; COST, ERC, ERDF, Horizon 2020, ICSC-NextGenerationEU and Marie Skłodowska-Curie Actions, European Union; Investissements d'Avenir Labex, Investissements d'Avenir Idex and ANR, France; DFG and AvH Foundation, Germany; Herakleitos, Thales and Aristeia programmes co-financed by EU-ESF and the Greek NSRF, Greece; BSF-NSF and MINERVA, Israel; Norwegian Financial Mechanism 2014-2021, Norway; NCN and NAWA, Poland; La Caixa Banking Foundation, CERCA Programme Generalitat de Catalunya and PROMETEO and GenT Programmes Generalitat Valenciana, Spain; Göran Gustafssons Stiftelse, Sweden; The Royal Society and Leverhulme Trust, United Kingdom.

The crucial computing support from all WLCG partners is acknowledged gratefully, in particular from CERN, the ATLAS Tier-1 facilities at TRIUMF (Canada), NDGF (Denmark, Norway, Sweden), CC-IN2P3 (France), KIT/GridKA (Germany), INFN-CNAF (Italy), NL-T1 (Netherlands), PIC (Spain), ASGC (Taiwan), RAL (U.K.) and BNL (U.S.A.), the Tier-2 facilities worldwide and large non-WLCG resource providers. Major contributors of computing resources are listed in ref. [130].

JHEP02(2024)197

A Upper limits on the production cross sections for additional tan β values

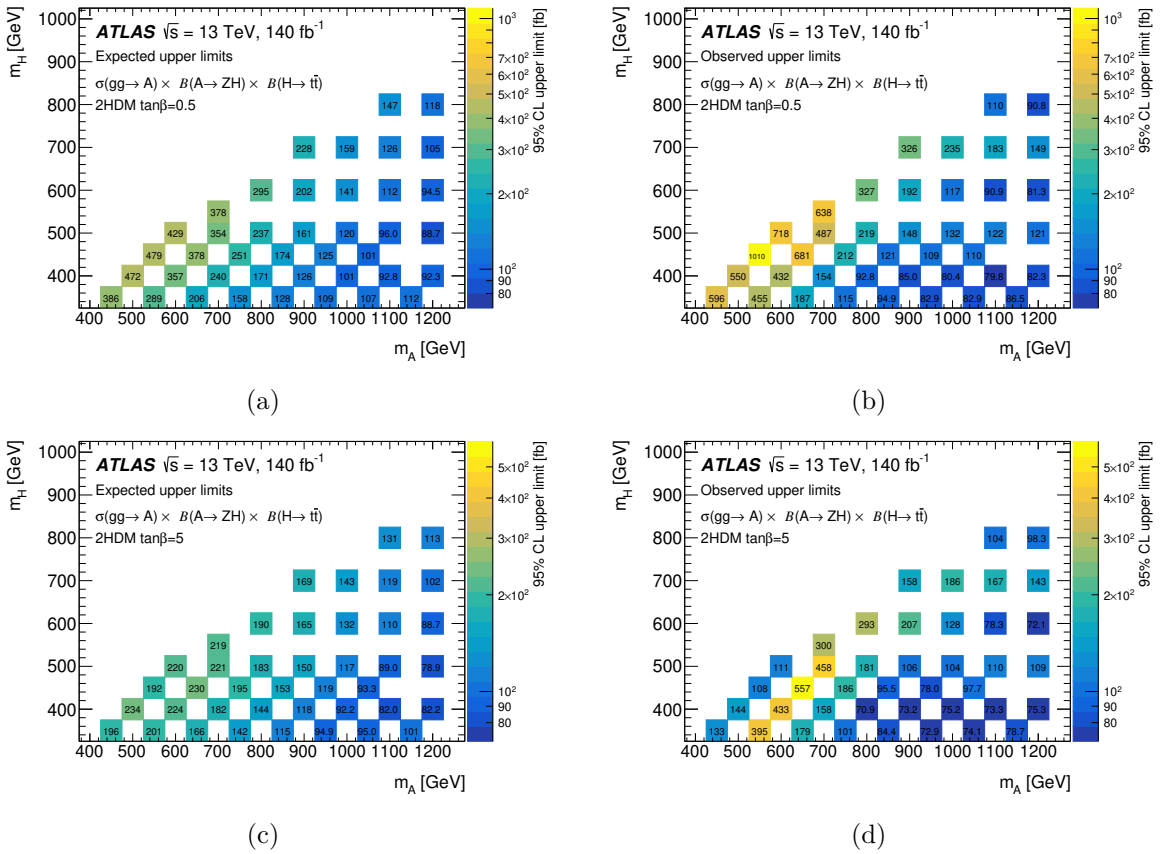

Figure 9. Expected and observed upper limits at 95% CL on $\sigma(gg \to A) \times B(A \to ZH) \times B(H \to t\bar{t})$. The limits are shown for $\tan\beta = 0.5$ (a,b) and $\tan\beta = 5$ (c,d). The $\tan\beta$ value is relevant only for the choice of A boson width.

JHEP02(2024)197

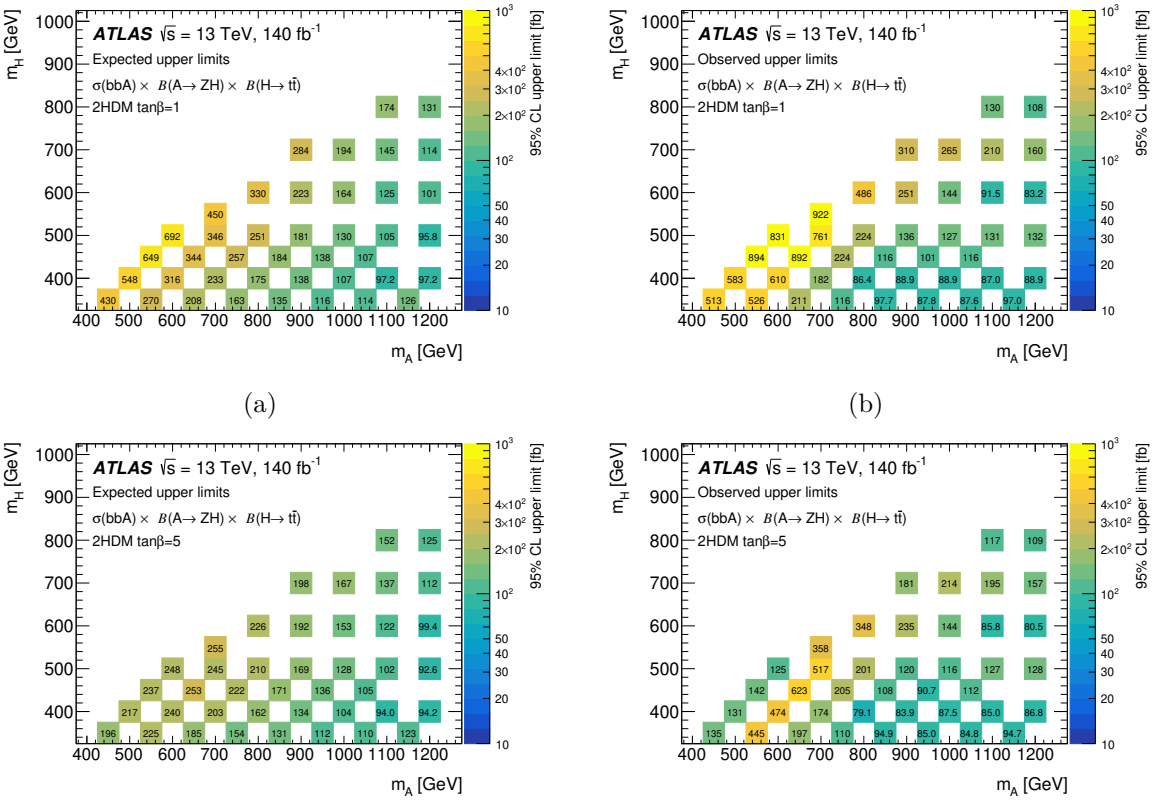

Figure 10. Expected and observed upper limits at 95% CL on $\sigma(b\bar{b}A) \times B(A \to ZH) \times B(H \to t\bar{t})$. The limits are shown for $\tan\beta = 1$ (a,b) and $\tan\beta = 5$ (c,d). The $\tan\beta$ value is relevant only for the choice of A boson width.

JHEP02(2024)197

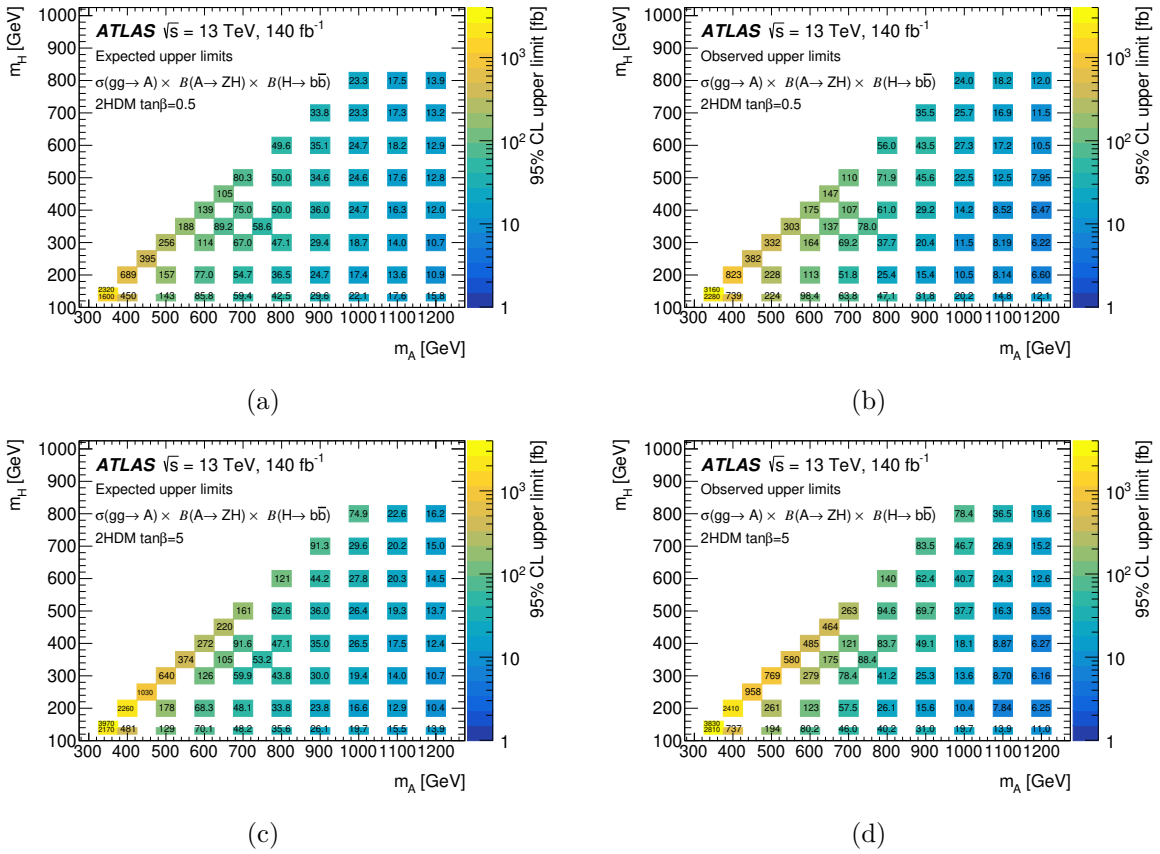

Figure 11. Expected and observed upper limits at 95% CL on $\sigma(gg \to A) \times B(A \to ZH) \times B(H \to b\bar{b})$. The limits are shown for $\tan\beta = 0.5$ (a,b) and $\tan\beta = 5$ (c,d). The $\tan\beta$ value is relevant only for the choice of A boson width.

JHEP02(2024)197

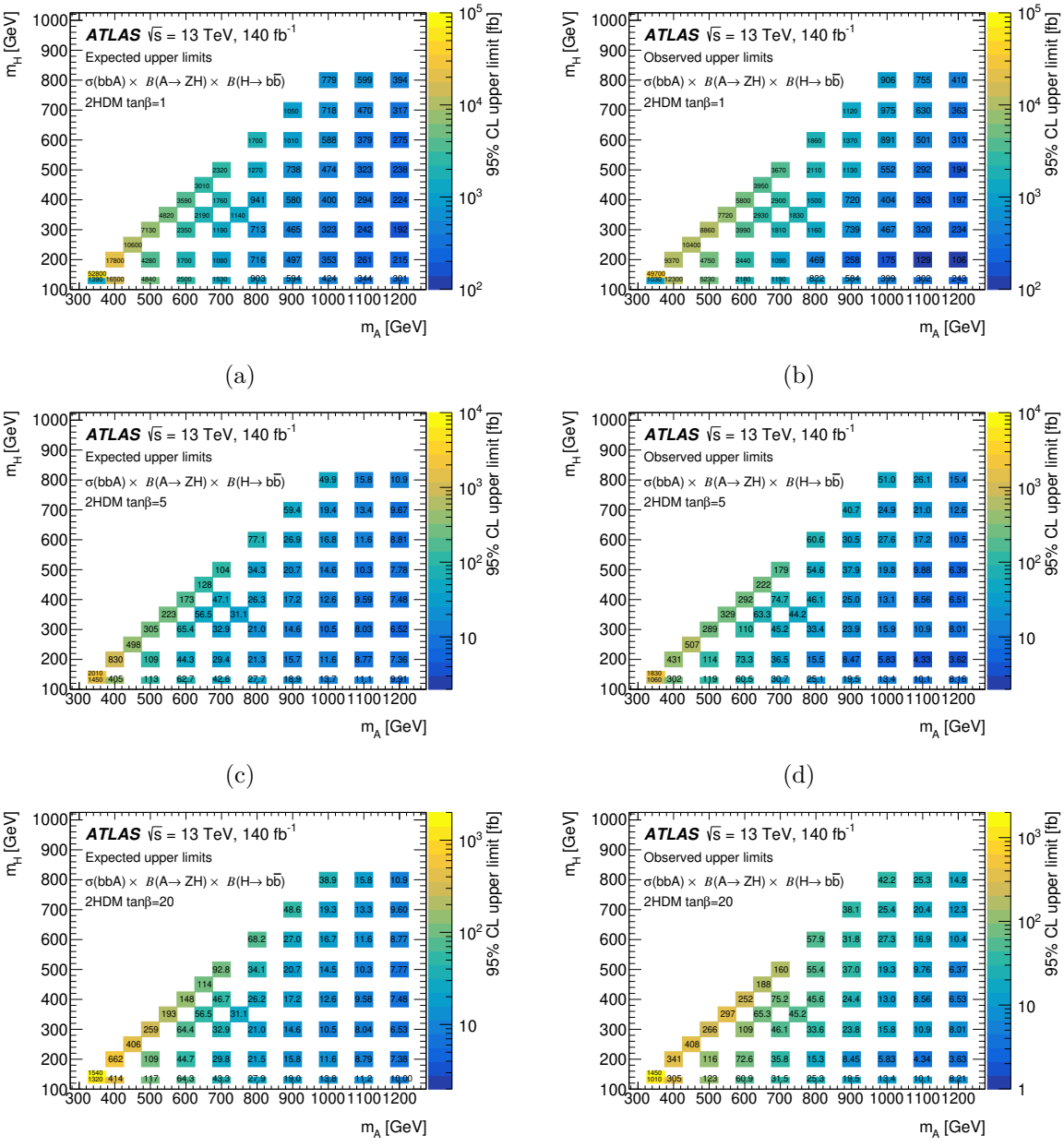

Figure 12. Expected and observed upper limits at 95% CL on $\sigma(b\bar{b}A) \times B(A \to ZH) \times B(H \to b\bar{b})$. The limits are shown for $\tan\beta = 1$ (a,b), $\tan\beta = 5$ (c,d) and $\tan\beta = 20$ (e,f). The $\tan\beta$ value is relevant only for the choice of A boson width.

JHEP02(2024)197

Open Access. This article is distributed under the terms of the Creative Commons Attribution License (CC-BY4.0), which permits any use, distribution and reproduction in any medium, provided the original author(s) and source are credited.

References

[1] ATLAS collaboration, *Observation of a new particle in the search for the Standard Model Higgs boson with the ATLAS detector at the LHC*, *Phys. Lett. B* **716** (2012) 1 [arXiv:1207.7214] [INSPIRE].

[2] CMS collaboration, *Observation of a new boson at a mass of* 125 *GeV with the CMS experiment at the LHC*, *Phys. Lett. B* **716** (2012) 30 [arXiv:1207.7235] [INSPIRE].

[3] A. Ferrari and N. Rompotis, *Exploration of extended Higgs sectors with run-2 proton-proton collision data at the LHC*, *Symmetry* **13** (2021) 2144 [*Erratum ibid.* **14** (2022) 1546] [INSPIRE].

[4] T.D. Lee, *A theory of spontaneous T violation*, *Phys. Rev. D* **8** (1973) 1226 [INSPIRE].

[5] G.C. Branco et al., *Theory and phenomenology of two-Higgs-doublet models*, *Phys. Rept.* **516** (2012) 1 [arXiv:1106.0034] [INSPIRE].

[6] A. Djouadi, *The anatomy of electro-weak symmetry breaking. II. The Higgs bosons in the minimal supersymmetric model*, *Phys. Rept.* **459** (2008) 1 [hep-ph/0503173] [INSPIRE].

[7] J. Abdallah et al., *Simplified models for dark matter searches at the LHC*, *Phys. Dark Univ.* **9-10** (2015) 8 [arXiv:1506.03116] [INSPIRE].

[8] M. Bauer, U. Haisch and F. Kahlhoefer, *Simplified dark matter models with two Higgs doublets. Part I. Pseudoscalar mediators*, *JHEP* **05** (2017) 138 [arXiv:1701.07427] [INSPIRE].

[9] J.E. Kim and G. Carosi, *Axions and the strong CP problem*, *Rev. Mod. Phys.* **82** (2010) 557 [*Erratum ibid.* **91** (2019) 049902] [arXiv:0807.3125] [INSPIRE].

[10] A.G. Cohen, D.B. Kaplan and A.E. Nelson, *Progress in electroweak baryogenesis*, *Ann. Rev. Nucl. Part. Sci.* **43** (1993) 27 [hep-ph/9302210] [INSPIRE].

[11] S.F. King, *Neutrino mass models*, *Rept. Prog. Phys.* **67** (2004) 107 [hep-ph/0310204] [INSPIRE].

[12] J.F. Gunion and H.E. Haber, *The CP conserving two Higgs doublet model: the approach to the decoupling limit*, *Phys. Rev. D* **67** (2003) 075019 [hep-ph/0207010] [INSPIRE].

[13] J. Haller et al., *Update of the global electroweak fit and constraints on two-Higgs-doublet models*, *Eur. Phys. J. C* **78** (2018) 675 [arXiv:1803.01853] [INSPIRE].

[14] ATLAS collaboration, *Search for heavy resonances decaying into a Z or W boson and a Higgs boson in final states with leptons and b-jets in* 139 fb^{-1} *of pp collisions at* $\sqrt{s} = 13$ *TeV with the ATLAS detector*, *JHEP* **06** (2023) 016 [arXiv:2207.00230] [INSPIRE].

[15] CMS collaboration, *Search for heavy resonances decaying into a vector boson and a Higgs boson in final states with charged leptons, neutrinos, and b quarks*, *Phys. Lett. B* **768** (2017) 137 [arXiv:1610.08066] [INSPIRE].

[16] G.C. Dorsch, S.J. Huber and J.M. No, *A strong electroweak phase transition in the* 2*HDM after LHC*8, *JHEP* **10** (2013) 029 [arXiv:1305.6610] [INSPIRE].

[17] G.C. Dorsch, S.J. Huber, K. Mimasu and J.M. No, *Echoes of the electroweak phase transition: discovering a second Higgs doublet through* $A_0 \to ZH_0$, *Phys. Rev. Lett.* **113** (2014) 211802 [arXiv:1405.5537] [INSPIRE].

JHEP02(2024)197

[18] N. Turok and J. Zadrozny, *Electroweak baryogenesis in the two doublet model*, *Nucl. Phys. B* **358** (1991) 471 [INSPIRE].

[19] L. Fromme, S.J. Huber and M. Seniuch, *Baryogenesis in the two-Higgs doublet model*, *JHEP* **11** (2006) 038 [hep-ph/0605242] [INSPIRE].

[20] P. Basler et al., *Strong first order electroweak phase transition in the CP-conserving 2HDM revisited*, *JHEP* **02** (2017) 121 [arXiv:1612.04086] [INSPIRE].

[21] W. Su, A.G. Williams and M. Zhang, *Strong first order electroweak phase transition in 2HDM confronting future Z & Higgs factories*, *JHEP* **04** (2021) 219 [arXiv:2011.04540] [INSPIRE].

[22] ATLAS collaboration, *Search for a heavy Higgs boson decaying into a Z boson and another heavy Higgs boson in the $\ell\ell bb$ and $\ell\ell WW$ final states in pp collisions at $\sqrt{s} = 13$ TeV with the ATLAS detector*, *Eur. Phys. J. C* **81** (2021) 396 [arXiv:2011.05639] [INSPIRE].

[23] CMS collaboration, *Search for neutral resonances decaying into a Z boson and a pair of b jets or τ leptons*, *Phys. Lett. B* **759** (2016) 369 [arXiv:1603.02991] [INSPIRE].

[24] CMS collaboration, *Search for new neutral Higgs bosons through the $H \to ZA \to \ell^+\ell^- b\bar{b}$ process in pp collisions at $\sqrt{s} = 13$ TeV*, *JHEP* **03** (2020) 055 [arXiv:1911.03781] [INSPIRE].

[25] ATLAS collaboration, *Search for Higgs boson pair production in association with a vector boson in pp collisions at $\sqrt{s} = 13$ TeV with the ATLAS detector*, *Eur. Phys. J. C* **83** (2023) 519 [arXiv:2210.05415] [INSPIRE].

[26] ATLAS collaboration, *Search for dark matter produced in association with a Standard Model Higgs boson decaying into b-quarks using the full run 2 dataset from the ATLAS detector*, *JHEP* **11** (2021) 209 [arXiv:2108.13391] [INSPIRE].

[27] ATLAS collaboration, *The ATLAS experiment at the CERN Large Hadron Collider*, 2008 *JINST* **3** S08003 [INSPIRE].

[28] ATLAS collaboration, *ATLAS Insertable B-Layer: technical design report*, ATLAS-TDR-19, CERN, Geneva, Switzerland (2010).

[29] ATLAS IBL collaboration, *Production and integration of the ATLAS Insertable B-Layer*, 2018 *JINST* **13** T05008 [arXiv:1803.00844] [INSPIRE].

[30] ATLAS collaboration, *Performance of the ATLAS trigger system in* 2015, *Eur. Phys. J. C* **77** (2017) 317 [arXiv:1611.09661] [INSPIRE].

[31] ATLAS collaboration, *The ATLAS collaboration software and firmware*, ATL-SOFT-PUB-2021-001, CERN, Geneva, Switzerland (2021).

[32] ATLAS collaboration, *ATLAS data quality operations and performance for* 2015–2018 *data-taking*, 2020 *JINST* **15** P04003 [arXiv:1911.04632] [INSPIRE].

[33] ATLAS collaboration, *Measurements of WH and ZH production in the $H \to b\bar{b}$ decay channel in pp collisions at* 13 *TeV with the ATLAS detector*, *Eur. Phys. J. C* **81** (2021) 178 [arXiv:2007.02873] [INSPIRE].

[34] J. Alwall et al., *The automated computation of tree-level and next-to-leading order differential cross sections, and their matching to parton shower simulations*, *JHEP* **07** (2014) 079 [arXiv:1405.0301] [INSPIRE].

[35] NNPDF collaboration, *Parton distributions for the LHC run II*, *JHEP* **04** (2015) 040 [arXiv:1410.8849] [INSPIRE].

[36] P. Artoisenet, V. Lemaitre, F. Maltoni and O. Mattelaer, *Automation of the matrix element reweighting method*, *JHEP* **12** (2010) 068 [arXiv:1007.3300] [INSPIRE].

JHEP02(2024)197

[37] S. Frixione, E. Laenen, P. Motylinski and B.R. Webber, *Angular correlations of lepton pairs from vector boson and top quark decays in Monte Carlo simulations*, *JHEP* **04** (2007) 081 [hep-ph/0702198] [INSPIRE].

[38] P. Artoisenet, R. Frederix, O. Mattelaer and R. Rietkerk, *Automatic spin-entangled decays of heavy resonances in Monte Carlo simulations*, *JHEP* **03** (2013) 015 [arXiv:1212.3460] [INSPIRE].

[39] T. Sjöstrand et al., *An introduction to PYTHIA* 8.2, *Comput. Phys. Commun.* **191** (2015) 159 [arXiv:1410.3012] [INSPIRE].

[40] ATLAS collaboration, *ATLAS Pythia* 8 *tunes to* 7 *TeV data*, ATL-PHYS-PUB-2014-021, CERN, Geneva, Switzerland (2014) [INSPIRE].

[41] U. Haisch and G. Polesello, *Searching for heavy Higgs bosons in the $t\bar{t}Z$ and tbW final states*, *JHEP* **09** (2018) 151 [arXiv:1807.07734] [INSPIRE].

[42] D.J. Lange, *The EvtGen particle decay simulation package*, *Nucl. Instrum. Meth. A* **462** (2001) 152 [INSPIRE].

[43] S. Schumann and F. Krauss, *A parton shower algorithm based on Catani-Seymour dipole factorisation*, *JHEP* **03** (2008) 038 [arXiv:0709.1027] [INSPIRE].

[44] T. Sjöstrand, S. Mrenna and P.Z. Skands, *A brief introduction to PYTHIA* 8.1, *Comput. Phys. Commun.* **178** (2008) 852 [arXiv:0710.3820] [INSPIRE].

[45] ATLAS collaboration, *The Pythia* 8 *A*3 *tune description of ATLAS minimum bias and inelastic measurements incorporating the Donnachie-Landshoff diffractive model*, ATL-PHYS-PUB-2016-017, CERN, Geneva, Switzerland (2016) [INSPIRE].

[46] GEANT4 collaboration, *GEANT*4 — *a simulation toolkit*, *Nucl. Instrum. Meth. A* **506** (2003) 250 [INSPIRE].

[47] ATLAS collaboration, *The ATLAS simulation infrastructure*, *Eur. Phys. J. C* **70** (2010) 823 [arXiv:1005.4568] [INSPIRE].

[48] R.D. Ball et al., *Parton distributions with LHC data*, *Nucl. Phys. B* **867** (2013) 244 [arXiv:1207.1303] [INSPIRE].

[49] J. Pumplin et al., *New generation of parton distributions with uncertainties from global QCD analysis*, *JHEP* **07** (2002) 012 [hep-ph/0201195] [INSPIRE].

[50] S. Frixione et al., *Single-top hadroproduction in association with a W boson*, *JHEP* **07** (2008) 029 [arXiv:0805.3067] [INSPIRE].

[51] S. Frixione, P. Nason and G. Ridolfi, *A positive-weight next-to-leading-order Monte Carlo for heavy flavour hadroproduction*, *JHEP* **09** (2007) 126 [arXiv:0707.3088] [INSPIRE].

[52] P. Nason, *A new method for combining NLO QCD with shower Monte Carlo algorithms*, *JHEP* **11** (2004) 040 [hep-ph/0409146] [INSPIRE].

[53] S. Frixione, P. Nason and C. Oleari, *Matching NLO QCD computations with parton shower simulations: the POWHEG method*, *JHEP* **11** (2007) 070 [arXiv:0709.2092] [INSPIRE].

[54] S. Alioli, P. Nason, C. Oleari and E. Re, *A general framework for implementing NLO calculations in shower Monte Carlo programs: the POWHEG BOX*, *JHEP* **06** (2010) 043 [arXiv:1002.2581] [INSPIRE].

[55] M. Beneke, P. Falgari, S. Klein and C. Schwinn, *Hadronic top-quark pair production with NNLL threshold resummation*, *Nucl. Phys. B* **855** (2012) 695 [arXiv:1109.1536] [INSPIRE].

JHEP02(2024)197

[56] M. Cacciari et al., *Top-pair production at hadron colliders with next-to-next-to-leading logarithmic soft-gluon resummation*, *Phys. Lett. B* **710** (2012) 612 [arXiv:1111.5869] [INSPIRE].

[57] P. Bärnreuther, M. Czakon and A. Mitov, *Percent level precision physics at the Tevatron: first genuine NNLO QCD corrections to $q\bar{q} \to t\bar{t} + X$*, *Phys. Rev. Lett.* **109** (2012) 132001 [arXiv:1204.5201] [INSPIRE].

[58] M. Czakon and A. Mitov, *NNLO corrections to top-pair production at hadron colliders: the all-fermionic scattering channels*, *JHEP* **12** (2012) 054 [arXiv:1207.0236] [INSPIRE].

[59] M. Czakon and A. Mitov, *NNLO corrections to top pair production at hadron colliders: the quark-gluon reaction*, *JHEP* **01** (2013) 080 [arXiv:1210.6832] [INSPIRE].

[60] M. Czakon, P. Fiedler and A. Mitov, *Total top-quark pair-production cross section at hadron colliders through $O(\alpha_S^4)$*, *Phys. Rev. Lett.* **110** (2013) 252004 [arXiv:1303.6254] [INSPIRE].

[61] M. Czakon and A. Mitov, *Top++: a program for the calculation of the top-pair cross-section at hadron colliders*, *Comput. Phys. Commun.* **185** (2014) 2930 [arXiv:1112.5675] [INSPIRE].

[62] E. Re, *Single-top Wt-channel production matched with parton showers using the POWHEG method*, *Eur. Phys. J. C* **71** (2011) 1547 [arXiv:1009.2450] [INSPIRE].

[63] N. Kidonakis, *Two-loop soft anomalous dimensions for single top quark associated production with a W^- or H^-*, *Phys. Rev. D* **82** (2010) 054018 [arXiv:1005.4451] [INSPIRE].

[64] N. Kidonakis, *Top quark production*, in the proceedings of the *Helmholtz international summer school on physics of heavy quarks and hadrons*, (2014), p. 139 [DOI:10.3204/DESY-PROC-2013-03/Kidonakis] [arXiv:1311.0283] [INSPIRE].

[65] R. Frederix, E. Re and P. Torrielli, *Single-top t-channel hadroproduction in the four-flavour scheme with POWHEG and aMC@NLO*, *JHEP* **09** (2012) 130 [arXiv:1207.5391] [INSPIRE].

[66] M. Aliev et al., *HATHOR: HAdronic Top and Heavy quarks crOss section calculatoR*, *Comput. Phys. Commun.* **182** (2011) 1034 [arXiv:1007.1327] [INSPIRE].

[67] P. Kant et al., *HatHor for single top-quark production: updated predictions and uncertainty estimates for single top-quark production in hadronic collisions*, *Comput. Phys. Commun.* **191** (2015) 74 [arXiv:1406.4403] [INSPIRE].

[68] SHERPA collaboration, *Event generation with Sherpa 2.2*, *SciPost Phys.* **7** (2019) 034 [arXiv:1905.09127] [INSPIRE].

[69] C. Anastasiou, L.J. Dixon, K. Melnikov and F. Petriello, *High precision QCD at hadron colliders: electroweak gauge boson rapidity distributions at NNLO*, *Phys. Rev. D* **69** (2004) 094008 [hep-ph/0312266] [INSPIRE].

[70] S. Höche, F. Krauss, M. Schönherr and F. Siegert, *A critical appraisal of NLO+PS matching methods*, *JHEP* **09** (2012) 049 [arXiv:1111.1220] [INSPIRE].

[71] S. Höche, F. Krauss, M. Schönherr and F. Siegert, *QCD matrix elements + parton showers: the NLO case*, *JHEP* **04** (2013) 027 [arXiv:1207.5030] [INSPIRE].

[72] S. Catani, F. Krauss, R. Kuhn and B.R. Webber, *QCD matrix elements + parton showers*, *JHEP* **11** (2001) 063 [hep-ph/0109231] [INSPIRE].

[73] S. Höche, F. Krauss, S. Schumann and F. Siegert, *QCD matrix elements and truncated showers*, *JHEP* **05** (2009) 053 [arXiv:0903.1219] [INSPIRE].

JHEP02(2024)197

[74] ATLAS collaboration, *Measurement of the Z/γ^* boson transverse momentum distribution in pp collisions at $\sqrt{s} = 7$ TeV with the ATLAS detector*, *JHEP* **09** (2014) 145 [arXiv:1406.3660] [INSPIRE].

[75] K. Hamilton, P. Nason and G. Zanderighi, *MINLO: Multi-scale Improved NLO*, *JHEP* **10** (2012) 155 [arXiv:1206.3572] [INSPIRE].

[76] G. Luisoni, P. Nason, C. Oleari and F. Tramontano, *$HW^{\pm}/HZ + 0$ and 1 jet at NLO with the POWHEG BOX interfaced to GoSam and their merging within MiNLO*, *JHEP* **10** (2013) 083 [arXiv:1306.2542] [INSPIRE].

[77] M.L. Ciccolini, S. Dittmaier and M. Krämer, *Electroweak radiative corrections to associated WH and ZH production at hadron colliders*, *Phys. Rev. D* **68** (2003) 073003 [hep-ph/0306234] [INSPIRE].

[78] O. Brein, A. Djouadi and R. Harlander, *NNLO QCD corrections to the Higgs-strahlung processes at hadron colliders*, *Phys. Lett. B* **579** (2004) 149 [hep-ph/0307206] [INSPIRE].

[79] G. Ferrera, M. Grazzini and F. Tramontano, *Associated WH production at hadron colliders: a fully exclusive QCD calculation at NNLO*, *Phys. Rev. Lett.* **107** (2011) 152003 [arXiv:1107.1164] [INSPIRE].

[80] O. Brein, R. Harlander, M. Wiesemann and T. Zirke, *Top-quark mediated effects in hadronic Higgs-strahlung*, *Eur. Phys. J. C* **72** (2012) 1868 [arXiv:1111.0761] [INSPIRE].

[81] G. Ferrera, M. Grazzini and F. Tramontano, *Higher-order QCD effects for associated WH production and decay at the LHC*, *JHEP* **04** (2014) 039 [arXiv:1312.1669] [INSPIRE].

[82] G. Ferrera, M. Grazzini and F. Tramontano, *Associated ZH production at hadron colliders: the fully differential NNLO QCD calculation*, *Phys. Lett. B* **740** (2015) 51 [arXiv:1407.4747] [INSPIRE].

[83] J.M. Campbell, R.K. Ellis and C. Williams, *Associated production of a Higgs boson at NNLO*, *JHEP* **06** (2016) 179 [arXiv:1601.00658] [INSPIRE].

[84] L. Altenkamp et al., *Gluon-induced Higgs-strahlung at next-to-leading order QCD*, *JHEP* **02** (2013) 078 [arXiv:1211.5015] [INSPIRE].

[85] R.V. Harlander, A. Kulesza, V. Theeuwes and T. Zirke, *Soft gluon resummation for gluon-induced Higgs Strahlung*, *JHEP* **11** (2014) 082 [arXiv:1410.0217] [INSPIRE].

[86] O. Brein, R.V. Harlander and T.J.E. Zirke, *vh@nnlo — Higgs Strahlung at hadron colliders*, *Comput. Phys. Commun.* **184** (2013) 998 [arXiv:1210.5347] [INSPIRE].

[87] LHC Higgs Cross Section Working Group collaboration, *Handbook of LHC Higgs cross sections: 4. Deciphering the nature of the Higgs sector*, arXiv:1610.07922 [DOI:10.23731/CYRM-2017-002] [INSPIRE].

[88] H.B. Hartanto, B. Jäger, L. Reina and D. Wackeroth, *Higgs boson production in association with top quarks in the POWHEG BOX*, *Phys. Rev. D* **91** (2015) 094003 [arXiv:1501.04498] [INSPIRE].

[89] ATLAS collaboration, *Vertex reconstruction performance of the ATLAS detector at $\sqrt{s} = 13$ TeV*, ATL-PHYS-PUB-2015-026, CERN, Geneva, Switzerland (2015) [INSPIRE].

[90] ATLAS collaboration, *Electron and photon performance measurements with the ATLAS detector using the* 2015–2017 *LHC proton-proton collision data*, 2019 *JINST* **14** P12006 [arXiv:1908.00005] [INSPIRE].

JHEP02(2024)197

[91] ATLAS collaboration, *Electron reconstruction and identification in the ATLAS experiment using the* 2015 *and* 2016 *LHC proton-proton collision data at* $\sqrt{s} = 13$ *TeV*, *Eur. Phys. J. C* **79** (2019) 639 [arXiv:1902.04655] [INSPIRE].

[92] ATLAS collaboration, *Muon reconstruction and identification efficiency in ATLAS using the full run* 2 *pp collision data set at* $\sqrt{s} = 13$ *TeV*, *Eur. Phys. J. C* **81** (2021) 578 [arXiv:2012.00578] [INSPIRE].

[93] ATLAS collaboration, *Reconstruction, energy calibration, and identification of hadronically decaying tau leptons in the ATLAS experiment for run-*2 *of the LHC*, ATL-PHYS-PUB-2015-045, CERN, Geneva, Switzerland (2015) [INSPIRE].

[94] M. Cacciari, G.P. Salam and G. Soyez, *The anti-*k_t *jet clustering algorithm*, *JHEP* **04** (2008) 063 [arXiv:0802.1189] [INSPIRE].

[95] M. Cacciari, G.P. Salam and G. Soyez, *FastJet user manual*, *Eur. Phys. J. C* **72** (2012) 1896 [arXiv:1111.6097] [INSPIRE].

[96] ATLAS collaboration, *Identification of hadronic tau lepton decays using neural networks in the ATLAS experiment*, ATL-PHYS-PUB-2019-033, CERN, Geneva, Switzerland (2019) [INSPIRE].

[97] ATLAS collaboration, *Jet reconstruction and performance using particle flow with the ATLAS detector*, *Eur. Phys. J. C* **77** (2017) 466 [arXiv:1703.10485] [INSPIRE].

[98] ATLAS collaboration, *Performance of pile-up mitigation techniques for jets in pp collisions at* $\sqrt{s} = 8$ *TeV using the ATLAS detector*, *Eur. Phys. J. C* **76** (2016) 581 [arXiv:1510.03823] [INSPIRE].

[99] ATLAS collaboration, *ATLAS b-jet identification performance and efficiency measurement with* $t\bar{t}$ *events in pp collisions at* $\sqrt{s} = 13$ *TeV*, *Eur. Phys. J. C* **79** (2019) 970 [arXiv:1907.05120] [INSPIRE].

[100] ATLAS collaboration, E_T^{miss} *performance in the ATLAS detector using* 2015–2016 *LHC pp collisions*, ATLAS-CONF-2018-023, CERN, Geneva, Switzerland (2018) [INSPIRE].

[101] ATLAS collaboration, *Object-based missing transverse momentum significance in the ATLAS detector*, ATLAS-CONF-2018-038, CERN, Geneva, Switzerland (2018) [INSPIRE].

[102] ATLAS collaboration, *Selection of jets produced in* 13 *TeV proton-proton collisions with the ATLAS detector*, ATLAS-CONF-2015-029, CERN, Geneva, Switzerland (2015) [INSPIRE].

[103] Particle Data Group collaboration, *Review of particle physics*, *PTEP* **2020** (2020) 083C01 [INSPIRE].

[104] ATLAS collaboration, *Jet energy scale and resolution measured in proton-proton collisions at* $\sqrt{s} = 13$ *TeV with the ATLAS detector*, *Eur. Phys. J. C* **81** (2021) 689 [arXiv:2007.02645] [INSPIRE].

[105] ATLAS collaboration, *Measurement of the c-jet mistagging efficiency in* $t\bar{t}$ *events using pp collision data at* $\sqrt{s} = 13$ *TeV collected with the ATLAS detector*, *Eur. Phys. J. C* **82** (2022) 95 [arXiv:2109.10627] [INSPIRE].

[106] ATLAS collaboration, *Calibration of light-flavour jet b-tagging rates on ATLAS proton-proton collision data at* $\sqrt{s} = 13$ *TeV*, ATLAS-CONF-2018-006, CERN, Geneva, Switzerland (2018) [INSPIRE].

[107] ATLAS collaboration, *Performance of missing transverse momentum reconstruction with the ATLAS detector using proton-proton collisions at* $\sqrt{s} = 13$ *TeV*, *Eur. Phys. J. C* **78** (2018) 903 [arXiv:1802.08168] [INSPIRE].

JHEP02(2024)197

[108] ATLAS collaboration, *Luminosity determination in pp collisions at $\sqrt{s} = 13$ TeV using the ATLAS detector at the LHC*, *Eur. Phys. J. C* **83** (2023) 982 [arXiv:2212.09379] [INSPIRE].

[109] G. Avoni et al., *The new LUCID-2 detector for luminosity measurement and monitoring in ATLAS*, 2018 *JINST* **13** P07017 [INSPIRE].

[110] J. Bellm et al., *Herwig* 7.1 *release note*, arXiv:1705.06919 [INSPIRE].

[111] M. Bähr et al., *Herwig++ physics and manual*, *Eur. Phys. J. C* **58** (2008) 639 [arXiv:0803.0883] [INSPIRE].

[112] J. Bellm et al., *Herwig* 7.0/*Herwig++* 3.0 *release note*, *Eur. Phys. J. C* **76** (2016) 196 [arXiv:1512.01178] [INSPIRE].

[113] J. Butterworth et al., *PDF4LHC recommendations for LHC run II*, *J. Phys. G* **43** (2016) 023001 [arXiv:1510.03865] [INSPIRE].

[114] G. Cowan, K. Cranmer, E. Gross and O. Vitells, *Asymptotic formulae for likelihood-based tests of new physics*, *Eur. Phys. J. C* **71** (2011) 1554 [*Erratum ibid.* **73** (2013) 2501] [arXiv:1007.1727] [INSPIRE].

[115] R.J. Barlow and C. Beeston, *Fitting using finite Monte Carlo samples*, *Comput. Phys. Commun.* **77** (1993) 219 [INSPIRE].

[116] A.L. Read, *Presentation of search results: the CL_s technique*, *J. Phys. G* **28** (2002) 2693 [INSPIRE].

[117] O. Vitells and E. Gross, *Estimating the significance of a signal in a multi-dimensional search*, *Astropart. Phys.* **35** (2011) 230 [arXiv:1105.4355] [INSPIRE].

[118] E. Gross and O. Vitells, *Trial factors for the look elsewhere effect in high energy physics*, *Eur. Phys. J. C* **70** (2010) 525 [arXiv:1005.1891] [INSPIRE].

[119] R.V. Harlander, S. Liebler and H. Mantler, *SusHi: a program for the calculation of Higgs production in gluon fusion and bottom-quark annihilation in the Standard Model and the MSSM*, *Comput. Phys. Commun.* **184** (2013) 1605 [arXiv:1212.3249] [INSPIRE].

[120] R. Harlander and P. Kant, *Higgs production and decay: analytic results at next-to-leading order QCD*, *JHEP* **12** (2005) 015 [hep-ph/0509189] [INSPIRE].

[121] R.V. Harlander and W.B. Kilgore, *Higgs boson production in bottom quark fusion at next-to-next-to leading order*, *Phys. Rev. D* **68** (2003) 013001 [hep-ph/0304035] [INSPIRE].

[122] R.V. Harlander and W.B. Kilgore, *Next-to-next-to-leading order Higgs production at hadron colliders*, *Phys. Rev. Lett.* **88** (2002) 201801 [hep-ph/0201206] [INSPIRE].

[123] S. Dawson, C.B. Jackson, L. Reina and D. Wackeroth, *Exclusive Higgs boson production with bottom quarks at hadron colliders*, *Phys. Rev. D* **69** (2004) 074027 [hep-ph/0311067] [INSPIRE].

[124] S. Dittmaier, M. Krämer and M. Spira, *Higgs radiation off bottom quarks at the Tevatron and the CERN LHC*, *Phys. Rev. D* **70** (2004) 074010 [hep-ph/0309204] [INSPIRE].

[125] R. Harlander, M. Krämer and M. Schumacher, *Bottom-quark associated Higgs-boson production: reconciling the four- and five-flavour scheme approach*, arXiv:1112.3478 [INSPIRE].

[126] D. Eriksson, J. Rathsman and O. Stal, *2HDMC: two-Higgs-doublet model calculator physics and manual*, *Comput. Phys. Commun.* **181** (2010) 189 [arXiv:0902.0851] [INSPIRE].

[127] DELPHES 3 collaboration, *DELPHES 3, a modular framework for fast simulation of a generic collider experiment*, *JHEP* **02** (2014) 057 [arXiv:1307.6346] [INSPIRE].

JHEP02(2024)197

[128] A. Buckley, D. Kar and K. Nordström, *Fast simulation of detector effects in Rivet*, *SciPost Phys.* **8** (2020) 025 [arXiv:1910.01637] [INSPIRE].

[129] C. Bierlich et al., *Robust Independent Validation of Experiment and Theory: Rivet version* 3, *SciPost Phys.* **8** (2020) 026 [arXiv:1912.05451] [INSPIRE].

[130] ATLAS collaboration, *ATLAS computing acknowledgements*, ATL-SOFT-PUB-2023-001, CERN, Geneva, Switzerland (2023).

JHEP02(2024)197

The ATLAS collaboration

G. Aad[102], B. Abbott[120], K. Abeling[55], N.J. Abicht[49], S.H. Abidi[29], A. Aboulhorma[35e], H. Abramowicz[151], H. Abreu[150], Y. Abulaiti[117], B.S. Acharya[69a,69b,m], C. Adam Bourdarios[4], L. Adamczyk[86a], S.V. Addepalli[26], M.J. Addison[101], J. Adelman[115], A. Adiguzel[21c], T. Adye[134], A.A. Affolder[136], Y. Afik[36], M.N. Agaras[13], J. Agarwala[73a,73b], A. Aggarwal[100], C. Agheorghiesei[27c], A. Ahmad[36], F. Ahmadov[38,y], W.S. Ahmed[104], S. Ahuja[95], X. Ai[62a], G. Aielli[76a,76b], A. Aikot[163], M. Ait Tamlihat[35e], B. Aitbenchikh[35a], I. Aizenberg[169], M. Akbiyik[100], T.P.A. Åkesson[98], A.V. Akimov[37], D. Akiyama[168], N.N. Akolkar[24], S. Aktas[21a], K. Al Khoury[41], G.L. Alberghi[23b], J. Albert[165], P. Albicocco[53], G.L. Albouy[60], S. Alderweireldt[52], M. Aleksa[36], I.N. Aleksandrov[38], C. Alexa[27b], T. Alexopoulos[10], F. Alfonsi[23b], M. Algren[56], M. Alhroob[120], B. Ali[132], H.M.J. Ali[91], S. Ali[148], S.W. Alibocus[92], M. Aliev[145], G. Alimonti[71a], W. Alkakhi[55], C. Allaire[66], B.M.M. Allbrooke[146], J.F. Allen[52], C.A. Allendes Flores[137f], P.P. Allport[20], A. Aloisio[72a,72b], F. Alonso[90], C. Alpigiani[138], M. Alvarez Estevez[99], A. Alvarez Fernandez[100], M. Alves Cardoso[56], M.G. Alviggi[72a,72b], M. Aly[101], Y. Amaral Coutinho[83b], A. Ambler[104], C. Amelung[36], M. Amerl[101], C.G. Ames[109], D. Amidei[106], S.P. Amor Dos Santos[130a], K.R. Amos[163], V. Ananiev[125], C. Anastopoulos[139], T. Andeen[11], J.K. Anders[36], S.Y. Andrean[47a,47b], A. Andreazza[71a,71b], S. Angelidakis[9], A. Angerami[41,ab], A.V. Anisenkov[37], A. Annovi[74a], C. Antel[56], M.T. Anthony[139], E. Antipov[145], M. Antonelli[53], F. Anulli[75a], M. Aoki[84], T. Aoki[153], J.A. Aparisi Pozo[163], M.A. Aparo[146], L. Aperio Bella[48], C. Appelt[18], A. Apyan[26], N. Aranzabal[36], S.J. Arbiol Val[87], C. Arcangeletti[53], A.T.H. Arce[51], E. Arena[92], J-F. Arguin[108], S. Argyropoulos[54], J.-H. Arling[48], O. Arnaez[4], H. Arnold[114], G. Artoni[75a,75b], H. Asada[111], K. Asai[118], S. Asai[153], N.A. Asbah[61], K. Assamagan[29], R. Astalos[28a], S. Atashi[160], R.J. Atkin[33a], M. Atkinson[162], H. Atmani[35f], P.A. Atmasiddha[128], K. Augsten[132], S. Auricchio[72a,72b], A.D. Auriol[20], V.A. Austrup[101], G. Avolio[36], K. Axiotis[56], G. Azuelos[108,af], D. Babal[28b], H. Bachacou[135], K. Bachas[152,p], A. Bachiu[34], F. Backman[47a,47b], A. Badea[61], T.M. Baer[106], P. Bagnaia[75a,75b], M. Bahmani[18], A.J. Bailey[163], V.R. Bailey[162], J.T. Baines[134], L. Baines[94], O.K. Baker[172], E. Bakos[15], D. Bakshi Gupta[8], V. Balakrishnan[120], R. Balasubramanian[114], E.M. Baldin[37], P. Balek[86a], E. Ballabene[23b,23a], F. Balli[135], L.M. Baltes[63a], W.K. Balunas[32], J. Balz[100], E. Banas[87], M. Bandieramonte[129], A. Bandyopadhyay[24], S. Bansal[24], L. Barak[151], M. Barakat[48], E.L. Barberio[105], D. Barberis[57b,57a], M. Barbero[102], M.Z. Barel[114], K.N. Barends[33a], T. Barillari[110], M-S. Barisits[36], T. Barklow[143], P. Baron[122], D.A. Baron Moreno[101], A. Baroncelli[62a], G. Barone[29], A.J. Barr[126], J.D. Barr[96], L. Barranco Navarro[47a,47b], F. Barreiro[99], J. Barreiro Guimarães da Costa[14a], U. Barron[151], M.G. Barros Teixeira[130a], S. Barsov[37], F. Bartels[63a], R. Bartoldus[143], A.E. Barton[91], P. Bartos[28a], A. Basan[100], M. Baselga[49], A. Bassalat[66,b], M.J. Basso[156a], C.R. Basson[101], R.L. Bates[59], S. Batlamous[35e], J.R. Batley[32], B. Batool[141], M. Battaglia[136], D. Battulga[18], M. Bauce[75a,75b], M. Bauer[36], P. Bauer[24], L.T. Bazzano Hurrell[30], J.B. Beacham[51], T. Beau[127], J.Y. Beaucamp[90], P.H. Beauchemin[158], F. Becherer[54], P. Bechtle[24], H.P. Beck[19,o], K. Becker[167], A.J. Beddall[82], V.A. Bednyakov[38], C.P. Bee[145], L.J. Beemster[15],

JHEP02(2024)197

T.A. Beermann[36], M. Begalli[83d], M. Begel[29], A. Behera[145], J.K. Behr[48], J.F. Beirer[36], F. Beisiegel[24], M. Belfkir[159], G. Bella[151], L. Bellagamba[23b], A. Bellerive[34], P. Bellos[20], K. Beloborodov[37], D. Benchekroun[35a], F. Bendebba[35a], Y. Benhammou[151], M. Benoit[29], J.R. Bensinger[26], S. Bentvelsen[114], L. Beresford[48], M. Beretta[53], E. Bergeaas Kuutmann[161], N. Berger[4], B. Bergmann[132], J. Beringer[17a], G. Bernardi[5], C. Bernius[143], F.U. Bernlochner[24], F. Bernon[36,102], A. Berrocal Guardia[13], T. Berry[95], P. Berta[133], A. Berthold[50], I.A. Bertram[91], S. Bethke[110], A. Betti[75a,75b], A.J. Bevan[94], N.K. Bhalla[54], M. Bhamjee[33c], S. Bhatta[145], D.S. Bhattacharya[166], P. Bhattarai[143], V.S. Bhopatkar[121], R. Bi[29,ai], R.M. Bianchi[129], G. Bianco[23b,23a], O. Biebel[109], R. Bielski[123], M. Biglietti[77a], M. Bindi[55], A. Bingul[21b], C. Bini[75a,75b], A. Biondini[92], C.J. Birch-sykes[101], G.A. Bird[20,134], M. Birman[169], M. Biros[133], S. Biryukov[146], T. Bisanz[49], E. Bisceglie[43b,43a], J.P. Biswal[134], D. Biswas[141], A. Bitadze[101], K. Bjørke[125], I. Bloch[48], A. Blue[59], U. Blumenschein[94], J. Blumenthal[100], G.J. Bobbink[114], V.S. Bobrovnikov[37], M. Boehler[54], B. Boehm[166], D. Bogavac[36], A.G. Bogdanchikov[37], C. Bohm[47a], V. Boisvert[95], P. Bokan[48], T. Bold[86a], M. Bomben[5], M. Bona[94], M. Boonekamp[135], C.D. Booth[95], A.G. Borbély[59], I.S. Bordulev[37], H.M. Borecka-Bielska[108], G. Borissov[91], D. Bortoletto[126], D. Boscherini[23b], M. Bosman[13], J.D. Bossio Sola[36], K. Bouaouda[35a], N. Bouchhar[163], J. Boudreau[129], E.V. Bouhova-Thacker[91], D. Boumediene[40], R. Bouquet[165], A. Boveia[119], J. Boyd[36], D. Boye[29], I.R. Boyko[38], J. Bracinik[20], N. Brahimi[62d], G. Brandt[171], O. Brandt[32], F. Braren[48], B. Brau[103], J.E. Brau[123], R. Brener[169], L. Brenner[114], R. Brenner[161], S. Bressler[169], D. Britton[59], D. Britzger[110], I. Brock[24], G. Brooijmans[41], W.K. Brooks[137f], E. Brost[29], L.M. Brown[165], L.E. Bruce[61], T.L. Bruckler[126], P.A. Bruckman de Renstrom[87], B. Brüers[48], A. Bruni[23b], G. Bruni[23b], M. Bruschi[23b], N. Bruscino[75a,75b], T. Buanes[16], Q. Buat[138], D. Buchin[110], A.G. Buckley[59], O. Bulekov[37], B.A. Bullard[143], S. Burdin[92], C.D. Burgard[49], A.M. Burger[40], B. Burghgrave[8], O. Burlayenko[54], J.T.P. Burr[32], C.D. Burton[11], J.C. Burzynski[142], E.L. Busch[41], V. Büscher[100], P.J. Bussey[59], J.M. Butler[25], C.M. Buttar[59], J.M. Butterworth[96], W. Buttinger[134], C.J. Buxo Vazquez[107], A.R. Buzykaev[37], S. Cabrera Urbán[163], L. Cadamuro[66], D. Caforio[58], H. Cai[129], Y. Cai[14a,14e], Y. Cai[14c], V.M.M. Cairo[36], O. Cakir[3a], N. Calace[36], P. Calafiura[17a], G. Calderini[127], P. Calfayan[68], G. Callea[59], L.P. Caloba[83b], D. Calvet[40], S. Calvet[40], T.P. Calvet[102], M. Calvetti[74a,74b], R. Camacho Toro[127], S. Camarda[36], D. Camarero Munoz[26], P. Camarri[76a,76b], M.T. Camerlingo[72a,72b], D. Cameron[36], C. Camincher[165], M. Campanelli[96], A. Camplani[42], V. Canale[72a,72b], A. Canesse[104], J. Cantero[163], Y. Cao[162], F. Capocasa[26], M. Capua[43b,43a], A. Carbone[71a,71b], R. Cardarelli[76a], J.C.J. Cardenas[8], F. Cardillo[163], G. Carducci[43b,43a], T. Carli[36], G. Carlino[72a], J.I. Carlotto[13], B.T. Carlson[129,q], E.M. Carlson[165,156a], L. Carminati[71a,71b], A. Carnelli[135], M. Carnesale[75a,75b], S. Caron[113], E. Carquin[137f], S. Carrá[71a], G. Carratta[23b,23a], F. Carrio Argos[33g], J.W.S. Carter[155], T.M. Carter[52], M.P. Casado[13,i], M. Caspar[48], F.L. Castillo[4], L. Castillo Garcia[13], V. Castillo Gimenez[163], N.F. Castro[130a,130e], A. Catinaccio[36], J.R. Catmore[125], V. Cavaliere[29], N. Cavalli[23b,23a], V. Cavasinni[74a,74b], Y.C. Cekmecelioglu[48], E. Celebi[21a], F. Celli[126], M.S. Centonze[70a,70b], V. Cepaitis[56],

JHEP02(2024)197

K. Cerny[122], A.S. Cerqueira[83a], A. Cerri[146], L. Cerrito[76a,76b], F. Cerutti[17a], B. Cervato[141], A. Cervelli[23b], G. Cesarini[53], S.A. Cetin[82], D. Chakraborty[115], J. Chan[170], W.Y. Chan[153], J.D. Chapman[32], E. Chapon[135], B. Chargeishvili[149b], D.G. Charlton[20], T.P. Charman[94], M. Chatterjee[19], C. Chauhan[133], S. Chekanov[6], S.V. Chekulaev[156a], G.A. Chelkov[38,a], A. Chen[106], B. Chen[151], B. Chen[165], H. Chen[14c], H. Chen[29], J. Chen[62c], J. Chen[142], M. Chen[126], S. Chen[153], S.J. Chen[14c], X. Chen[62c,135], X. Chen[14b,ae], Y. Chen[62a], C.L. Cheng[170], H.C. Cheng[64a], S. Cheong[143], A. Cheplakov[38], E. Cheremushkina[48], E. Cherepanova[114], R. Cherkaoui El Moursli[35e], E. Cheu[7], K. Cheung[65], L. Chevalier[135], V. Chiarella[53], G. Chiarelli[74a], N. Chiedde[102], G. Chiodini[70a], A.S. Chisholm[20], A. Chitan[27b], M. Chitishvili[163], M.V. Chizhov[38], K. Choi[11], A.R. Chomont[75a,75b], Y. Chou[103], E.Y.S. Chow[113], T. Chowdhury[33g], K.L. Chu[169], M.C. Chu[64a], X. Chu[14a,14e], J. Chudoba[131], J.J. Chwastowski[87], D. Cieri[110], K.M. Ciesla[86a], V. Cindro[93], A. Ciocio[17a], F. Cirotto[72a,72b], Z.H. Citron[169,k], M. Citterio[71a], D.A. Ciubotaru[27b], A. Clark[56], P.J. Clark[52], C. Clarry[155], J.M. Clavijo Columbie[48], S.E. Clawson[48], C. Clement[47a,47b], J. Clercx[48], Y. Coadou[102], M. Cobal[69a,69c], A. Coccaro[57b], R.F. Coelho Barrue[130a], R. Coelho Lopes De Sa[103], S. Coelli[71a], A.E.C. Coimbra[71a,71b], B. Cole[41], J. Collot[60], P. Conde Muiño[130a,130g], M.P. Connell[33c], S.H. Connell[33c], I.A. Connelly[59], E.I. Conroy[126], F. Conventi[72a,ag], H.G. Cooke[20], A.M. Cooper-Sarkar[126], A. Cordeiro Oudot Choi[127], L.D. Corpe[40], M. Corradi[75a,75b], F. Corriveau[104,w], A. Cortes-Gonzalez[18], M.J. Costa[163], F. Costanza[4], D. Costanzo[139], B.M. Cote[119], G. Cowan[95], K. Cranmer[170], D. Cremonini[23b,23a], S. Crépé-Renaudin[60], F. Crescioli[127], M. Cristinziani[141], M. Cristoforetti[78a,78b], V. Croft[114], J.E. Crosby[121], G. Crosetti[43b,43a], A. Cueto[99], T. Cuhadar Donszelmann[160], H. Cui[14a,14e], Z. Cui[7], W.R. Cunningham[59], F. Curcio[43b,43a], P. Czodrowski[36], M.M. Czurylo[63b], M.J. Da Cunha Sargedas De Sousa[57b,57a], J.V. Da Fonseca Pinto[83b], C. Da Via[101], W. Dabrowski[86a], T. Dado[49], S. Dahbi[33g], T. Dai[106], D. Dal Santo[19], C. Dallapiccola[103], M. Dam[42], G. D'amen[29], V. D'Amico[109], J. Damp[100], J.R. Dandoy[34], M.F. Daneri[30], M. Danninger[142], V. Dao[36], G. Darbo[57b], S. Darmora[6], S.J. Das[29,ai], S. D'Auria[71a,71b], C. David[156b], T. Davidek[133], B. Davis-Purcell[34], I. Dawson[94], H.A. Day-hall[132], K. De[8], R. De Asmundis[72a], N. De Biase[48], S. De Castro[23b,23a], N. De Groot[113], P. de Jong[114], H. De la Torre[115], A. De Maria[14c], A. De Salvo[75a], U. De Sanctis[76a,76b], A. De Santo[146], J.B. De Vivie De Regie[60], D.V. Dedovich[38], J. Degens[114], A.M. Deiana[44], F. Del Corso[23b,23a], J. Del Peso[99], F. Del Rio[63a], F. Deliot[135], C.M. Delitzsch[49], M. Della Pietra[72a,72b], D. Della Volpe[56], A. Dell'Acqua[36], L. Dell'Asta[71a,71b], M. Delmastro[4], P.A. Delsart[60], S. Demers[172], M. Demichev[38], S.P. Denisov[37], L. D'Eramo[40], D. Derendarz[87], F. Derue[127], P. Dervan[92], K. Desch[24], C. Deutsch[24], F.A. Di Bello[57b,57a], A. Di Ciaccio[76a,76b], L. Di Ciaccio[4], A. Di Domenico[75a,75b], C. Di Donato[72a,72b], A. Di Girolamo[36], G. Di Gregorio[36], A. Di Luca[78a,78b], B. Di Micco[77a,77b], R. Di Nardo[77a,77b], C. Diaconu[102], M. Diamantopoulou[34], F.A. Dias[114], T. Dias Do Vale[142], M.A. Diaz[137a,137b], F.G. Diaz Capriles[24], M. Didenko[163], E.B. Diehl[106], L. Diehl[54], S. Díez Cornell[48], C. Diez Pardos[141], C. Dimitriadi[161,24], A. Dimitrievska[17a], J. Dingfelder[24], I-M. Dinu[27b], S.J. Dittmeier[63b], F. Dittus[36], F. Djama[102], T. Djobava[149b], J.I. Djuvsland[16],

JHEP02(2024)197

C. Doglioni[101,98], A. Dohnalova[28a], J. Dolejsi[133], Z. Dolezal[133], K.M. Dona[39], M. Donadelli[83c], B. Dong[107], J. Donini[40], A. D'Onofrio[72a,72b], M. D'Onofrio[92], J. Dopke[134], A. Doria[72a], N. Dos Santos Fernandes[130a], P. Dougan[101], M.T. Dova[90], A.T. Doyle[59], M.A. Draguet[126], E. Dreyer[169], I. Drivas-koulouris[10], M. Drnevich[117], A.S. Drobac[158], M. Drozdova[56], D. Du[62a], T.A. du Pree[114], F. Dubinin[37], M. Dubovsky[28a], E. Duchovni[169], G. Duckeck[109], O.A. Ducu[27b], D. Duda[52], A. Dudarev[36], E.R. Duden[26], M. D'uffizi[101], L. Duflot[66], M. Dührssen[36], C. Dülsen[171], A.E. Dumitriu[27b], M. Dunford[63a], S. Dungs[49], K. Dunne[47a,47b], A. Duperrin[102], H. Duran Yildiz[3a], M. Düren[58], A. Durglishvili[149b], B.L. Dwyer[115], G.I. Dyckes[17a], M. Dyndal[86a], B.S. Dziedzic[87], Z.O. Earnshaw[146], G.H. Eberwein[126], B. Eckerova[28a], S. Eggebrecht[55], E. Egidio Purcino De Souza[127], L.F. Ehrke[56], G. Eigen[16], K. Einsweiler[17a], T. Ekelof[161], P.A. Ekman[98], S. El Farkh[35b], Y. El Ghazali[35b], H. El Jarrari[36], A. El Moussaouy[108], V. Ellajosyula[161], M. Ellert[161], F. Ellinghaus[171], N. Ellis[36], J. Elmsheuser[29], M. Elsing[36], D. Emeliyanov[134], Y. Enari[153], I. Ene[17a], S. Epari[13], J. Erdmann[49], P.A. Erland[87], M. Errenst[171], M. Escalier[66], C. Escobar[163], E. Etzion[151], G. Evans[130a], H. Evans[68], L.S. Evans[95], M.O. Evans[146], A. Ezhilov[37], S. Ezzarqtouni[35a], F. Fabbri[59], L. Fabbri[23b,23a], G. Facini[96], V. Fadeyev[136], R.M. Fakhrutdinov[37], S. Falciano[75a], L.F. Falda Ulhoa Coelho[36], P.J. Falke[24], J. Faltova[133], C. Fan[162], Y. Fan[14a], Y. Fang[14a,14e], M. Fanti[71a,71b], M. Faraj[69a,69b], Z. Farazpay[97], A. Farbin[8], A. Farilla[77a], T. Farooque[107], S.M. Farrington[52], F. Fassi[35e], D. Fassouliotis[9], M. Faucci Giannelli[76a,76b], W.J. Fawcett[32], L. Fayard[66], P. Federic[133], P. Federicova[131], O.L. Fedin[37,a], G. Fedotov[37], M. Feickert[170], L. Feligioni[102], D.E. Fellers[123], C. Feng[62b], M. Feng[14b], Z. Feng[114], M.J. Fenton[160], A.B. Fenyuk[37], L. Ferencz[48], R.A.M. Ferguson[91], S.I. Fernandez Luengo[137f], P. Fernandez Martinez[13], M.J.V. Fernoux[102], J. Ferrando[48], A. Ferrari[161], P. Ferrari[114,113], R. Ferrari[73a], D. Ferrere[56], C. Ferretti[106], F. Fiedler[100], P. Fiedler[132], A. Filipčič[93], E.K. Filmer[1], F. Filthaut[113], M.C.N. Fiolhais[130a,130c,c], L. Fiorini[163], W.C. Fisher[107], T. Fitschen[101], P.M. Fitzhugh[135], I. Fleck[141], P. Fleischmann[106], T. Flick[171], M. Flores[33d,ac], L.R. Flores Castillo[64a], L. Flores Sanz De Acedo[36], F.M. Follega[78a,78b], N. Fomin[16], J.H. Foo[155], B.C. Forland[68], A. Formica[135], A.C. Forti[101], E. Fortin[36], A.W. Fortman[61], M.G. Foti[17a], L. Fountas[9,j], D. Fournier[66], H. Fox[91], P. Francavilla[74a,74b], S. Francescato[61], S. Franchellucci[56], M. Franchini[23b,23a], S. Franchino[63a], D. Francis[36], L. Franco[113], V. Franco Lima[36], L. Franconi[48], M. Franklin[61], G. Frattari[26], A.C. Freegard[94], W.S. Freund[83b], Y.Y. Frid[151], J. Friend[59], N. Fritzsche[50], A. Froch[54], D. Froidevaux[36], J.A. Frost[126], Y. Fu[62a], S. Fuenzalida Garrido[137f], M. Fujimoto[102], K.Y. Fung[64a], E. Furtado De Simas Filho[83b], M. Furukawa[153], J. Fuster[163], A. Gabrielli[23b,23a], A. Gabrielli[155], P. Gadow[36], G. Gagliardi[57b,57a], L.G. Gagnon[17a], E.J. Gallas[126], B.J. Gallop[134], K.K. Gan[119], S. Ganguly[153], Y. Gao[52], F.M. Garay Walls[137a,137b], B. Garcia[29], C. García[163], A. Garcia Alonso[114], A.G. Garcia Caffaro[172], J.E. García Navarro[163], M. Garcia-Sciveres[17a], G.L. Gardner[128], R.W. Gardner[39], N. Garelli[158], D. Garg[80], R.B. Garg[143,n], J.M. Gargan[52], C.A. Garner[155], C.M. Garvey[33a], P. Gaspar[83b], V.K. Gassmann[158], G. Gaudio[73a], V. Gautam[13], P. Gauzzi[75a,75b], I.L. Gavrilenko[37], A. Gavrilyuk[37], C. Gay[164], G. Gaycken[48],

JHEP02(2024)197

E.N. Gazis[10], A.A. Geanta[27b], C.M. Gee[136], A. Gekow[119], C. Gemme[57b], M.H. Genest[60], S. Gentile[75a,75b], A.D. Gentry[112], S. George[95], W.F. George[20], T. Geralis[46], P. Gessinger-Befurt[36], M.E. Geyik[171], M. Ghani[167], M. Ghneimat[141], K. Ghorbanian[94], A. Ghosal[141], A. Ghosh[160], A. Ghosh[7], B. Giacobbe[23b], S. Giagu[75a,75b], T. Giani[114], P. Giannetti[74a], A. Giannini[62a], S.M. Gibson[95], M. Gignac[136], D.T. Gil[86b], A.K. Gilbert[86a], B.J. Gilbert[41], D. Gillberg[34], G. Gilles[114], N.E.K. Gillwald[48], L. Ginabat[127], D.M. Gingrich[2,af], M.P. Giordani[69a,69c], P.F. Giraud[135], G. Giugliarelli[69a,69c], D. Giugni[71a], F. Giuli[36], I. Gkialas[9,j], L.K. Gladilin[37], C. Glasman[99], G.R. Gledhill[123], G. Glemža[48], M. Glisic[123], I. Gnesi[43b,f], Y. Go[29,ai], M. Goblirsch-Kolb[36], B. Gocke[49], D. Godin[108], B. Gokturk[21a], S. Goldfarb[105], T. Golling[56], M.G.D. Gololo[33g], D. Golubkov[37], J.P. Gombas[107], A. Gomes[130a,130b], G. Gomes Da Silva[141], A.J. Gomez Delegido[163], R. Gonçalo[130a,130c], G. Gonella[123], L. Gonella[20], A. Gongadze[149c], F. Gonnella[20], J.L. Gonski[41], R.Y. González Andana[52], S. González de la Hoz[163], S. Gonzalez Fernandez[13], R. Gonzalez Lopez[92], C. Gonzalez Renteria[17a], M.V. Gonzalez Rodrigues[48], R. Gonzalez Suarez[161], S. Gonzalez-Sevilla[56], G.R. Gonzalvo Rodriguez[163], L. Goossens[36], B. Gorini[36], E. Gorini[70a,70b], A. Gorišek[93], T.C. Gosart[128], A.T. Goshaw[51], M.I. Gostkin[38], S. Goswami[121], C.A. Gottardo[36], S.A. Gotz[109], M. Gouighri[35b], V. Goumarre[48], A.G. Goussiou[138], N. Govender[33c], I. Grabowska-Bold[86a], K. Graham[34], E. Gramstad[125], S. Grancagnolo[70a,70b], M. Grandi[146], C.M. Grant[1,135], P.M. Gravila[27f], F.G. Gravili[70a,70b], H.M. Gray[17a], M. Greco[70a,70b], C. Grefe[24], I.M. Gregor[48], P. Grenier[143], S.G. Grewe[110], C. Grieco[13], A.A. Grillo[136], K. Grimm[31], S. Grinstein[13,s], J.-F. Grivaz[66], E. Gross[169], J. Grosse-Knetter[55], C. Grud[106], J.C. Grundy[126], L. Guan[106], W. Guan[29], C. Gubbels[164], J.G.R. Guerrero Rojas[163], G. Guerrieri[69a,69c], F. Guescini[110], R. Gugel[100], J.A.M. Guhit[106], A. Guida[18], E. Guilloton[167,134], S. Guindon[36], F. Guo[14a,14e], J. Guo[62c], L. Guo[48], Y. Guo[106], R. Gupta[48], R. Gupta[129], S. Gurbuz[24], S.S. Gurdasani[54], G. Gustavino[36], M. Guth[56], P. Gutierrez[120], L.F. Gutierrez Zagazeta[128], M. Gutsche[50], C. Gutschow[96], C. Gwenlan[126], C.B. Gwilliam[92], E.S. Haaland[125], A. Haas[117], M. Habedank[48], C. Haber[17a], H.K. Hadavand[8], A. Hadef[50], S. Hadzic[110], A.I. Hagan[91], J.J. Hahn[141], E.H. Haines[96], M. Haleem[166], J. Haley[121], J.J. Hall[139], G.D. Hallewell[102], L. Halser[19], K. Hamano[165], M. Hamer[24], G.N. Hamity[52], E.J. Hampshire[95], J. Han[62b], K. Han[62a], L. Han[14c], L. Han[62a], S. Han[17a], Y.F. Han[155], K. Hanagaki[84], M. Hance[136], D.A. Hangal[41,ab], H. Hanif[142], M.D. Hank[128], R. Hankache[101], J.B. Hansen[42], J.D. Hansen[42], P.H. Hansen[42], K. Hara[157], D. Harada[56], T. Harenberg[171], S. Harkusha[37], M.L. Harris[103], Y.T. Harris[126], J. Harrison[13], N.M. Harrison[119], P.F. Harrison[167], N.M. Hartman[110], N.M. Hartmann[109], Y. Hasegawa[140], R. Hauser[107], C.M. Hawkes[20], R.J. Hawkings[36], Y. Hayashi[153], S. Hayashida[111], D. Hayden[107], C. Hayes[106], R.L. Hayes[114], C.P. Hays[126], J.M. Hays[94], H.S. Hayward[92], F. He[62a], M. He[14a,14e], Y. He[154], Y. He[48], N.B. Heatley[94], V. Hedberg[98], A.L. Heggelund[125], N.D. Hehir[94,*], C. Heidegger[54], K.K. Heidegger[54], W.D. Heidorn[81], J. Heilman[34], S. Heim[48], T. Heim[17a], J.G. Heinlein[128], J.J. Heinrich[123], L. Heinrich[110,ad], J. Hejbal[131], L. Helary[48], A. Held[170], S. Hellesund[16], C.M. Helling[164], S. Hellman[47a,47b], R.C.W. Henderson[91], L. Henkelmann[32], A.M. Henriques Correia[36],

JHEP02(2024)197

H. Herde[98], Y. Hernández Jiménez[145], L.M. Herrmann[24], T. Herrmann[50], G. Herten[54], R. Hertenberger[109], L. Hervas[36], M.E. Hesping[100], N.P. Hessey[156a], H. Hibi[85], E. Hill[155], S.J. Hillier[20], J.R. Hinds[107], F. Hinterkeuser[24], M. Hirose[124], S. Hirose[157], D. Hirschbuehl[171], T.G. Hitchings[101], B. Hiti[93], J. Hobbs[145], R. Hobincu[27e], N. Hod[169], M.C. Hodgkinson[139], B.H. Hodkinson[32], A. Hoecker[36], D.D. Hofer[106], J. Hofer[48], T. Holm[24], M. Holzbock[110], L.B.A.H. Hommels[32], B.P. Honan[101], J. Hong[62c], T.M. Hong[129], B.H. Hooberman[162], W.H. Hopkins[6], Y. Horii[111], S. Hou[148], A.S. Howard[93], J. Howarth[59], J. Hoya[6], M. Hrabovsky[122], A. Hrynevich[48], T. Hryn'ova[4], P.J. Hsu[65], S.-C. Hsu[138], Q. Hu[62a], Y.F. Hu[14a,14e], S. Huang[64b], X. Huang[14c], X. Huang[14a,14e], Y. Huang[139], Y. Huang[14a], Z. Huang[101], Z. Hubacek[132], M. Huebner[24], F. Huegging[24], T.B. Huffman[126], C.A. Hugli[48], M. Huhtinen[36], S.K. Huiberts[16], R. Hulsken[104], N. Huseynov[12], J. Huston[107], J. Huth[61], R. Hyneman[143], G. Iacobucci[56], G. Iakovidis[29], I. Ibragimov[141], L. Iconomidou-Fayard[66], P. Iengo[72a,72b], R. Iguchi[153], T. Iizawa[126], Y. Ikegami[84], N. Ilic[155], H. Imam[35a], M. Ince Lezki[56], T. Ingebretsen Carlson[47a,47b], G. Introzzi[73a,73b], M. Iodice[77a], V. Ippolito[75a,75b], R.K. Irwin[92], M. Ishino[153], W. Islam[170], C. Issever[18,48], S. Istin[21a,ak], H. Ito[168], J.M. Iturbe Ponce[64a], R. Iuppa[78a,78b], A. Ivina[169], J.M. Izen[45], V. Izzo[72a], P. Jacka[131,132], P. Jackson[1], R.M. Jacobs[48], B.P. Jaeger[142], C.S. Jagfeld[109], G. Jain[156a], P. Jain[54], K. Jakobs[54], T. Jakoubek[169], J. Jamieson[59], K.W. Janas[86a], M. Javurkova[103], F. Jeanneau[135], L. Jeanty[123], J. Jejelava[149a,z], P. Jenni[54,g], C.E. Jessiman[34], S. Jézéquel[4], C. Jia[62b], J. Jia[145], X. Jia[61], X. Jia[14a,14e], Z. Jia[14c], S. Jiggins[48], J. Jimenez Pena[13], S. Jin[14c], A. Jinaru[27b], O. Jinnouchi[154], P. Johansson[139], K.A. Johns[7], J.W. Johnson[136], D.M. Jones[32], E. Jones[48], P. Jones[32], R.W.L. Jones[91], T.J. Jones[92], H.L. Joos[55,36], R. Joshi[119], J. Jovicevic[15], X. Ju[17a], J.J. Junggeburth[103], T. Junkermann[63a], A. Juste Rozas[13,s], M.K. Juzek[87], S. Kabana[137e], A. Kaczmarska[87], M. Kado[110], H. Kagan[119], M. Kagan[143], A. Kahn[41], A. Kahn[128], C. Kahra[100], T. Kaji[153], E. Kajomovitz[150], N. Kakati[169], I. Kalaitzidou[54], C.W. Kalderon[29], A. Kamenshchikov[155], N.J. Kang[136], D. Kar[33g], K. Karava[126], M.J. Kareem[156b], E. Karentzos[54], I. Karkanias[152], O. Karkout[114], S.N. Karpov[38], Z.M. Karpova[38], V. Kartvelishvili[91], A.N. Karyukhin[37], E. Kasimi[152], J. Katzy[48], S. Kaur[34], K. Kawade[140], M.P. Kawale[120], C. Kawamoto[88], T. Kawamoto[62a], E.F. Kay[36], F.I. Kaya[158], S. Kazakos[107], V.F. Kazanin[37], Y. Ke[145], J.M. Keaveney[33a], R. Keeler[165], G.V. Kehris[61], J.S. Keller[34], A.S. Kelly[96], J.J. Kempster[146], K.E. Kennedy[41], P.D. Kennedy[100], O. Kepka[131], B.P. Kerridge[167], S. Kersten[171], B.P. Kerševan[93], S. Keshri[66], L. Keszeghova[28a], S. Ketabchi Haghighat[155], R.A. Khan[129], M. Khandoga[127], A. Khanov[121], A.G. Kharlamov[37], T. Kharlamova[37], E.E. Khoda[138], M. Kholodenko[37], T.J. Khoo[18], G. Khoriauli[166], J. Khubua[149b], Y.A.R. Khwaira[66], A. Kilgallon[123], D.W. Kim[47a,47b], Y.K. Kim[39], N. Kimura[96], M.K. Kingston[55], A. Kirchhoff[55], C. Kirfel[24], F. Kirfel[24], J. Kirk[134], A.E. Kiryunin[110], C. Kitsaki[10], O. Kivernyk[24], M. Klassen[63a], C. Klein[34], L. Klein[166], M.H. Klein[106], M. Klein[92], S.B. Klein[56], U. Klein[92], P. Klimek[36], A. Klimentov[29], T. Klioutchnikova[36], P. Kluit[114], S. Kluth[110], E. Kneringer[79], T.M. Knight[155], A. Knue[49], R. Kobayashi[88], D. Kobylianskii[169], S.F. Koch[126], M. Kocian[143], P. Kodyš[133], D.M. Koeck[123], P.T. Koenig[24], T. Koffas[34],

JHEP02(2024)197

O. Kolay[50], I. Koletsou[4], T. Komarek[122], K. Köneke[54], A.X.Y. Kong[1], T. Kono[118], N. Konstantinidis[96], P. Kontaxakis[56], B. Konya[98], R. Kopeliansky[68], S. Koperny[86a], K. Korcyl[87], K. Kordas[152,e], G. Koren[151], A. Korn[96], S. Korn[55], I. Korolkov[13], N. Korotkova[37], B. Kortman[114], O. Kortner[110], S. Kortner[110], W.H. Kostecka[115], V.V. Kostyukhin[141], A. Kotsokechagia[135], A. Kotwal[51], A. Koulouris[36], A. Kourkoumeli-Charalampidi[73a,73b], C. Kourkoumelis[9], E. Kourlitis[110,ad], O. Kovanda[146], R. Kowalewski[165], W. Kozanecki[135], A.S. Kozhin[37], V.A. Kramarenko[37], G. Kramberger[93], P. Kramer[100], M.W. Krasny[127], A. Krasznahorkay[36], J.W. Kraus[171], J.A. Kremer[48], T. Kresse[50], J. Kretzschmar[92], K. Kreul[18], P. Krieger[155], S. Krishnamurthy[103], M. Krivos[133], K. Krizka[20], K. Kroeninger[49], H. Kroha[110], J. Kroll[131], J. Kroll[128], K.S. Krowpman[107], U. Kruchonak[38], H. Krüger[24], N. Krumnack[81], M.C. Kruse[51], O. Kuchinskaia[37], S. Kuday[3a], S. Kuehn[36], R. Kuesters[54], T. Kuhl[48], V. Kukhtin[38], Y. Kulchitsky[37,a], S. Kuleshov[137d,137b], M. Kumar[33g], N. Kumari[48], A. Kupco[131], T. Kupfer[49], A. Kupich[37], O. Kuprash[54], H. Kurashige[85], L.L. Kurchaninov[156a], O. Kurdysh[66], Y.A. Kurochkin[37], A. Kurova[37], M. Kuze[154], A.K. Kvam[103], J. Kvita[122], T. Kwan[104], N.G. Kyriacou[106], L.A.O. Laatu[102], C. Lacasta[163], F. Lacava[75a,75b], H. Lacker[18], D. Lacour[127], N.N. Lad[96], E. Ladygin[38], B. Laforge[127], T. Lagouri[137e], F.Z. Lahbabi[35a], S. Lai[55], I.K. Lakomiec[86a], N. Lalloue[60], J.E. Lambert[165], S. Lammers[68], W. Lampl[7], C. Lampoudis[152,e], A.N. Lancaster[115], E. Lançon[29], U. Landgraf[54], M.P.J. Landon[94], V.S. Lang[54], R.J. Langenberg[103], O.K.B. Langrekken[125], A.J. Lankford[160], F. Lanni[36], K. Lantzsch[24], A. Lanza[73a], A. Lapertosa[57b,57a], J.F. Laporte[135], T. Lari[71a], F. Lasagni Manghi[23b], M. Lassnig[36], V. Latonova[131], A. Laudrain[100], A. Laurier[150], S.D. Lawlor[139], Z. Lawrence[101], R. Lazaridou[167], M. Lazzaroni[71a,71b], B. Le[101], E.M. Le Boulicaut[51], B. Leban[93], A. Lebedev[81], M. LeBlanc[101], F. Ledroit-Guillon[60], A.C.A. Lee[96], S.C. Lee[148], S. Lee[47a,47b], T.F. Lee[92], L.L. Leeuw[33c], H.P. Lefebvre[95], M. Lefebvre[165], C. Leggett[17a], G. Lehmann Miotto[36], M. Leigh[56], W.A. Leight[103], W. Leinonen[113], A. Leisos[152,r], M.A.L. Leite[83c], C.E. Leitgeb[48], R. Leitner[133], K.J.C. Leney[44], T. Lenz[24], S. Leone[74a], C. Leonidopoulos[52], A. Leopold[144], C. Leroy[108], R. Les[107], C.G. Lester[32], M. Levchenko[37], J. Levêque[4], D. Levin[106], L.J. Levinson[169], M.P. Lewicki[87], D.J. Lewis[4], A. Li[5], B. Li[62b], C. Li[62a], C-Q. Li[110], H. Li[62a], H. Li[62b], H. Li[14c], H. Li[14b], H. Li[62b], J. Li[62c], K. Li[138], L. Li[62c], M. Li[14a,14e], Q.Y. Li[62a], S. Li[14a,14e], S. Li[62d,62c,d], T. Li[5], X. Li[104], Z. Li[126], Z. Li[104], Z. Li[92], Z. Li[14a,14e], S. Liang[14a,14e], Z. Liang[14a], M. Liberatore[135], B. Liberti[76a], K. Lie[64c], J. Lieber Marin[83b], H. Lien[68], K. Lin[107], R.E. Lindley[7], J.H. Lindon[2], E. Lipeles[128], A. Lipniacka[16], A. Lister[164], J.D. Little[4], B. Liu[14a], B.X. Liu[142], D. Liu[62d,62c], J.B. Liu[62a], J.K.K. Liu[32], K. Liu[62d,62c], M. Liu[62a], M.Y. Liu[62a], P. Liu[14a], Q. Liu[62d,138,62c], X. Liu[62a], Y. Liu[14d,14e], Y.L. Liu[62b], Y.W. Liu[62a], J. Llorente Merino[142], S.L. Lloyd[94], E.M. Lobodzinska[48], P. Loch[7], T. Lohse[18], K. Lohwasser[139], E. Loiacono[48], M. Lokajicek[131,*], J.D. Lomas[20], J.D. Long[162], I. Longarini[160], L. Longo[70a,70b], R. Longo[162], I. Lopez Paz[67], A. Lopez Solis[48], N. Lorenzo Martinez[4], A.M. Lory[109], G. Löschcke Centeno[146], O. Loseva[37], X. Lou[47a,47b], X. Lou[14a,14e], A. Lounis[66], J. Love[6], P.A. Love[91], G. Lu[14a,14e], M. Lu[80], S. Lu[128], Y.J. Lu[65], H.J. Lubatti[138],

JHEP02(2024)197

C. Luci[75a,75b], F.L. Lucio Alves[14c], A. Lucotte[60], F. Luehring[68], I. Luise[145], O. Lukianchuk[66], O. Lundberg[144], B. Lund-Jensen[144], N.A. Luongo[6], M.S. Lutz[151], A.B. Lux[25], D. Lynn[29], H. Lyons[92], R. Lysak[131], E. Lytken[98], V. Lyubushkin[38], T. Lyubushkina[38], M.M. Lyukova[145], H. Ma[29], K. Ma[62a], L.L. Ma[62b], W. Ma[62a], Y. Ma[121], D.M. Mac Donell[165], G. Maccarrone[53], J.C. MacDonald[100], P.C. Machado De Abreu Farias[83b], R. Madar[40], W.F. Mader[50], T. Madula[96], J. Maeda[85], T. Maeno[29], H. Maguire[139], V. Maiboroda[135], A. Maio[130a,130b,130d], K. Maj[86a], O. Majersky[48], S. Majewski[123], N. Makovec[66], V. Maksimovic[15], B. Malaescu[127], Pa. Malecki[87], V.P. Maleev[37], F. Malek[60], M. Mali[93], D. Malito[95], U. Mallik[80], S. Maltezos[10], S. Malyukov[38], J. Mamuzic[13], G. Mancini[53], G. Manco[73a,73b], J.P. Mandalia[94], I. Mandić[93], L. Manhaes de Andrade Filho[83a], I.M. Maniatis[169], J. Manjarres Ramos[102,aa], D.C. Mankad[169], A. Mann[109], B. Mansoulie[135], S. Manzoni[36], L. Mao[62c], X. Mapekula[33c], A. Marantis[152,r], G. Marchiori[5], M. Marcisovsky[131], C. Marcon[71a], M. Marinescu[20], S. Marium[48], M. Marjanovic[120], E.J. Marshall[91], Z. Marshall[17a], S. Marti-Garcia[163], T.A. Martin[167], V.J. Martin[52], B. Martin dit Latour[16], L. Martinelli[75a,75b], M. Martinez[13,s], P. Martinez Agullo[163], V.I. Martinez Outschoorn[103], P. Martinez Suarez[13], S. Martin-Haugh[134], V.S. Martoiu[27b], A.C. Martyniuk[96], A. Marzin[36], D. Mascione[78a,78b], L. Masetti[100], T. Mashimo[153], J. Masik[101], A.L. Maslennikov[37], L. Massa[23b], P. Massarotti[72a,72b], P. Mastrandrea[74a,74b], A. Mastroberardino[43b,43a], T. Masubuchi[153], T. Mathisen[161], J. Matousek[133], N. Matsuzawa[153], J. Maurer[27b], B. Maček[93], D.A. Maximov[37], R. Mazini[148], I. Maznas[152], M. Mazza[107], S.M. Mazza[136], E. Mazzeo[71a,71b], C. Mc Ginn[29], J.P. Mc Gowan[104], S.P. Mc Kee[106], E.F. McDonald[105], A.E. McDougall[114], J.A. Mcfayden[146], R.P. McGovern[128], G. Mchedlidze[149b], R.P. Mckenzie[33g], T.C. Mclachlan[48], D.J. Mclaughlin[96], S.J. McMahon[134], C.M. Mcpartland[92], R.A. McPherson[165,w], S. Mehlhase[109], A. Mehta[92], D. Melini[150], B.R. Mellado Garcia[33g], A.H. Melo[55], F. Meloni[48], A.M. Mendes Jacques Da Costa[101], H.Y. Meng[155], L. Meng[91], S. Menke[110], M. Mentink[36], E. Meoni[43b,43a], G. Mercado[115], C. Merlassino[69a,69c], L. Merola[72a,72b], C. Meroni[71a,71b], G. Merz[106], O. Meshkov[37], J. Metcalfe[6], A.S. Mete[6], C. Meyer[68], J-P. Meyer[135], R.P. Middleton[134], L. Mijović[52], G. Mikenberg[169], M. Mikestikova[131], M. Mikuž[93], H. Mildner[100], A. Milic[36], C.D. Milke[44], D.W. Miller[39], L.S. Miller[34], A. Milov[169], D.A. Milstead[47a,47b], T. Min[14c], A.A. Minaenko[37], I.A. Minashvili[149b], L. Mince[59], A.I. Mincer[117], B. Mindur[86a], M. Mineev[38], Y. Mino[88], L.M. Mir[13], M. Miralles Lopez[163], M. Mironova[17a], A. Mishima[153], M.C. Missio[113], A. Mitra[167], V.A. Mitsou[163], Y. Mitsumori[111], O. Miu[155], P.S. Miyagawa[94], T. Mkrtchyan[63a], M. Mlinarevic[96], T. Mlinarevic[96], M. Mlynarikova[36], S. Mobius[19], P. Moder[48], P. Mogg[109], A.F. Mohammed[14a,14e], S. Mohapatra[41], G. Mokgatitswane[33g], L. Moleri[169], B. Mondal[141], S. Mondal[132], K. Mönig[48], E. Monnier[102], L. Monsonis Romero[163], J. Montejo Berlingen[13], M. Montella[119], F. Montereali[77a,77b], F. Monticelli[90], S. Monzani[69a,69c], N. Morange[66], A.L. Moreira De Carvalho[130a], M. Moreno Llácer[163], C. Moreno Martinez[56], P. Morettini[57b], S. Morgenstern[36], M. Morii[61], M. Morinaga[153], A.K. Morley[36], F. Morodei[75a,75b], L. Morvaj[36], P. Moschovakos[36], B. Moser[36], M. Mosidze[149b], T. Moskalets[54], P. Moskvitina[113], J. Moss[31,l], E.J.W. Moyse[103],

JHEP02(2024)197

O. Mtintsilana[33g], S. Muanza[102], J. Mueller[129], D. Muenstermann[91], R. Müller[19], G.A. Mullier[161], A.J. Mullin[32], J.J. Mullin[128], D.P. Mungo[155], D. Munoz Perez[163], F.J. Munoz Sanchez[101], M. Murin[101], W.J. Murray[167,134], A. Murrone[71a,71b], M. Muškinja[17a], C. Mwewa[29], A.G. Myagkov[37,a], A.J. Myers[8], G. Myers[68], M. Myska[132], B.P. Nachman[17a], O. Nackenhorst[49], A. Nag[50], K. Nagai[126], K. Nagano[84], J.L. Nagle[29,ai], E. Nagy[102], A.M. Nairz[36], Y. Nakahama[84], K. Nakamura[84], K. Nakkalil[5], H. Nanjo[124], R. Narayan[44], E.A. Narayanan[112], I. Naryshkin[37], M. Naseri[34], S. Nasri[159], C. Nass[24], G. Navarro[22a], J. Navarro-Gonzalez[163], R. Nayak[151], A. Nayaz[18], P.Y. Nechaeva[37], F. Nechansky[48], L. Nedic[126], T.J. Neep[20], A. Negri[73a,73b], M. Negrini[23b], C. Nellist[114], C. Nelson[104], K. Nelson[106], S. Nemecek[131], M. Nessi[36,h], M.S. Neubauer[162], F. Neuhaus[100], J. Neundorf[48], R. Newhouse[164], P.R. Newman[20], C.W. Ng[129], Y.W.Y. Ng[48], B. Ngair[35e], H.D.N. Nguyen[108], R.B. Nickerson[126], R. Nicolaidou[135], J. Nielsen[136], M. Niemeyer[55], J. Niermann[55,36], N. Nikiforou[36], V. Nikolaenko[37,a], I. Nikolic-Audit[127], K. Nikolopoulos[20], P. Nilsson[29], I. Ninca[48], H.R. Nindhito[56], G. Ninio[151], A. Nisati[75a], N. Nishu[2], R. Nisius[110], J-E. Nitschke[50], E.K. Nkadimeng[33g], T. Nobe[153], D.L. Noel[32], T. Nommensen[147], M.B. Norfolk[139], R.R.B. Norisam[96], B.J. Norman[34], M. Noury[35a], J. Novak[93], T. Novak[48], L. Novotny[132], R. Novotny[112], L. Nozka[122], K. Ntekas[160], N.M.J. Nunes De Moura Junior[83b], E. Nurse[96], J. Ocariz[127], A. Ochi[85], I. Ochoa[130a], S. Oerdek[48], J.T. Offermann[39], A. Ogrodnik[133], A. Oh[101], C.C. Ohm[144], H. Oide[84], R. Oishi[153], M.L. Ojeda[48], M.W. O'Keefe[92], Y. Okumura[153], L.F. Oleiro Seabra[130a], S.A. Olivares Pino[137d], D. Oliveira Damazio[29], D. Oliveira Goncalves[83a], J.L. Oliver[160], Ö.O. Öncel[54], A.P. O'Neill[19], A. Onofre[130a,130e], P.U.E. Onyisi[11], M.J. Oreglia[39], G.E. Orellana[90], D. Orestano[77a,77b], N. Orlando[13], R.S. Orr[155], V. O'Shea[59], L.M. Osojnak[128], R. Ospanov[62a], G. Otero y Garzon[30], H. Otono[89], P.S. Ott[63a], G.J. Ottino[17a], M. Ouchrif[35d], J. Ouellette[29], F. Ould-Saada[125], M. Owen[59], R.E. Owen[134], K.Y. Oyulmaz[21a], V.E. Ozcan[21a], F. Ozturk[87], N. Ozturk[8], S. Ozturk[82], H.A. Pacey[126], A. Pacheco Pages[13], C. Padilla Aranda[13], G. Padovano[75a,75b], S. Pagan Griso[17a], G. Palacino[68], A. Palazzo[70a,70b], S. Palestini[36], J. Pan[172], T. Pan[64a], D.K. Panchal[11], C.E. Pandini[114], J.G. Panduro Vazquez[95], H.D. Pandya[1], H. Pang[14b], P. Pani[48], G. Panizzo[69a,69c], L. Paolozzi[56], C. Papadatos[108], S. Parajuli[44], A. Paramonov[6], C. Paraskevopoulos[10], D. Paredes Hernandez[64b], K.R. Park[41], T.H. Park[155], M.A. Parker[32], F. Parodi[57b,57a], E.W. Parrish[115], V.A. Parrish[52], J.A. Parsons[41], U. Parzefall[54], B. Pascual Dias[108], L. Pascual Dominguez[151], E. Pasqualucci[75a], S. Passaggio[57b], F. Pastore[95], P. Pasuwan[47a,47b], P. Patel[87], U.M. Patel[51], J.R. Pater[101], T. Pauly[36], J. Pearkes[143], M. Pedersen[125], R. Pedro[130a], S.V. Peleganchuk[37], O. Penc[36], E.A. Pender[52], K.E. Penski[109], M. Penzin[37], B.S. Peralva[83d], A.P. Pereira Peixoto[60], L. Pereira Sanchez[47a,47b], D.V. Perepelitsa[29,ai], E. Perez Codina[156a], M. Perganti[10], L. Perini[71a,71b,*], H. Pernegger[36], O. Perrin[40], K. Peters[48], R.F.Y. Peters[101], B.A. Petersen[36], T.C. Petersen[42], E. Petit[102], V. Petousis[132], C. Petridou[152,e], A. Petrukhin[141], M. Pettee[17a], N.E. Pettersson[36], A. Petukhov[37], K. Petukhova[133], R. Pezoa[137f], L. Pezzotti[36], G. Pezzullo[172], T.M. Pham[170], T. Pham[105], P.W. Phillips[134], G. Piacquadio[145], E. Pianori[17a], F. Piazza[123], R. Piegaia[30], D. Pietreanu[27b], A.D. Pilkington[101], M. Pinamonti[69a,69c],

JHEP02(2024)197

J.L. Pinfold[2], B.C. Pinheiro Pereira[130a], A.E. Pinto Pinoargote[100,135], L. Pintucci[69a,69c], K.M. Piper[146], A. Pirttikoski[56], D.A. Pizzi[34], L. Pizzimento[64b], A. Pizzini[114], M.-A. Pleier[29], V. Plesanovs[54], V. Pleskot[133], E. Plotnikova[38], G. Poddar[4], R. Poettgen[98], L. Poggioli[127], I. Pokharel[55], S. Polacek[133], G. Polesello[73a], A. Poley[142,156a], R. Polifka[132], A. Polini[23b], C.S. Pollard[167], Z.B. Pollock[119], V. Polychronakos[29], E. Pompa Pacchi[75a,75b], D. Ponomarenko[113], L. Pontecorvo[36], S. Popa[27a], G.A. Popeneciu[27d], A. Poreba[36], D.M. Portillo Quintero[156a], S. Pospisil[132], M.A. Postill[139], P. Postolache[27c], K. Potamianos[167], P.A. Potepa[86a], I.N. Potrap[38], C.J. Potter[32], H. Potti[1], T. Poulsen[48], J. Poveda[163], M.E. Pozo Astigarraga[36], A. Prades Ibanez[163], J. Pretel[54], D. Price[101], M. Primavera[70a], M.A. Principe Martin[99], R. Privara[122], T. Procter[59], M.L. Proffitt[138], N. Proklova[128], K. Prokofiev[64c], G. Proto[110], S. Protopopescu[29], J. Proudfoot[6], M. Przybycien[86a], W.W. Przygoda[86b], J.E. Puddefoot[139], D. Pudzha[37], D. Pyatiizbyantseva[37], J. Qian[106], D. Qichen[101], Y. Qin[101], T. Qiu[52], A. Quadt[55], M. Queitsch-Maitland[101], G. Quetant[56], R.P. Quinn[164], G. Rabanal Bolanos[61], D. Rafanoharana[54], F. Ragusa[71a,71b], J.L. Rainbolt[39], J.A. Raine[56], S. Rajagopalan[29], E. Ramakoti[37], I.A. Ramirez-Berend[34], K. Ran[48,14e], N.P. Rapheeha[33g], H. Rasheed[27b], V. Raskina[127], D.F. Rassloff[63a], S. Rave[100], B. Ravina[55], I. Ravinovich[169], M. Raymond[36], A.L. Read[125], N.P. Readioff[139], D.M. Rebuzzi[73a,73b], G. Redlinger[29], A.S. Reed[110], K. Reeves[26], J.A. Reidelsturz[171], D. Reikher[151], A. Rej[49], C. Rembser[36], A. Renardi[48], M. Renda[27b], M.B. Rendel[110], F. Renner[48], A.G. Rennie[160], A.L. Rescia[48], S. Resconi[71a], M. Ressegotti[57b,57a], S. Rettie[36], J.G. Reyes Rivera[107], E. Reynolds[17a], O.L. Rezanova[37], P. Reznicek[133], N. Ribaric[91], E. Ricci[78a,78b], R. Richter[110], S. Richter[47a,47b], E. Richter-Was[86b], M. Ridel[127], S. Ridouani[35d], P. Rieck[117], P. Riedler[36], E.M. Riefel[47a,47b], J.O. Rieger[114], M. Rijssenbeek[145], A. Rimoldi[73a,73b], M. Rimoldi[36], L. Rinaldi[23b,23a], T.T. Rinn[29], M.P. Rinnagel[109], G. Ripellino[161], I. Riu[13], P. Rivadeneira[48], J.C. Rivera Vergara[165], F. Rizatdinova[121], E. Rizvi[94], B.A. Roberts[167], B.R. Roberts[17a], S.H. Robertson[104,w], D. Robinson[32], C.M. Robles Gajardo[137f], M. Robles Manzano[100], A. Robson[59], A. Rocchi[76a,76b], C. Roda[74a,74b], S. Rodriguez Bosca[63a], Y. Rodriguez Garcia[22a], A. Rodriguez Rodriguez[54], A.M. Rodríguez Vera[156b], S. Roe[36], J.T. Roemer[160], A.R. Roepe-Gier[136], J. Roggel[171], O. Røhne[125], R.A. Rojas[103], C.P.A. Roland[127], J. Roloff[29], A. Romaniouk[37], E. Romano[73a,73b], M. Romano[23b], A.C. Romero Hernandez[162], N. Rompotis[92], L. Roos[127], S. Rosati[75a], B.J. Rosser[39], E. Rossi[126], E. Rossi[72a,72b], L.P. Rossi[57b], L. Rossini[54], R. Rosten[119], M. Rotaru[27b], B. Rottler[54], C. Rougier[102,aa], D. Rousseau[66], D. Rousso[32], A. Roy[162], S. Roy-Garand[155], A. Rozanov[102], Z.M.A. Rozario[59], Y. Rozen[150], X. Ruan[33g], A. Rubio Jimenez[163], A.J. Ruby[92], V.H. Ruelas Rivera[18], T.A. Ruggeri[1], A. Ruggiero[126], A. Ruiz-Martinez[163], A. Rummler[36], Z. Rurikova[54], N.A. Rusakovich[38], H.L. Russell[165], G. Russo[75a,75b], J.P. Rutherfoord[7], S. Rutherford Colmenares[32], K. Rybacki[91], M. Rybar[133], E.B. Rye[125], A. Ryzhov[44], J.A. Sabater Iglesias[56], P. Sabatini[163], H.F-W. Sadrozinski[136], F. Safai Tehrani[75a], B. Safarzadeh Samani[134], M. Safdari[143], S. Saha[165], M. Sahinsoy[110], A. Saibel[163], M. Saimpert[135], M. Saito[153], T. Saito[153], D. Salamani[36], A. Salnikov[143], J. Salt[163], A. Salvador Salas[151], D. Salvatore[43b,43a], F. Salvatore[146], A. Salzburger[36], D. Sammel[54], D. Sampsonidis[152,e],

JHEP02(2024)197

D. Sampsonidou[123], J. Sánchez[163], A. Sanchez Pineda[4], V. Sanchez Sebastian[163], H. Sandaker[125], C.O. Sander[48], J.A. Sandesara[103], M. Sandhoff[171], C. Sandoval[22b], D.P.C. Sankey[134], T. Sano[88], A. Sansoni[53], L. Santi[75a,75b], C. Santoni[40], H. Santos[130a,130b], S.N. Santpur[17a], A. Santra[169], K.A. Saoucha[116b], J.G. Saraiva[130a,130d], J. Sardain[7], O. Sasaki[84], K. Sato[157], C. Sauer[63b], F. Sauerburger[54], E. Sauvan[4], P. Savard[155,af], R. Sawada[153], C. Sawyer[134], L. Sawyer[97], I. Sayago Galvan[163], C. Sbarra[23b], A. Sbrizzi[23b,23a], T. Scanlon[96], J. Schaarschmidt[138], P. Schacht[110], U. Schäfer[100], A.C. Schaffer[66,44], D. Schaile[109], R.D. Schamberger[145], C. Scharf[18], M.M. Schefer[19], V.A. Schegelsky[37], D. Scheirich[133], F. Schenck[18], M. Schernau[160], C. Scheulen[55], C. Schiavi[57b,57a], E.J. Schioppa[70a,70b], M. Schioppa[43b,43a], B. Schlag[143,n], K.E. Schleicher[54], S. Schlenker[36], J. Schmeing[171], M.A. Schmidt[171], K. Schmieden[100], C. Schmitt[100], N. Schmitt[100], S. Schmitt[48], L. Schoeffel[135], A. Schoening[63b], P.G. Scholer[54], E. Schopf[126], M. Schott[100], J. Schovancova[36], S. Schramm[56], F. Schroeder[171], T. Schroer[56], H-C. Schultz-Coulon[63a], M. Schumacher[54], B.A. Schumm[136], Ph. Schune[135], A.J. Schuy[138], H.R. Schwartz[136], A. Schwartzman[143], T.A. Schwarz[106], Ph. Schwemling[135], R. Schwienhorst[107], A. Sciandra[136], G. Sciolla[26], F. Scuri[74a], C.D. Sebastiani[92], K. Sedlaczek[115], P. Seema[18], S.C. Seidel[112], A. Seiden[136], B.D. Seidlitz[41], C. Seitz[48], J.M. Seixas[83b], G. Sekhniaidze[72a], S.J. Sekula[44], L. Selem[60], N. Semprini-Cesari[23b,23a], D. Sengupta[56], V. Senthilkumar[163], L. Serin[66], L. Serkin[69a,69b], M. Sessa[76a,76b], H. Severini[120], F. Sforza[57b,57a], A. Sfyrla[56], E. Shabalina[55], R. Shaheen[144], J.D. Shahinian[128], D. Shaked Renous[169], L.Y. Shan[14a], M. Shapiro[17a], A. Sharma[36], A.S. Sharma[164], P. Sharma[80], S. Sharma[48], P.B. Shatalov[37], K. Shaw[146], S.M. Shaw[101], A. Shcherbakova[37], Q. Shen[62c,5], D.J. Sheppard[142], P. Sherwood[96], L. Shi[96], X. Shi[14a], C.O. Shimmin[172], J.D. Shinner[95], I.P.J. Shipsey[126], S. Shirabe[56,h], M. Shiyakova[38,u], J. Shlomi[169], M.J. Shochet[39], J. Shojaii[105], D.R. Shope[125], B. Shrestha[120], S. Shrestha[119,aj], E.M. Shrif[33g], M.J. Shroff[165], P. Sicho[131], A.M. Sickles[162], E. Sideras Haddad[33g], A. Sidoti[23b], F. Siegert[50], Dj. Sijacki[15], F. Sili[90], J.M. Silva[20], M.V. Silva Oliveira[29], S.B. Silverstein[47a], S. Simion[66], R. Simoniello[36], E.L. Simpson[59], H. Simpson[146], L.R. Simpson[106], N.D. Simpson[98], S. Simsek[82], S. Sindhu[55], P. Sinervo[155], S. Singh[155], S. Sinha[48], S. Sinha[101], M. Sioli[23b,23a], I. Siral[36], E. Sitnikova[48], S.Yu. Sivoklokov[37,*], J. Sjölin[47a,47b], A. Skaf[55], E. Skorda[20], P. Skubic[120], M. Slawinska[87], V. Smakhtin[169], B.H. Smart[134], J. Smiesko[36], S.Yu. Smirnov[37], Y. Smirnov[37], L.N. Smirnova[37,a], O. Smirnova[98], A.C. Smith[41], E.A. Smith[39], H.A. Smith[126], J.L. Smith[92], R. Smith[143], M. Smizanska[91], K. Smolek[132], A.A. Snesarev[37], S.R. Snider[155], H.L. Snoek[114], S. Snyder[29], R. Sobie[165,w], A. Soffer[151], C.A. Solans Sanchez[36], E.Yu. Soldatov[37], U. Soldevila[163], A.A. Solodkov[37], S. Solomon[26], A. Soloshenko[38], K. Solovieva[54], O.V. Solovyanov[40], V. Solovyev[37], P. Sommer[36], A. Sonay[13], W.Y. Song[156b], J.M. Sonneveld[114], A. Sopczak[132], A.L. Sopio[96], F. Sopkova[28b], I.R. Sotarriva Alvarez[154], V. Sothilingam[63a], O.J. Soto Sandoval[137c,137b], S. Sottocornola[68], R. Soualah[116b], Z. Soumaimi[35e], D. South[48], N. Soybelman[169], S. Spagnolo[70a,70b], M. Spalla[110], D. Sperlich[54], G. Spigo[36], S. Spinali[91], D.P. Spiteri[59], M. Spousta[133], E.J. Staats[34], A. Stabile[71a,71b], R. Stamen[63a], A. Stampekis[20], M. Standke[24], E. Stanecka[87], M.V. Stange[50], B. Stanislaus[17a], M.M. Stanitzki[48],

JHEP02(2024)197

B. Stapf[48], E.A. Starchenko[37], G.H. Stark[136], J. Stark[102,aa], D.M. Starko[156b], P. Staroba[131], P. Starovoitov[63a], S. Stärz[104], R. Staszewski[87], G. Stavropoulos[46], J. Steentoft[161], P. Steinberg[29], B. Stelzer[142,156a], H.J. Stelzer[129], O. Stelzer-Chilton[156a], H. Stenzel[58], T.J. Stevenson[146], G.A. Stewart[36], J.R. Stewart[121], M.C. Stockton[36], G. Stoicea[27b], M. Stolarski[130a], S. Stonjek[110], A. Straessner[50], J. Strandberg[144], S. Strandberg[47a,47b], M. Stratmann[171], M. Strauss[120], T. Strebler[102], P. Strizenec[28b], R. Ströhmer[166], D.M. Strom[123], R. Stroynowski[44], A. Strubig[47a,47b], S.A. Stucci[29], B. Stugu[16], J. Stupak[120], N.A. Styles[48], D. Su[143], S. Su[62a], W. Su[62d], X. Su[62a,66], K. Sugizaki[153], V.V. Sulin[37], M.J. Sullivan[92], D.M.S. Sultan[78a,78b], L. Sultanaliyeva[37], S. Sultansoy[3b], T. Sumida[88], S. Sun[106], S. Sun[170], O. Sunneborn Gudnadottir[161], N. Sur[102], M.R. Sutton[146], H. Suzuki[157], M. Svatos[131], M. Swiatlowski[156a], T. Swirski[166], I. Sykora[28a], M. Sykora[133], T. Sykora[133], D. Ta[100], K. Tackmann[48,t], A. Taffard[160], R. Tafirout[156a], J.S. Tafoya Vargas[66], E.P. Takeva[52], Y. Takubo[84], M. Talby[102], A.A. Talyshev[37], K.C. Tam[64b], N.M. Tamir[151], A. Tanaka[153], J. Tanaka[153], R. Tanaka[66], M. Tanasini[57b,57a], Z. Tao[164], S. Tapia Araya[137f], S. Tapprogge[100], A. Tarek Abouelfadl Mohamed[107], S. Tarem[150], K. Tariq[14a], G. Tarna[102,27b], G.F. Tartarelli[71a], P. Tas[133], M. Tasevsky[131], E. Tassi[43b,43a], A.C. Tate[162], G. Tateno[153], Y. Tayalati[35e,v], G.N. Taylor[105], W. Taylor[156b], A.S. Tee[170], R. Teixeira De Lima[143], P. Teixeira-Dias[95], J.J. Teoh[155], K. Terashi[153], J. Terron[99], S. Terzo[13], M. Testa[53], R.J. Teuscher[155,w], A. Thaler[79], O. Theiner[56], N. Themistokleous[52], T. Theveneaux-Pelzer[102], O. Thielmann[171], D.W. Thomas[95], J.P. Thomas[20], E.A. Thompson[17a], P.D. Thompson[20], E. Thomson[128], Y. Tian[55], V. Tikhomirov[37,a], Yu.A. Tikhonov[37], S. Timoshenko[37], D. Timoshyn[133], E.X.L. Ting[1], P. Tipton[172], S.H. Tlou[33g], A. Tnourji[40], K. Todome[154], S. Todorova-Nova[133], S. Todt[50], M. Togawa[84], J. Tojo[89], S. Tokár[28a], K. Tokushuku[84], O. Toldaiev[68], R. Tombs[32], M. Tomoto[84,111], L. Tompkins[143,n], K.W. Topolnicki[86b], E. Torrence[123], H. Torres[102,aa], E. Torró Pastor[163], M. Toscani[30], C. Tosciri[39], M. Tost[11], D.R. Tovey[139], A. Traeet[16], I.S. Trandafir[27b], T. Trefzger[166], A. Tricoli[29], I.M. Trigger[156a], S. Trincaz-Duvoid[127], D.A. Trischuk[26], B. Trocmé[60], C. Troncon[71a], L. Truong[33c], M. Trzebinski[87], A. Trzupek[87], F. Tsai[145], M. Tsai[106], A. Tsiamis[152,e], P.V. Tsiareshka[37], S. Tsigaridas[156a], A. Tsirigotis[152,r], V. Tsiskaridze[155], E.G. Tskhadadze[149a], M. Tsopoulou[152,e], Y. Tsujikawa[88], I.I. Tsukerman[37], V. Tsulaia[17a], S. Tsuno[84], K. Tsuri[118], D. Tsybychev[145], Y. Tu[64b], A. Tudorache[27b], V. Tudorache[27b], A.N. Tuna[61], S. Turchikhin[57b,57a], I. Turk Cakir[3a], R. Turra[71a], T. Turtuvshin[38,x], P.M. Tuts[41], S. Tzamarias[152,e], P. Tzanis[10], E. Tzovara[100], F. Ukegawa[157], P.A. Ulloa Poblete[137c,137b], E.N. Umaka[29], G. Unal[36], M. Unal[11], A. Undrus[29], G. Unel[160], J. Urban[28b], P. Urquijo[105], P. Urrejola[137a], G. Usai[8], R. Ushioda[154], M. Usman[108], Z. Uysal[21b], V. Vacek[132], B. Vachon[104], K.O.H. Vadla[125], T. Vafeiadis[36], A. Vaitkus[96], C. Valderanis[109], E. Valdes Santurio[47a,47b], M. Valente[156a], S. Valentinetti[23b,23a], A. Valero[163], E. Valiente Moreno[163], A. Vallier[102,aa], J.A. Valls Ferrer[163], D.R. Van Arneman[114], T.R. Van Daalen[138], A. Van Der Graaf[49], P. Van Gemmeren[6], M. Van Rijnbach[125,36], S. Van Stroud[96], I. Van Vulpen[114], M. Vanadia[76a,76b], W. Vandelli[36], M. Vandenbroucke[135], E.R. Vandewall[121], D. Vannicola[151], L. Vannoli[57b,57a], R. Vari[75a], E.W. Varnes[7], C. Varni[17b], T. Varol[148],

JHEP02(2024)197

D. Varouchas[66], L. Varriale[163], K.E. Varvell[147], M.E. Vasile[27b], L. Vaslin[84], G.A. Vasquez[165], A. Vasyukov[38], F. Vazeille[40], T. Vazquez Schroeder[36], J. Veatch[31], V. Vecchio[101], M.J. Veen[103], I. Veliscek[126], L.M. Veloce[155], F. Veloso[130a,130c], S. Veneziano[75a], A. Ventura[70a,70b], S. Ventura Gonzalez[135], A. Verbytskyi[110], M. Verducci[74a,74b], C. Vergis[24], M. Verissimo De Araujo[83b], W. Verkerke[114], J.C. Vermeulen[114], C. Vernieri[143], M. Vessella[103], M.C. Vetterli[142,af], A. Vgenopoulos[152,e], N. Viaux Maira[137f], T. Vickey[139], O.E. Vickey Boeriu[139], G.H.A. Viehhauser[126], L. Vigani[63b], M. Villa[23b,23a], M. Villaplana Perez[163], E.M. Villhauer[52], E. Vilucchi[53], M.G. Vincter[34], G.S. Virdee[20], A. Vishwakarma[52], A. Visibile[114], C. Vittori[36], I. Vivarelli[146], E. Voevodina[110], F. Vogel[109], J.C. Voigt[50], P. Vokac[132], Yu. Volkotrub[86a], J. Von Ahnen[48], E. Von Toerne[24], B. Vormwald[36], V. Vorobel[133], K. Vorobev[37], M. Vos[163], K. Voss[141], J.H. Vossebeld[92], M. Vozak[114], L. Vozdecky[94], N. Vranjes[15], M. Vranjes Milosavljevic[15], M. Vreeswijk[114], R. Vuillermet[36], O. Vujinovic[100], I. Vukotic[39], S. Wada[157], C. Wagner[103], J.M. Wagner[17a], W. Wagner[171], S. Wahdan[171], H. Wahlberg[90], M. Wakida[111], J. Walder[134], R. Walker[109], W. Walkowiak[141], A. Wall[128], T. Wamorkar[6], A.Z. Wang[136], C. Wang[100], C. Wang[62c], H. Wang[17a], J. Wang[64a], R.-J. Wang[100], R. Wang[61], R. Wang[6], S.M. Wang[148], S. Wang[62b], T. Wang[62a], W.T. Wang[80], W. Wang[14a], X. Wang[14c], X. Wang[162], X. Wang[62c], Y. Wang[62d], Y. Wang[14c], Z. Wang[106], Z. Wang[62d,51,62c], Z. Wang[106], A. Warburton[104], R.J. Ward[20], N. Warrack[59], A.T. Watson[20], H. Watson[59], M.F. Watson[20], E. Watton[59,134], G. Watts[138], B.M. Waugh[96], C. Weber[29], H.A. Weber[18], M.S. Weber[19], S.M. Weber[63a], C. Wei[62a], Y. Wei[126], A.R. Weidberg[126], E.J. Weik[117], J. Weingarten[49], M. Weirich[100], C. Weiser[54], C.J. Wells[48], T. Wenaus[29], B. Wendland[49], T. Wengler[36], N.S. Wenke[110], N. Wermes[24], M. Wessels[63a], A.M. Wharton[91], A.S. White[61], A. White[8], M.J. White[1], D. Whiteson[160], L. Wickremasinghe[124], W. Wiedenmann[170], C. Wiel[50], M. Wielers[134], C. Wiglesworth[42], D.J. Wilbern[120], H.G. Wilkens[36], D.M. Williams[41], H.H. Williams[128], S. Williams[32], S. Willocq[103], B.J. Wilson[101], P.J. Windischhofer[39], F.I. Winkel[30], F. Winklmeier[123], B.T. Winter[54], J.K. Winter[101], M. Wittgen[143], M. Wobisch[97], Z. Wolffs[114], J. Wollrath[160], M.W. Wolter[87], H. Wolters[130a,130c], A.F. Wongel[48], E.L. Woodward[41], S.D. Worm[48], B.K. Wosiek[87], K.W. Woźniak[87], S. Wozniewski[55], K. Wraight[59], C. Wu[20], J. Wu[14a,14e], M. Wu[64a], M. Wu[113], S.L. Wu[170], X. Wu[56], Y. Wu[62a], Z. Wu[135], J. Wuerzinger[110,ad], T.R. Wyatt[101], B.M. Wynne[52], S. Xella[42], L. Xia[14c], M. Xia[14b], J. Xiang[64c], M. Xie[62a], X. Xie[62a], S. Xin[14a,14e], A. Xiong[123], J. Xiong[17a], D. Xu[14a], H. Xu[62a], L. Xu[62a], R. Xu[128], T. Xu[106], Y. Xu[14b], Z. Xu[52], Z. Xu[14c], B. Yabsley[147], S. Yacoob[33a], Y. Yamaguchi[154], E. Yamashita[153], H. Yamauchi[157], T. Yamazaki[17a], Y. Yamazaki[85], J. Yan[62c], S. Yan[126], Z. Yan[25], H.J. Yang[62c,62d], H.T. Yang[62a], S. Yang[62a], T. Yang[64c], X. Yang[36], X. Yang[14a], Y. Yang[44], Y. Yang[62a], Z. Yang[62a], W-M. Yao[17a], Y.C. Yap[48], H. Ye[14c], H. Ye[55], J. Ye[14a], S. Ye[29], X. Ye[62a], Y. Yeh[96], I. Yeletskikh[38], B.K. Yeo[17b], M.R. Yexley[96], P. Yin[41], K. Yorita[168], S. Younas[27b], C.J.S. Young[36], C. Young[143], C. Yu[14a,14e,ah], Y. Yu[62a], M. Yuan[106], R. Yuan[62b], L. Yue[96], M. Zaazoua[62a], B. Zabinski[87], E. Zaid[52], Z.K. Zak[87], T. Zakareishvili[149b], N. Zakharchuk[34], S. Zambito[56], J.A. Zamora Saa[137d,137b], J. Zang[153], D. Zanzi[54],

JHEP02(2024)197

O. Zaplatilek[132], C. Zeitnitz[171], H. Zeng[14a], J.C. Zeng[162], D.T. Zenger Jr[26], O. Zenin[37], T. Ženiš[28a], S. Zenz[94], S. Zerradi[35a], D. Zerwas[66], M. Zhai[14a,14e], B. Zhang[14c], D.F. Zhang[139], J. Zhang[62b], J. Zhang[6], K. Zhang[14a,14e], L. Zhang[14c], P. Zhang[14a,14e], R. Zhang[170], S. Zhang[106], S. Zhang[44], T. Zhang[153], X. Zhang[62c], X. Zhang[62b], Y. Zhang[62c,5], Y. Zhang[96], Y. Zhang[14c], Z. Zhang[17a], Z. Zhang[66], H. Zhao[138], T. Zhao[62b], Y. Zhao[136], Z. Zhao[62a], A. Zhemchugov[38], J. Zheng[14c], K. Zheng[162], X. Zheng[62a], Z. Zheng[143], D. Zhong[162], B. Zhou[106], H. Zhou[7], N. Zhou[62c], Y. Zhou[7], C.G. Zhu[62b], J. Zhu[106], Y. Zhu[62c], Y. Zhu[62a], X. Zhuang[14a], K. Zhukov[37], V. Zhulanov[37], N.I. Zimine[38], J. Zinsser[63b], M. Ziolkowski[141], L. Živković[15], A. Zoccoli[23b,23a], K. Zoch[61], T.G. Zorbas[139], O. Zormpa[46], W. Zou[41], L. Zwalinski[36]

[1] *Department of Physics, University of Adelaide, Adelaide; Australia*
[2] *Department of Physics, University of Alberta, Edmonton AB; Canada*
[3] [(a)] *Department of Physics, Ankara University, Ankara;* [(b)] *Division of Physics, TOBB University of Economics and Technology, Ankara; Türkiye*
[4] *LAPP, Université Savoie Mont Blanc, CNRS/IN2P3, Annecy; France*
[5] *APC, Université Paris Cité, CNRS/IN2P3, Paris; France*
[6] *High Energy Physics Division, Argonne National Laboratory, Argonne IL; United States of America*
[7] *Department of Physics, University of Arizona, Tucson AZ; United States of America*
[8] *Department of Physics, University of Texas at Arlington, Arlington TX; United States of America*
[9] *Physics Department, National and Kapodistrian University of Athens, Athens; Greece*
[10] *Physics Department, National Technical University of Athens, Zografou; Greece*
[11] *Department of Physics, University of Texas at Austin, Austin TX; United States of America*
[12] *Institute of Physics, Azerbaijan Academy of Sciences, Baku; Azerbaijan*
[13] *Institut de Física d'Altes Energies (IFAE), Barcelona Institute of Science and Technology, Barcelona; Spain*
[14] [(a)] *Institute of High Energy Physics, Chinese Academy of Sciences, Beijing;* [(b)] *Physics Department, Tsinghua University, Beijing;* [(c)] *Department of Physics, Nanjing University, Nanjing;* [(d)] *School of Science, Shenzhen Campus of Sun Yat-sen University;* [(e)] *University of Chinese Academy of Science (UCAS), Beijing; China*
[15] *Institute of Physics, University of Belgrade, Belgrade; Serbia*
[16] *Department for Physics and Technology, University of Bergen, Bergen; Norway*
[17] [(a)] *Physics Division, Lawrence Berkeley National Laboratory, Berkeley CA;* [(b)] *University of California, Berkeley CA; United States of America*
[18] *Institut für Physik, Humboldt Universität zu Berlin, Berlin; Germany*
[19] *Albert Einstein Center for Fundamental Physics and Laboratory for High Energy Physics, University of Bern, Bern; Switzerland*
[20] *School of Physics and Astronomy, University of Birmingham, Birmingham; United Kingdom*
[21] [(a)] *Department of Physics, Bogazici University, Istanbul;* [(b)] *Department of Physics Engineering, Gaziantep University, Gaziantep;* [(c)] *Department of Physics, Istanbul University, Istanbul; Türkiye*
[22] [(a)] *Facultad de Ciencias y Centro de Investigaciónes, Universidad Antonio Nariño, Bogotá;* [(b)] *Departamento de Física, Universidad Nacional de Colombia, Bogotá; Colombia*
[23] [(a)] *Dipartimento di Fisica e Astronomia A. Righi, Università di Bologna, Bologna;* [(b)] *INFN Sezione di Bologna; Italy*
[24] *Physikalisches Institut, Universität Bonn, Bonn; Germany*
[25] *Department of Physics, Boston University, Boston MA; United States of America*
[26] *Department of Physics, Brandeis University, Waltham MA; United States of America*
[27] [(a)] *Transilvania University of Brasov, Brasov;* [(b)] *Horia Hulubei National Institute of Physics and Nuclear Engineering, Bucharest;* [(c)] *Department of Physics, Alexandru Ioan Cuza University of Iasi, Iasi;* [(d)] *National Institute for Research and Development of Isotopic and Molecular Technologies, Physics Department, Cluj-Napoca;* [(e)] *University Politehnica Bucharest, Bucharest;* [(f)] *West University in Timisoara, Timisoara;* [(g)] *Faculty of Physics, University of Bucharest, Bucharest; Romania*

JHEP02(2024)197

[28] [(a)] Faculty of Mathematics, Physics and Informatics, Comenius University, Bratislava;[(b)] Department of Subnuclear Physics, Institute of Experimental Physics of the Slovak Academy of Sciences, Kosice; Slovak Republic
[29] Physics Department, Brookhaven National Laboratory, Upton NY; United States of America
[30] Universidad de Buenos Aires, Facultad de Ciencias Exactas y Naturales, Departamento de Física, y CONICET, Instituto de Física de Buenos Aires (IFIBA), Buenos Aires; Argentina
[31] California State University, CA; United States of America
[32] Cavendish Laboratory, University of Cambridge, Cambridge; United Kingdom
[33] [(a)] Department of Physics, University of Cape Town, Cape Town;[(b)] iThemba Labs, Western Cape;[(c)] Department of Mechanical Engineering Science, University of Johannesburg, Johannesburg;[(d)] National Institute of Physics, University of the Philippines Diliman (Philippines);[(e)] University of South Africa, Department of Physics, Pretoria;[(f)] University of Zululand, KwaDlangezwa;[(g)] School of Physics, University of the Witwatersrand, Johannesburg; South Africa
[34] Department of Physics, Carleton University, Ottawa ON; Canada
[35] [(a)] Faculté des Sciences Ain Chock, Réseau Universitaire de Physique des Hautes Energies — Université Hassan II, Casablanca;[(b)] Faculté des Sciences, Université Ibn-Tofail, Kénitra;[(c)] Faculté des Sciences Semlalia, Université Cadi Ayyad, LPHEA-Marrakech;[(d)] LPMR, Faculté des Sciences, Université Mohamed Premier, Oujda;[(e)] Faculté des sciences, Université Mohammed V, Rabat;[(f)] Institute of Applied Physics, Mohammed VI Polytechnic University, Ben Guerir; Morocco
[36] CERN, Geneva; Switzerland
[37] Affiliated with an institute covered by a cooperation agreement with CERN
[38] Affiliated with an international laboratory covered by a cooperation agreement with CERN
[39] Enrico Fermi Institute, University of Chicago, Chicago IL; United States of America
[40] LPC, Université Clermont Auvergne, CNRS/IN2P3, Clermont-Ferrand; France
[41] Nevis Laboratory, Columbia University, Irvington NY; United States of America
[42] Niels Bohr Institute, University of Copenhagen, Copenhagen; Denmark
[43] [(a)] Dipartimento di Fisica, Università della Calabria, Rende;[(b)] INFN Gruppo Collegato di Cosenza, Laboratori Nazionali di Frascati; Italy
[44] Physics Department, Southern Methodist University, Dallas TX; United States of America
[45] Physics Department, University of Texas at Dallas, Richardson TX; United States of America
[46] National Centre for Scientific Research "Demokritos", Agia Paraskevi; Greece
[47] [(a)] Department of Physics, Stockholm University;[(b)] Oskar Klein Centre, Stockholm; Sweden
[48] Deutsches Elektronen-Synchrotron DESY, Hamburg and Zeuthen; Germany
[49] Fakultät Physik, Technische Universität Dortmund, Dortmund; Germany
[50] Institut für Kern- und Teilchenphysik, Technische Universität Dresden, Dresden; Germany
[51] Department of Physics, Duke University, Durham NC; United States of America
[52] SUPA — School of Physics and Astronomy, University of Edinburgh, Edinburgh; United Kingdom
[53] INFN e Laboratori Nazionali di Frascati, Frascati; Italy
[54] Physikalisches Institut, Albert-Ludwigs-Universität Freiburg, Freiburg; Germany
[55] II. Physikalisches Institut, Georg-August-Universität Göttingen, Göttingen; Germany
[56] Département de Physique Nucléaire et Corpusculaire, Université de Genève, Genève; Switzerland
[57] [(a)] Dipartimento di Fisica, Università di Genova, Genova;[(b)] INFN Sezione di Genova; Italy
[58] II. Physikalisches Institut, Justus-Liebig-Universität Giessen, Giessen; Germany
[59] SUPA — School of Physics and Astronomy, University of Glasgow, Glasgow; United Kingdom
[60] LPSC, Université Grenoble Alpes, CNRS/IN2P3, Grenoble INP, Grenoble; France
[61] Laboratory for Particle Physics and Cosmology, Harvard University, Cambridge MA; United States of America
[62] [(a)] Department of Modern Physics and State Key Laboratory of Particle Detection and Electronics, University of Science and Technology of China, Hefei;[(b)] Institute of Frontier and Interdisciplinary Science and Key Laboratory of Particle Physics and Particle Irradiation (MOE), Shandong University, Qingdao;[(c)] School of Physics and Astronomy, Shanghai Jiao Tong University, Key Laboratory for Particle Astrophysics and Cosmology (MOE), SKLPPC, Shanghai;[(d)] Tsung-Dao Lee Institute, Shanghai;[(e)] School of Physics and Microelectronics, Zhengzhou University; China

JHEP02(2024)197

[63] [(a)] Kirchhoff-Institut für Physik, Ruprecht-Karls-Universität Heidelberg, Heidelberg;[(b)] Physikalisches Institut, Ruprecht-Karls-Universität Heidelberg, Heidelberg; Germany
[64] [(a)] Department of Physics, Chinese University of Hong Kong, Shatin, N.T., Hong Kong;[(b)] Department of Physics, University of Hong Kong, Hong Kong;[(c)] Department of Physics and Institute for Advanced Study, Hong Kong University of Science and Technology, Clear Water Bay, Kowloon, Hong Kong; China
[65] Department of Physics, National Tsing Hua University, Hsinchu; Taiwan
[66] IJCLab, Université Paris-Saclay, CNRS/IN2P3, 91405, Orsay; France
[67] Centro Nacional de Microelectrónica (IMB-CNM-CSIC), Barcelona; Spain
[68] Department of Physics, Indiana University, Bloomington IN; United States of America
[69] [(a)] INFN Gruppo Collegato di Udine, Sezione di Trieste, Udine;[(b)] ICTP, Trieste;[(c)] Dipartimento Politecnico di Ingegneria e Architettura, Università di Udine, Udine; Italy
[70] [(a)] INFN Sezione di Lecce;[(b)] Dipartimento di Matematica e Fisica, Università del Salento, Lecce; Italy
[71] [(a)] INFN Sezione di Milano;[(b)] Dipartimento di Fisica, Università di Milano, Milano; Italy
[72] [(a)] INFN Sezione di Napoli;[(b)] Dipartimento di Fisica, Università di Napoli, Napoli; Italy
[73] [(a)] INFN Sezione di Pavia;[(b)] Dipartimento di Fisica, Università di Pavia, Pavia; Italy
[74] [(a)] INFN Sezione di Pisa;[(b)] Dipartimento di Fisica E. Fermi, Università di Pisa, Pisa; Italy
[75] [(a)] INFN Sezione di Roma;[(b)] Dipartimento di Fisica, Sapienza Università di Roma, Roma; Italy
[76] [(a)] INFN Sezione di Roma Tor Vergata;[(b)] Dipartimento di Fisica, Università di Roma Tor Vergata, Roma; Italy
[77] [(a)] INFN Sezione di Roma Tre;[(b)] Dipartimento di Matematica e Fisica, Università Roma Tre, Roma; Italy
[78] [(a)] INFN-TIFPA;[(b)] Università degli Studi di Trento, Trento; Italy
[79] Universität Innsbruck, Department of Astro and Particle Physics, Innsbruck; Austria
[80] University of Iowa, Iowa City IA; United States of America
[81] Department of Physics and Astronomy, Iowa State University, Ames IA; United States of America
[82] Istinye University, Sariyer, Istanbul; Türkiye
[83] [(a)] Departamento de Engenharia Elétrica, Universidade Federal de Juiz de Fora (UFJF), Juiz de Fora;[(b)] Universidade Federal do Rio De Janeiro COPPE/EE/IF, Rio de Janeiro;[(c)] Instituto de Física, Universidade de São Paulo, São Paulo;[(d)] Rio de Janeiro State University, Rio de Janeiro; Brazil
[84] KEK, High Energy Accelerator Research Organization, Tsukuba; Japan
[85] Graduate School of Science, Kobe University, Kobe; Japan
[86] [(a)] AGH University of Krakow, Faculty of Physics and Applied Computer Science, Krakow;[(b)] Marian Smoluchowski Institute of Physics, Jagiellonian University, Krakow; Poland
[87] Institute of Nuclear Physics Polish Academy of Sciences, Krakow; Poland
[88] Faculty of Science, Kyoto University, Kyoto; Japan
[89] Research Center for Advanced Particle Physics and Department of Physics, Kyushu University, Fukuoka; Japan
[90] Instituto de Física La Plata, Universidad Nacional de La Plata and CONICET, La Plata; Argentina
[91] Physics Department, Lancaster University, Lancaster; United Kingdom
[92] Oliver Lodge Laboratory, University of Liverpool, Liverpool; United Kingdom
[93] Department of Experimental Particle Physics, Jožef Stefan Institute and Department of Physics, University of Ljubljana, Ljubljana; Slovenia
[94] School of Physics and Astronomy, Queen Mary University of London, London; United Kingdom
[95] Department of Physics, Royal Holloway University of London, Egham; United Kingdom
[96] Department of Physics and Astronomy, University College London, London; United Kingdom
[97] Louisiana Tech University, Ruston LA; United States of America
[98] Fysiska institutionen, Lunds universitet, Lund; Sweden
[99] Departamento de Física Teorica C-15 and CIAFF, Universidad Autónoma de Madrid, Madrid; Spain
[100] Institut für Physik, Universität Mainz, Mainz; Germany
[101] School of Physics and Astronomy, University of Manchester, Manchester; United Kingdom
[102] CPPM, Aix-Marseille Université, CNRS/IN2P3, Marseille; France
[103] Department of Physics, University of Massachusetts, Amherst MA; United States of America
[104] Department of Physics, McGill University, Montreal QC; Canada
[105] School of Physics, University of Melbourne, Victoria; Australia

JHEP02(2024)197

[106] Department of Physics, University of Michigan, Ann Arbor MI; United States of America
[107] Department of Physics and Astronomy, Michigan State University, East Lansing MI; United States of America
[108] Group of Particle Physics, University of Montreal, Montreal QC; Canada
[109] Fakultät für Physik, Ludwig-Maximilians-Universität München, München; Germany
[110] Max-Planck-Institut für Physik (Werner-Heisenberg-Institut), München; Germany
[111] Graduate School of Science and Kobayashi-Maskawa Institute, Nagoya University, Nagoya; Japan
[112] Department of Physics and Astronomy, University of New Mexico, Albuquerque NM; United States of America
[113] Institute for Mathematics, Astrophysics and Particle Physics, Radboud University/Nikhef, Nijmegen; Netherlands
[114] Nikhef National Institute for Subatomic Physics and University of Amsterdam, Amsterdam; Netherlands
[115] Department of Physics, Northern Illinois University, DeKalb IL; United States of America
[116] [(a)] New York University Abu Dhabi, Abu Dhabi;[(b)] University of Sharjah, Sharjah; United Arab Emirates
[117] Department of Physics, New York University, New York NY; United States of America
[118] Ochanomizu University, Otsuka, Bunkyo-ku, Tokyo; Japan
[119] Ohio State University, Columbus OH; United States of America
[120] Homer L. Dodge Department of Physics and Astronomy, University of Oklahoma, Norman OK; United States of America
[121] Department of Physics, Oklahoma State University, Stillwater OK; United States of America
[122] Palacký University, Joint Laboratory of Optics, Olomouc; Czech Republic
[123] Institute for Fundamental Science, University of Oregon, Eugene, OR; United States of America
[124] Graduate School of Science, Osaka University, Osaka; Japan
[125] Department of Physics, University of Oslo, Oslo; Norway
[126] Department of Physics, Oxford University, Oxford; United Kingdom
[127] LPNHE, Sorbonne Université, Université Paris Cité, CNRS/IN2P3, Paris; France
[128] Department of Physics, University of Pennsylvania, Philadelphia PA; United States of America
[129] Department of Physics and Astronomy, University of Pittsburgh, Pittsburgh PA; United States of America
[130] [(a)] Laboratório de Instrumentação e Física Experimental de Partículas — LIP, Lisboa;[(b)] Departamento de Física, Faculdade de Ciências, Universidade de Lisboa, Lisboa;[(c)] Departamento de Física, Universidade de Coimbra, Coimbra;[(d)] Centro de Física Nuclear da Universidade de Lisboa, Lisboa;[(e)] Departamento de Física, Universidade do Minho, Braga;[(f)] Departamento de Física Teórica y del Cosmos, Universidad de Granada, Granada (Spain);[(g)] Departamento de Física, Instituto Superior Técnico, Universidade de Lisboa, Lisboa; Portugal
[131] Institute of Physics of the Czech Academy of Sciences, Prague; Czech Republic
[132] Czech Technical University in Prague, Prague; Czech Republic
[133] Charles University, Faculty of Mathematics and Physics, Prague; Czech Republic
[134] Particle Physics Department, Rutherford Appleton Laboratory, Didcot; United Kingdom
[135] IRFU, CEA, Université Paris-Saclay, Gif-sur-Yvette; France
[136] Santa Cruz Institute for Particle Physics, University of California Santa Cruz, Santa Cruz CA; United States of America
[137] [(a)] Departamento de Física, Pontificia Universidad Católica de Chile, Santiago;[(b)] Millennium Institute for Subatomic physics at high energy frontier (SAPHIR), Santiago;[(c)] Instituto de Investigación Multidisciplinario en Ciencia y Tecnología, y Departamento de Física, Universidad de La Serena;[(d)] Universidad Andres Bello, Department of Physics, Santiago;[(e)] Instituto de Alta Investigación, Universidad de Tarapacá, Arica;[(f)] Departamento de Física, Universidad Técnica Federico Santa María, Valparaíso; Chile
[138] Department of Physics, University of Washington, Seattle WA; United States of America
[139] Department of Physics and Astronomy, University of Sheffield, Sheffield; United Kingdom
[140] Department of Physics, Shinshu University, Nagano; Japan
[141] Department Physik, Universität Siegen, Siegen; Germany
[142] Department of Physics, Simon Fraser University, Burnaby BC; Canada
[143] SLAC National Accelerator Laboratory, Stanford CA; United States of America

JHEP02(2024)197

[144] Department of Physics, Royal Institute of Technology, Stockholm; Sweden
[145] Departments of Physics and Astronomy, Stony Brook University, Stony Brook NY; United States of America
[146] Department of Physics and Astronomy, University of Sussex, Brighton; United Kingdom
[147] School of Physics, University of Sydney, Sydney; Australia
[148] Institute of Physics, Academia Sinica, Taipei; Taiwan
[149] [(a)] E. Andronikashvili Institute of Physics, Iv. Javakhishvili Tbilisi State University, Tbilisi;[(b)] High Energy Physics Institute, Tbilisi State University, Tbilisi;[(c)] University of Georgia, Tbilisi; Georgia
[150] Department of Physics, Technion, Israel Institute of Technology, Haifa; Israel
[151] Raymond and Beverly Sackler School of Physics and Astronomy, Tel Aviv University, Tel Aviv; Israel
[152] Department of Physics, Aristotle University of Thessaloniki, Thessaloniki; Greece
[153] International Center for Elementary Particle Physics and Department of Physics, University of Tokyo, Tokyo; Japan
[154] Department of Physics, Tokyo Institute of Technology, Tokyo; Japan
[155] Department of Physics, University of Toronto, Toronto ON; Canada
[156] [(a)] TRIUMF, Vancouver BC;[(b)] Department of Physics and Astronomy, York University, Toronto ON; Canada
[157] Division of Physics and Tomonaga Center for the History of the Universe, Faculty of Pure and Applied Sciences, University of Tsukuba, Tsukuba; Japan
[158] Department of Physics and Astronomy, Tufts University, Medford MA; United States of America
[159] United Arab Emirates University, Al Ain; United Arab Emirates
[160] Department of Physics and Astronomy, University of California Irvine, Irvine CA; United States of America
[161] Department of Physics and Astronomy, University of Uppsala, Uppsala; Sweden
[162] Department of Physics, University of Illinois, Urbana IL; United States of America
[163] Instituto de Física Corpuscular (IFIC), Centro Mixto Universidad de Valencia — CSIC, Valencia; Spain
[164] Department of Physics, University of British Columbia, Vancouver BC; Canada
[165] Department of Physics and Astronomy, University of Victoria, Victoria BC; Canada
[166] Fakultät für Physik und Astronomie, Julius-Maximilians-Universität Würzburg, Würzburg; Germany
[167] Department of Physics, University of Warwick, Coventry; United Kingdom
[168] Waseda University, Tokyo; Japan
[169] Department of Particle Physics and Astrophysics, Weizmann Institute of Science, Rehovot; Israel
[170] Department of Physics, University of Wisconsin, Madison WI; United States of America
[171] Fakultät für Mathematik und Naturwissenschaften, Fachgruppe Physik, Bergische Universität Wuppertal, Wuppertal; Germany
[172] Department of Physics, Yale University, New Haven CT; United States of America

[a] Also Affiliated with an institute covered by a cooperation agreement with CERN
[b] Also at An-Najah National University, Nablus; Palestine
[c] Also at Borough of Manhattan Community College, City University of New York, New York NY; United States of America
[d] Also at Center for High Energy Physics, Peking University; China
[e] Also at Center for Interdisciplinary Research and Innovation (CIRI-AUTH), Thessaloniki; Greece
[f] Also at Centro Studi e Ricerche Enrico Fermi; Italy
[g] Also at CERN, Geneva; Switzerland
[h] Also at Département de Physique Nucléaire et Corpusculaire, Université de Genève, Genève; Switzerland
[i] Also at Departament de Fisica de la Universitat Autonoma de Barcelona, Barcelona; Spain
[j] Also at Department of Financial and Management Engineering, University of the Aegean, Chios; Greece
[k] Also at Department of Physics, Ben Gurion University of the Negev, Beer Sheva; Israel
[l] Also at Department of Physics, California State University, Sacramento; United States of America
[m] Also at Department of Physics, King's College London, London; United Kingdom
[n] Also at Department of Physics, Stanford University, Stanford CA; United States of America
[o] Also at Department of Physics, University of Fribourg, Fribourg; Switzerland
[p] Also at Department of Physics, University of Thessaly; Greece

JHEP02(2024)197

[q] Also at Department of Physics, Westmont College, Santa Barbara; United States of America
[r] Also at Hellenic Open University, Patras; Greece
[s] Also at Institucio Catalana de Recerca i Estudis Avancats, ICREA, Barcelona; Spain
[t] Also at Institut für Experimentalphysik, Universität Hamburg, Hamburg; Germany
[u] Also at Institute for Nuclear Research and Nuclear Energy (INRNE) of the Bulgarian Academy of Sciences, Sofia; Bulgaria
[v] Also at Institute of Applied Physics, Mohammed VI Polytechnic University, Ben Guerir; Morocco
[w] Also at Institute of Particle Physics (IPP); Canada
[x] Also at Institute of Physics and Technology, Ulaanbaatar; Mongolia
[y] Also at Institute of Physics, Azerbaijan Academy of Sciences, Baku; Azerbaijan
[z] Also at Institute of Theoretical Physics, Ilia State University, Tbilisi; Georgia
[aa] Also at L2IT, Université de Toulouse, CNRS/IN2P3, UPS, Toulouse; France
[ab] Also at Lawrence Livermore National Laboratory, Livermore; United States of America
[ac] Also at National Institute of Physics, University of the Philippines Diliman (Philippines); Philippines
[ad] Also at Technical University of Munich, Munich; Germany
[ae] Also at The Collaborative Innovation Center of Quantum Matter (CICQM), Beijing; China
[af] Also at TRIUMF, Vancouver BC; Canada
[ag] Also at Università di Napoli Parthenope, Napoli; Italy
[ah] Also at University of Chinese Academy of Sciences (UCAS), Beijing; China
[ai] Also at University of Colorado Boulder, Department of Physics, Colorado; United States of America
[aj] Also at Washington College, Chestertown, MD; United States of America
[ak] Also at Yeditepe University, Physics Department, Istanbul; Türkiye
[*] Deceased

JHEP02(2024)197